Faculty of Engineering of University of Porto


# CROSS
# Monte Carlo Simulation and Cross-Entropy

João Meneses Figueiredo Costa

FINAL VERSION

Dissertation submitted in fulfillment of the requirements
for the Master in Electrical and Computers Engineering
in the Major of Energy

Supervisor: Vladimiro Henrique Barrosa Pinto de Miranda (Ph.D.)
Co- supervisor: Leonel de Magalhães Carvalho (Ph.D.)

Porto, Portugal, July, 2016

# Abstract

The planning of power system operations is a complex problem, mostly due to the presence of uncertainties tied to the multiple variables of such system. Given the liberalization of the power systems in late 20th century, early 21st century, and its continued evolution as well as the expanding accessibility of the transmission and distribution networks provided to the distributors and the consumers with the introduction of micro-production and renewable energy options, this planning problem grows in complexity at an exponential rate.

Initially treating these problems and modelling them based in probabilistic concepts, presented a problem due to the lack of data related to the behavior of each variable. The Sequential Monte Carlo simulation (MCS) method is one of the most powerful tools for power systems reliability assessment.

Through sequentially sampling the durations of the different states for the multiple components that compose the power systems, this method can somehow simulate the stochastic behavior of such components. Therefore, time-dependent issues like the renewable power production, micro-grid operation, scheduled maintenance, hydric thermal power systems, the evolution of the system load, etc.

Presenting itself with numerous advantages, such as making it possible to estimate average durations for different events and their frequency, as well as quantify the power unavailability associated with each system failure. The MCS major downside is the simulation time, sometimes too slow due to computational effort of the method itself.

As so the main objectives of this dissertation are to investigate alternative and incorporated methods based on the Cross-Entropy theory and propose algorithmic advances that can effectively improve the time-efficiency of the sequential MCS simulation.

# Resumo

O planeamento das operações do sistema de energia é um problema complexo, principalmente devido à presença de incertezas ligadas às múltiplas variáveis do referido sistema. Dada a liberalização dos sistemas de energia no final do século 20, início do século 21, e sua evolução contínua, bem como a acessibilidade a expansão das redes de transmissão e distribuição dadas aos distribuidores e os consumidores, com a introdução de microprodução e opções de energia renovável, este problema de planeamento cresce em complexidade a uma taxa exponencial.

Inicialmente, o tratamento destes problemas e modelização baseada em conceitos de probabilidade, apresentou um problema devido à falta de dados relacionados com o comportamento de cada variável. O método de simulação Monte Carlo Sequencial (MCS) é uma das ferramentas mais poderosas para avaliação da fiabilidade de sistemas de energia, através da sequencial amostragem as durações das diferentes estados para os vários componentes que compõem os sistemas de energia, este método pode de alguma forma simular o comportamento estocástico dos ditos componentes, os mesmos problemas dependentes do tempo, como a produção de energia renovável, a operação micro-rede, manutenção programada, os sistemas de energia hídrico-térmicos, a evolução da carga do sistema, etc.

Apresentando-se com inúmeras vantagens, como tornando-se possível estimar durações médias para diferentes eventos e sua frequência, bem como quantificar a indisponibilidade de energia associada a cada falha do sistema, a principal desvantagem MCS é o tempo de simulação, por vezes demasiado lento devido ao esforço computacional do próprio método.

Como assim os principais objetivos desta tese são, investigar métodos alternativos incorporados com base na teoria entropia cruzada e propor avanços algorítmicos que possam melhorar eficazmente o tempo-eficiência da simulação MCS sequencial.

# Acknowledgment's

First of all, I'd like to talk about my supervisor, Professor Doctor Vladimiro Henrique Barrosa Pinto de Miranda, who I met in my 4rd year o MIEEC and have learned a lot from him the last two years, and when the opportunity arose to work together, I didn't think twice. I'd like to express my sincere gratitude, for a major contribution in helping refine this work, for his brilliant insights, encouragement, for the opportunity granted to me. Most of all for believing and supporting my commitment in what he warned me it was going to be an overwhelming exercise of overcoming and suffering that, nonetheless, in the end proved out to be incredibly rewarding.

I could never have imagined the great opportunity that was yet to come, work with Doctor Leonel Magalhães Carvalho, to him I'd like to express my deepest gratitude, whose availability, hard work, endless patience, and correct guidance throughout this work helped overcome all and any difficulties. I feel proud and honored to have learned so much with such a brilliant engineer and exceptional human being, who I believe to be and undeniable role model for all of us who seek to accomplish more and better each day.

I'd like to address a special thanks to everyone I came in contact in INESCTEC Porto, for their sympathy, friendliness and availability, who made this brief passage warmly comfortable. The same goes to everyone I met at FEUP, who helped me become what I am today, from the many teachers that passed me their knowledge and the pride in their job, as well as the many friends I've made and who have enriched my heart and soul.

Above all, the last and most important thanks goes to my family, I owe everything I have to them, they have been a constant pillar of strength, hope, endurance and belief, the very foundation of what I am today. A family that despite the sacrifices and difficulties faced, gave me the opportunity to improve my education and that never ceased to support me and my dreams, even when my biggest dream is and will always be to make them proud of what they achieved. If the time comes, I can only hope to be as good of a parent as mine were to me.

# Contents

# List of figures

# List of tables

# List of Abbreviations

| | |
|---|---|
| COPT | Capacity Outage Probability Table |
| CE | Cross-Entropy |
| CDF | Cumulative Distribution Function |
| CMC | Conditional Monte Carlo |
| CV | Control Variables |
| CS | Cauchy-Schwarz |
| EENS | Expected Energy Not Supplied |
| EPSO | Evolutionary Particle Swarm Optimization |
| EU | European Union |
| HL1 | Hierarchical Level One |
| HL2 | Hierarchical Level Two |
| HL3 | Hierarchical Level Three |
| IS | Importance Sampling |
| KL | Kullback-Leibler |
| LOLC | Loss of Load Cost |
| LOLD | Loss of Load Duration |
| LOLE | Loss of Load Expectation |
| LOLF | Loss of Load Frequency |
| LOLP | Loss of Load Probability |
| MCS | Monte Carlo Simulation |
| MTTF | Mean Time to Failure |
| MTTR | Mean Time to Repair |
| PDF | Probability Density Function |
| PRF | Peak Reduction Factor |
| SMCS | Sequential Monte Carlo Simulation |
| WF | Wind Farm |
| WTG | Wind Turbine Generator |

# List of Symbols

| | |
|---|---|
| $\lambda$ | Failure Rate |
| $\mu$ | Repair Rate |
| R | Reliability |
| Q | Unreliability |
| m | Mean Time to Failure |
| r | Mean Time to Repair |
| L | Load |
| $\hat{E}$ | Estimated Expected Value |
| $E$ | Expected Value |
| $\hat{V}$ | Estimated Variance |
| $V$ | Variance |
| $\beta$ | Coefficient of Variation |
| $N$ | Sample Dimension |
| $\sigma$ | Standard Deviation |
| $C$ | Covariance |
| $\rho$ | Correlation Coefficient |
| $D_{KL}$ | Kullback-Leibler Divergence |
| $D_{KL}$ | Cauchy-Schwarz Divergence |
| $u_i$ | Unavailability of i group for the original distribution |
| $v_i$ | Unavailability of i group for the distorted distribution |

# Chapter 1

# Introduction

This chapter serves as exhibition of the complex problem at hand, along with its context and the ideas behind this dissertation. Firstly, the context and the importance of problem will be explained as well as the importance of the reliability assessment, followed by the current means of calculating these indices and their significance, finally the motivation for this dissertation will be defended along with its organization.

## 1.1. Context and Importance of Electric Power Systems Reliability Assessment

The concept of reliability took a vital Role mid-20th century, when the dimension and complexity of power systems started to rapidly grow. Its modern definition as we know it dates back to 1940 when the U.S. Military started to develop advanced systems of armament which in turn resulted in some of the first reliability studies through computer simulation [1].

Modern power system, nowadays, consist of a complex network of electrical components progressively more interconnected, geographically dispersed across the world, focused on the production, transfer and distribution of electric power, delivering energy downstream to the final consumers. The high number of components, coupled with the demand uncertainties and the fluctuation of energy resources, both renewable and fossil-fueled make the design and its compartmentalized operation extremely complex. Requiring a frequent and precise monitoring by the different operators that compose the system, due to the enormous quantity of components, combined with their unique operation characteristics, there is a possibility of failure of the entire system simply by failing a crucial or a set of crucial components. These phenomena are classified as rare events due to the low probability associated with them.

With its constant growing expansion and complexity, many depend on its normal operation to be as smooth as possible, the economy of a country depends on it, seeing as most of its industry depend on it to boost their activity, as well as possibly its security, with all the electronic equipment used by the military depending mostly to direct connections to the grid, making the power grid of a country a strategic aspect of its defense, presently, not only is the power system delegated to supply the end costumers with energy but likewise to assure that the system functions with a set of standards

in continuity, quality and security, to further develop the economic and social sectors of a modern society [2].

Constant interruptions on electric energy supply can dramatically affect multiple sectors of the economy, forcing them to "buy" reliability, usually in the form of emergency generators, in worst scenarios, these economic agents are forced to move its activities to other countries with high losses in the economic sector as well as a shift of scenery in the social environment.

These setbacks can often be repaired, following short term government measures put in place to attract the industries with other benefits such as tax reductions, financial compensations, etc. Nevertheless, these setbacks lead to more investment both in the power grid and the financial incentives, in turn leading to an unsustainable economic development.

In order to decrease the probability as well as the frequency and the duration of these rare events, more investment is required, however, the tendency to postpone these investments, operating the system near its limits, leaves the decision makers these contradictory requirements when the time comes to reinforce the electric system in order to increase its reliability.

The recent changes in the sector, such as the progressive deregulation with the purpose of creating an electric market, raised the degree of importance to the continuity of service, being the responsibility of the electricity provider to assure a continuous power supply. The operation scenery of the electric power systems has changed, due to new concepts, distributed generation, micro-grids, the increased penetration of energy from fluctuating sources, brought the necessity describe the energy system minutely, to correctly assess its reliability.

## 1.2. Current Methodology and Motivation

The development of accurate models for the increasing uncertainties and the fluctuating power sources presents itself as a problem with the reliability assessment of modern power systems. Other difficulties are related to the increasing size of the set of the stochastic variables of these models. Even with the current computational power available, the reliability assessment of complex power systems is still time-consuming [3-6].

The creation of efficient methodologies that cope with the new and increasing complexities affecting the reliability of modern power systems is of the utmost importance. The new methodologies must provide satisfactory results with sufficient accuracy, attainable in useful time and must be competitive with existing methods.

The Monte Carlo Simulation (MCS) is, of the available current methods, the most used for reliability assessment of power systems [7-8]. The MCS method is based on the frequentist theory of sampling, which defines the probability of an event as its long-run expected frequency of occurrence [9]. According to this theory, the population mean, in this case is a reliability index, can be estimated by drawing successive samples from the population. The resulting estimate is used to create a

confidence interval for the population mean, which is centered at the sample mean. The MCS methods used for the reliability assessment of power systems are in fact stochastic simulation methods given the random behavior of these systems varying with time [2].

The MCS methods can be subdivided into two different approaches: the non-sequential (non-Chronological) and the sequential (Chronological) [10], the non-sequential MCS method, which is closely related to random sampling, differs from the sequential MCS method which can accurately reproduce the whole cycle of interruptions, as so, this method can easily include all chronological characteristics of power systems into the simulation, such as time fluctuating load models and power sources, the time-dependency of primary energy resources, loss of load cost, maintenance schedules, weather effects, calendar patterns, etc.

## 1.3. Hypothesis and Purpose of this Dissertation

For the reasons above, the sequential MCS method can be considered the most complete approach to model accurately the increasing complexity of modern power systems. Unfortunately, the advantages of the sequential MCS method are met by the considerable disadvantageous simulation time necessary to accurately estimate the reliability indices.

The MCS method already has adequate mechanisms to accelerate its convergence time, namely, the Control Variable (CV), or the Importance Sampling (IS), [11]. The Control Variable method assumes it's possible to calculate an approximate value for that we wish to know, through an analytical method independent in relation to the Monte Carlo. Importance Sampling is based on a distribution distortion in order to increase the probability of rare events. This technique seeks to reduce the variance without changing the expected value.

The purpose of this dissertation is to research more ways to accelerate the MCS method. The research explores the notions of importance sampling and Cauchy-Schwarz Probability Distribution Function (PDF) distance, and further developing the implementation of cross-entropy methods currently based on the Kullback-Leibler PDF distance. This study is motivated by the theoretical hypothesis that the optimal distribution distortion would require only one iteration of the method to converge, and therefore obtain accurate results with less simulation time. That being said we, will be looking for a parallelism between the current methodologies to facilitate the implementation of new algorithms to distort such distribution.

## 1.4. Dissertation's Structure

This dissertation's work is compartmentalized in 5 chapters, that obey the following structure:

**Chapter 1** consists of a brief, yet important, contextualization of the problem, this dissertation and its studies will revolve around, along with some of the implications of power systems reliability in the world as we know it and lastly, the motivation and scope of this work.

**Chapter 2** serves as a more detailed and structured introduction to the current methodologies. Starts with a brief explanation on reliability assessment, followed by the different reliability indices, describing the hierarchical levels, the analytical methods, finishes with the MCS and the basic concepts associated, as well as the complementary mechanisms used in conjunction with the MCS to accelerate its convergence.

**Chapter 3** will introduce the model IEEE RTS 79 used in all of this work's tests, as well as, show the current CE and MCS results and efficiency, through a battery of different tests using both methods in conjunction and the crude MCS alone. Finishes by comparing and discussing the obtained results.

**Chapter 4** introduces the *Cauchy-Schwarz Inequality*, along with the possibilities of introduction in the MCS method, investigates the parallelism with the current Cross-Entropy methods based on the *Kullback-Leibler Divergence*. The second part of this chapter presents the results obtained with the new method and compares them with the current one.

**Chapter 5** finally closes this dissertation with the conclusions attained in the previous chapters, trough research and extrapolations, and the reference list to the main scientific knowledge contributors.

# Chapter 2

# State of the Art

## 2.1. Reliability Assessment

Reliability is a branch of engineering knowledge that seeks to establish behavior models for systems with components subjected to, partial or full, malfunctions that may impede the normal operation, for which the system was conceived [11].

The reliability assessment studies concern systems, more or less complex. The representation of such failures in the system's equipment is done with basis in probabilistic models, allowing us to represent the uncertainty of those events, especially when there is insufficient statistical sampling [11].

Due to the probabilistic nature of the events, it's assumed that such events related with the system occur randomly, and there is no way to predict with enough precision the moments when the components fail. Therefore, probabilistic distributions are used, based on the statistical analysis of the behavior of similar systems of components [11].

As an example, if we assume X as random variable representing a component's lifetime the likelihood of such component surviving a certain time t or past that certain time t, can be respectively represented as $P(X \leq t)$ and $P(X > t)$. The probability of a component surviving past a certain time, is designated as reliability, which can be represented by the letter R. We can establish:

$$R(t) = P(X > t), \tag{2. 1}$$

if we assume f(x) as the PDF of X, we have

$$R(t) = \int_t^{\infty} f(x)dx\,. \tag{2. 2}$$

Another important concept associated to these studies is the failure rate, often represent by the Greek letter λ, the failure rate is defined as follows:

$$\lambda(\mathrm{t}) = \frac{f(t)}{R(t)} \Rightarrow \lambda(\mathrm{t}) = -\frac{dR(t)}{R(t)dt}. \quad \textbf{(2. 3)}$$

The failure rate can be perceived as the frequency with which an engineered system or component fails, in a determined interval between t and t+dt. Upon expansion of the following equation

$$\lambda(t)dt = -\frac{dR(t)}{R(t)}, \quad \textbf{(2. 4)}$$

we obtain

$$\int_0^t \lambda(t)dt = -\int_1^{R(t)} \frac{1}{R(t)} dR(t), \quad \textbf{(2. 5)}$$

which is equivalent to

$$R(t) = e^{-\int_0^t \lambda(t)dt}. \quad \textbf{(2. 6)}$$

Thus we have the reliability of a component as function of the failure rate. If the failure rate is considered constant throughout time, $\lambda(t) = \lambda$, and so independent from time, comes

$$R(t) = e^{-\lambda t} \quad \textbf{(2. 7)}$$

As equation 2.7 shows, this is one of the justifications for the use of exponential distribution. Nevertheless, the failure rate can't always be assumed as constant, and so it's possible to observe two different patterns for its evolution throughout time in the following figure.

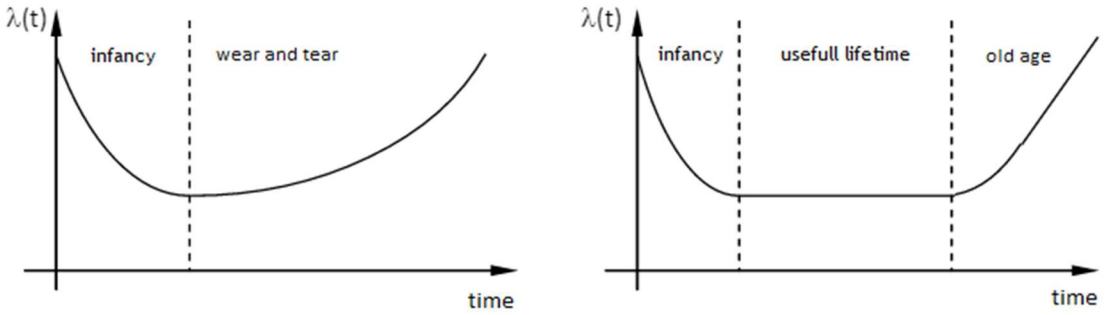


**Figure 2.1** - Models of the development of failure rate throughout time. On the left, typical case of mechanical components subject to wear and tear. To the right typical case of electronic or electrical components, wherein the aging factors are different.

### 2.1.1. Exponential Distribution

If a random continuous variable, is non negative, X will present an exponential distribution with the failure rate λ, if its PDF it's given by

$$f(t) = \lambda e^{-\lambda t} \text{, for } t \geq 0, \qquad \textbf{(2. 8)}$$

if we integrate function f(t), we have $\int_0^{\infty} f(t)dt \quad 1$, which in turn represents a PDF:

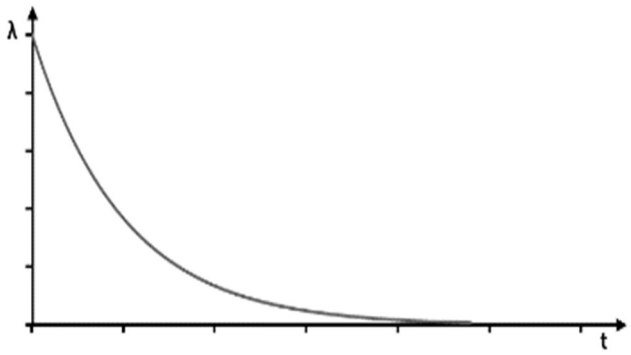


**Figure 2.2** - Probability Distribution Function of an Exponential Distribution

Therefore, we can define the PDF of an Exponential distribution as:

$$f(t;\lambda) = \begin{cases} \lambda e^{-\lambda t}, x \geq 0 \\ 0, x \leq 0 \end{cases}. \qquad \textbf{(2. 9)}$$

The exponential distribution plays a practical central role in the establishment of component behavior models, particularly in power systems, despite other distributions being used in reliability models. Namely the Gauss distribution and Weibull, having no memory, is a good representation of electrical and electronic systems, in particular the ones subjected to maintenance in order to keep them working within their lifetime.

### 2.1.2. Markov Models for repairable components

The Markov models assume a special importance, because they can serve as a reference model to most of the studies. However, they require a certain data precision, which in many cases it's not compatible with the existing or the stored database. Nonetheless the Markov processes allow us to model many phenomena, in this particular case the electric power systems [11-13].

In order to build a Markov model for the reliability assessment problem, it's necessary that we begin with defining the possible residing states for a component. In this case, it can be as simple as a component being in two states, enabled (E) and disabled (D). It's also necessary to describe the transitions between states: admitting such state might change or maintain we have the following possible Markov diagram:

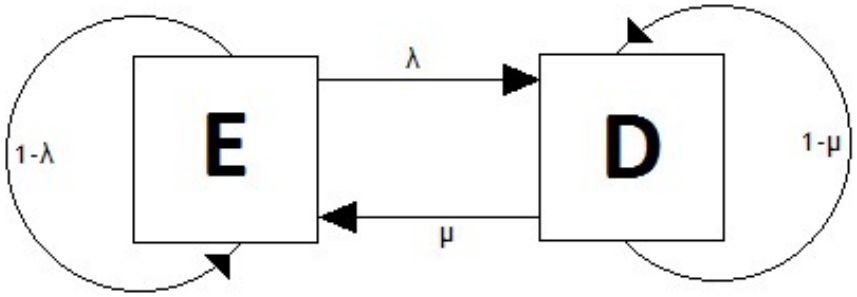


**Figure 2.3** - Markov diagram for a component with two possible states

Assuming that time is a sequence of discrete leaps, we are in the presence of a discrete Markov process, and the system's evolution is a sequence of states. This allows us to mathematically represent the process through the so called Markov matrix, that states

$$\begin{bmatrix} 1-\lambda & \mu \\ \lambda & 1-\mu \end{bmatrix} \begin{bmatrix} P_E(t) \\ P_D(t) \end{bmatrix} = \begin{bmatrix} P_E(t+1) \\ P_D(t+1) \end{bmatrix}, \quad \textbf{(2. 10)}$$

with:

- $P_E(t)$ - Probability of the component being enabled in the time instance t;
- $P_D(t)$- Probability of the component being disabled in the time instance t;
- λ – failure rate (constant);
- μ - repair rate (constant);

### 2.1.3. Basic Indices in Electrical Systems Reliability

In most of the electrical reliability assessment studies, the analysis and calculus are based in basic statistical indices, such indices, commonly represented by traditional letter are as follows [11]:

- λ – Failure Rate, [failures/year];
- FOR – forced outage rate, [%];
- μ – Repair Rate, [year$^{-1}$];
- r – Mean time to repair, [hours];
- U – unavailability, [hours/year];
- PNS – Average power cut, [kW, MW];
- E – Average Annual Non Supplied Energy, [kW, MW/year]

The first five are a result of the probabilistic models, the last two measure the impacts in the system, the average power cut corresponds to the expected value of the power cut distributions because of the unscheduled service interruption

The average annual non supplied energy corresponds to the expected value of the product of each power cut in each incident by the respective duration.

Although there are more indices that help define a systems reliability, but these five form the necessary conceptual basis.

### 2.1.4. Mean time to failure and to repair

The operation of a component continuously repairable, may be represented as follows:

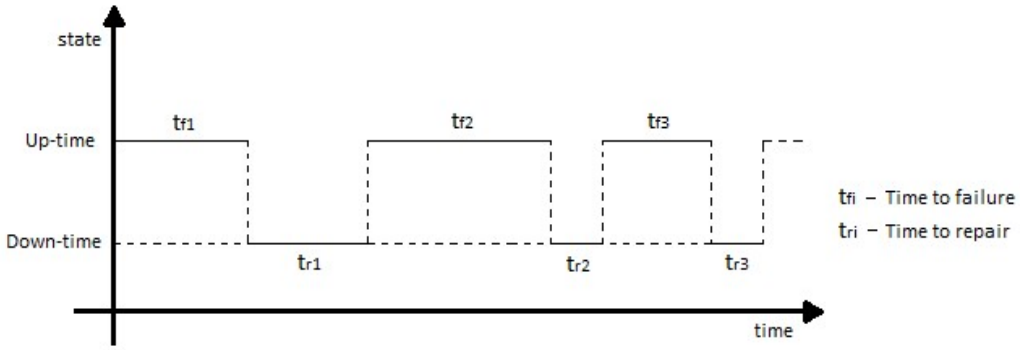


**Figure 2.4** - Historical representation of a continuously repairable component

The definition of the mean time to failure and mean time to repair is depicted by the following equations [11] [13]:

$$m = MTTF = \frac{\sum_{i=1}^{n_f} t_{fi}}{n_f} = \frac{1}{\lambda}, \quad \textbf{(2. 11)}$$

$$r = MTTR = \frac{\sum_{i=1}^{n_r} t_{ri}}{n_r} = \frac{1}{\mu}. \quad \textbf{(2. 12)}$$

These indices can be easily diagrammed, as it can be seen below, along with another important index, the mean time between failures (MTBF), $MTBF = m + r$ :

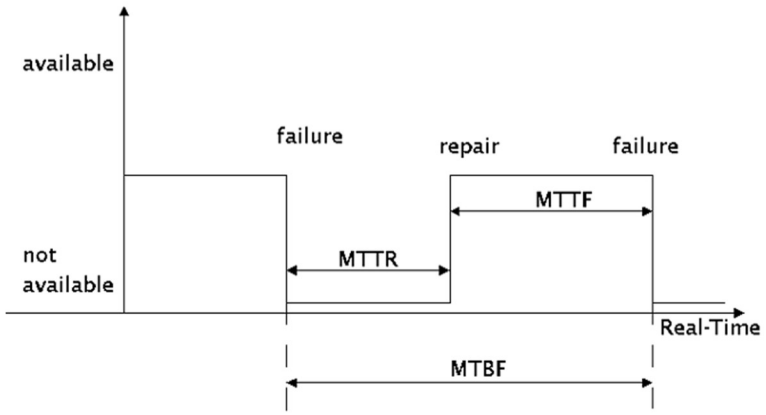


**Figure 2.5** - Graphical representation of the MTTF, MTTR and the MTBF of a component

Therefore, the probabilities of a component being available or not, at any moment are given by:

$$P(Available) = \frac{r}{m+r} = \frac{\mu}{\lambda+\mu}, \quad \textbf{(2. 13)}$$

$$P(notAvailable) = \frac{m}{m+r} = \frac{\lambda}{\lambda+\mu}. \quad \textbf{(2. 14)}$$

## 2.2. Reliability Indices

Reliability assessment studies, as we would expect result in reliability indices that help define the systems and characterize the service quality. Reliability indices can provide information on the reliability of a system, which are most commonly associated to the planning phase. These indices can be called predictive indices, in turn there are the past performance indices which refer the actual system reliability, presenting the events observed in the studies. Considering this dissertation addresses mostly the planning phases with simulation methods, only predictive indices are used [14].

The main objective of these studies is not to solve decision problems, but instead to provide quantitative information, whether of economic nature or risk, which constitutes aid elements to decision. Below are some of the most common reliability indices, addressing frequency, duration, cost and even the energy associated with each event [13]:

- Load of Loss Probability - LOLP [%]– Probability associated with load shedding;
- Load of Loss Expectation - LOLE [hour/year} - Average hours with load shedding during a year;
- Expected Energy Not Supplied – EENS [MWh/year] – Average energy shedding during a year;
- Expected Power Not Supplied – EPNS [MW] – Average load shedding;
- Loss of Load Frequency – LOLF [occurrence/year] – Average number of load shedding occurrences during a year;
- Loss of Load Duration – LOLD [hour/occurrence] – Average duration of load shedding occurrences;
- Loss of Load Cost – LOLC [currency/year] – Average cost of load shedding during a year;

Although there are more indices that help define a systems reliability, these are the ones that will be use in this dissertation due to the nature of this work.

### 2.2.1. Hierarchical Levels of Reliability of a Power System

Power systems can be divided in three hierarchical levels (HL). Firstly, the HL1 refers to the generation facilities, HL2 is concerned to the so called composite system, which includes both the generation and transmission facilities, lastly HL3 concerns the entirety of the power system, including the composite systems and the distribution facilities up to consumer load [15].

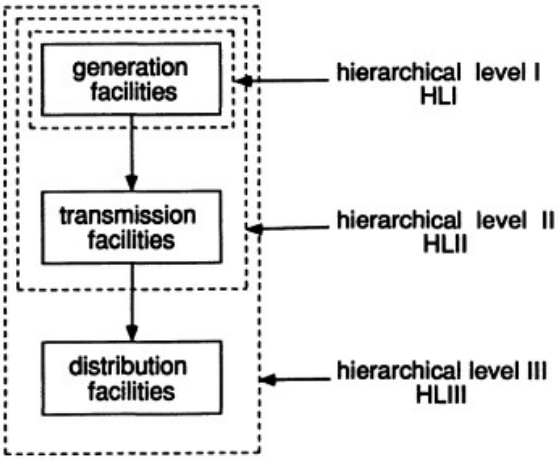


**Figure 2.6** - Hierarchical Levels [15]

In this dissertation we will mostly deal with HL1 reliability, which is enough to test the efficiency of current and the researched methodologies.

### 2.2.2. Hierarchical Level 1 (Generating System)

Planning the expansion or the operation of a production system, requires taking into account the economic rationalization objectives and goals or restrictions associated with service quality assurance. In particular, it's imperative, as a first concern, to focus in having sufficient production capacity to supply the load (forecast) system [11].

The necessity for these studies results from the dramatic consequence, of not having enough capacity to satisfy the peak demand, that in turn derives from component breakdowns, unseasonable forced outages and schedule maintenance. Therefore, the determination of the appropriate values of availability of power production, in the form of installed capacity in the core, is at the center of static reserve studies. In general, these studies attempt to determine the suitability of building up a central or adding new groups, so that we may numerically determine the assurance that the system load will be powered entirely.

### 2.2.3. Hierarchical Level 2 (Composite System)

These HL2 studies, no longer concern only the generating systems as well as the transmission, as so, it's required to include the detailed model for the transmission grid. Another important aspect is the inclusion of more restrictions in comparison to the HL1 studies, due to the characteristic of components that compose the transmission grid, such as, voltage and loading limits of the circuit and the active and reactive power transit [2] [15]

The more complete model approach of these studies, allows, in turn, for a more accurate, way of determining the effects of the geographic dispersion of the loads and energy sources. The necessity for these studies comes from the independent nature of the components, that can cause load shedding even with the generating system fully operational, as such, they attempt to determine the suitability of building new transmission lines or reinforcing existing ones, so that we may numerically determine the assurance that the composite system.

## 2.3. Analytical Methodology

Analytical methods, aim to solve the mathematically modeled problem, resorting to the calculus of the reliability indices through the obtainment of the probability mass functions. This approach is computationally more efficient, however, the systems have to be simple to mathematically model and with a reduced number of components due to exponential increase in complexity [14] [11].

### 2.3.1. Capacity Outage Probability Table

The capacity outage probability table, is one of the steps to calculate a basic system's reliability indices, this table is an enumeration of all possible systems states and their probability of occurrence. Nevertheless, the information obtained calculating it, is of the utmost importance because it gathers pertinent values and allows us to proceed to the calculus of the Loss of Load Probability and other reliability indices [11].

### 2.3.2. Loss of Load risk calculus

Given the values obtained from the capacity outage probability table, it's possible to calculate the risk values known as LOLP and LOLE, both concern to the probability of load shedding events throughout an evaluation period commonly set as a year. The main difference between LOLP and the LOLE, is that the LOLP is dimensionless, considered as a probability percentage and the LOLE expresses the same value in days or hours per year [11]. With that in consideration the formula is as it follows:

$$LOLP = \sum_{i=1}^{n} p(x_i) \times p(L > X_{\max} - X_i). \quad \textbf{(2. 15)}$$

In which:

- $p(x_i)$ - lost capacity probability of $x_i$ kW or MW:
- $X_{\max}$ - total installed capacity in Kw or MW;
- $L$ - load peak;
- $p(L > X_{\max} - X_i)$ - probability that the load peak exceeds the available capacity at the i state;
- n – total number of states;

$$LOLE(Risk) = LOLP \times 365 \text{ (Days in a year)} \quad \textbf{(2. 16)}$$

## 2.4. Simulation Methodology

Simulation methods are mostly based in the MCS [3] [8], these methods integrate optimization techniques into simulation analysis, due to the complex nature of some of the simulations the objective function may prove hard to evaluate and optimize.

The MCS is a powerful tool, evaluating phenomena which can be characterized as probabilistic. The main idea behind the model is to form a representative sample of the system's behavior, by drawing and analyzing each state in order to evaluate the average values of the results and other parameters, and thus, deducing the system's behavior from the behavior of the sample.

The estimates that result from these studies, do so, not only delivering the reliability indices, as well as a confidence interval, plausible to obtain due to the computer-based simulation of the stochastic behavior of these mathematically modeled systems [12-13].

The main advantages that derive from using the MCS are:

- It allows us to use any probability distribution function;
- Easy to include dependency relations between events;
- Easily adjustable to any system alterations;

Despite the obvious advantages, this method can present as well some disadvantages:

- Great number of experiments, necessary to perform;
- If the study of each state proves to be complex, it may end up requiring a great computational effort, and in turn more computational time;

The MCS method, as previously said, can be divided in two approaches, classified according to how each system state is sampled. If the state's space representation is used then, we might call the MCS as non-sequential or non-chronological, in turn, if the state's sampling, is done following a chronology of the events such as those in figure (2.4), the method is called sequential or chronological. A more simplistic and metaphoric approach would be comparing the non-sequential MCS states to pictures, a collection of static images of the system in different moments, and the sequential MCS states chronology, as a film's timeline, in both methods each state is the aggregation of the states of each component [12-13].

The sequential MCS allows as well to integrate generating capacity from fluctuating or time dependent power sources such as renewable resources, which are modeled with uncertainty.

From a generic point of view, the MCS method consist of the following basic steps:

- Drawing the samples (states) to analyze;
- Analysis of the sample depending on the value to study;
- Preforming a convergence test to verify if the estimate possesses the required accuracy and quality;

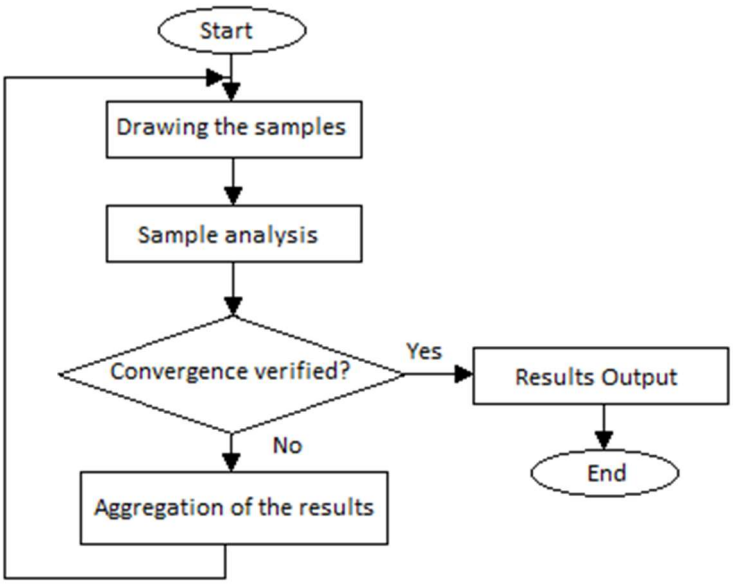


**Figure 2.7** - Generic algorithm for the MCS method

### 2.4.1. Non-sequential MCS method initialization

As previously stated the non-sequential MCS, draws each sample, as static images of the system's stochastic behavior, that being said, each components current state is completely independent from previous or future states [14].

The estimated reliability indices are mathematically calculated as

$$\hat{E}[H(X)] = \frac{1}{N}\sum_{i=1}^{N} H(x_i), \qquad \textbf{(2. 17)}$$

considering $X = [x_1, x_2, x_i, \ldots, x_n]$ to be a real vector, in which $x_1$, $x_2$, $x_3$, …, $x_n$, are the sampled system states, with N concerning the number of samples, and H being the test function every state is submitted, $H(x_i)$ will be the outcome in the following terms

$$H(x_i) = \begin{cases} 1 & if \quad x_i \in S_{Xf} \\ 0 & if \quad x_i \in S_{Xs} \end{cases}, \qquad \textbf{(2. 18)}$$

where, $S_{Xf}$ and $S_{Xs}$ are respectively all the failure states and the success states.

### 2.4.2. Sequential MCS method initialization

The sequential approach, requires more information, it's no longer sufficient knowing the component's FOR, it's now necessary to know the PDF functions associated with the time to failure and time to repair. If we assume exponential distributions these will be characterized by the failure and repair rate [11].

It's also necessary to have a model for the load fluctuation based on a forecast, it can consist of a deterministic load curve, with no uncertainty, that must be chronological, in other words it can no longer be an accumulated load diagram, otherwise it might as well be a load forecast with a probabilistic model or uncertainty.

The generation of a random time value t normally distributed (Gaussian function), is done, firstly by evenly drawing a value y in [0,1], and then intersecting from the Y-axis the distribution curve, we find the correspondent value of t, due to the exponential character of the function,

$$F(t) = \left(1 - e^{-\lambda t}\right) = y\,, \qquad \textbf{(2. 19)}$$

it's possible to resort the inverse function,

$$t = F^{-1(y)} = -\frac{1}{\lambda}\log(1-y). \qquad \textbf{(2. 20)}$$

As so this allows us to evenly distribute in [0,1] and immediately calculate the exponential distributed value of y.

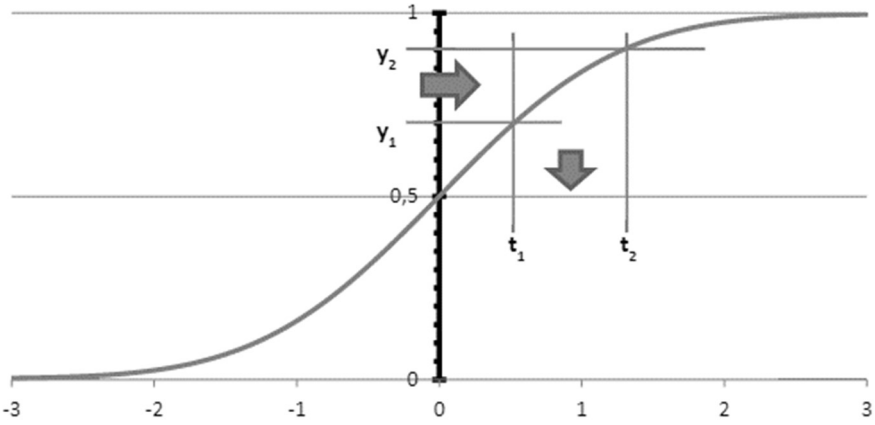


**Figure 2.8** - Values of t distributed according to the Gaussian distribution, following the reverse function of the evenly drawn values of y [11]

Consequently, all the simulated lifecycles are aggregated to create the system lifetime, which in turn will be evaluated every step of the way to see if the systems composition is enough to supply the respective load in that moment, to guarantee each component resides in 2 states (on and off). The timeline simulation is done by chaining successively drawn times to failure and times to repair [14]. The estimated reliability indices are mathematically calculated as

$$\hat{E}\left[H(X)\right] = \frac{1}{N}\sum_{i=1}^{N} H\left(\{x_n\}_{n=1}^{S_i}\right), \qquad \textbf{(2. 21)}$$

considering $\{x_n\}_{n=1}^{Si} = \{x_1, x_2, x_i, \dots, x_{Si}\}$ , $S_i \in \mathbb{N}$, is the chronologically sampled system states x, concerning the period *i*, with N the number of periods simulated, and H being the test function every state is submitted, the outcome will be in the following terms

$$H\left(\{x_n\}_{n=1}^{S_i}\right) = \frac{1}{T}\sum_{n=1}^{S_i} d(x_n) \times H\left(x_n\right). \qquad \textbf{(2. 22)}$$

where $x_n$ is the $n^{th}$ state of the sequence, *T* is the total duration of the simulated period (typically *T* = 8760 h), *d* ($x_n$) is the duration of the state $x_n$ and *H* ($x_n$) is the outcome of (2.18) with $x_n$ as argument.

### 2.4.3. MCS method convergence

In the MCS, we estimate $E[H]$, from equations (2. 16) and (2. 20), depending on the simulation approach, however $\hat{E}[H]$, is an estimate and not the "real" expected value $E[H]$, which is unknown. As in most sampling processes, the average sample value, distributes itself around the "real" value in such way that the uncertainty of the estimate may be represented as a variance $V(\hat{E}[H])$ of the estimator [11]:

$$V(\hat{E}[H]) = \frac{V(H)}{N}, \qquad \textbf{(2. 23)}$$

where $V(H)$ is the real variance of H, as this one is also unknown, we resort to an unbiased estimator, given by,

$$\hat{V}(H) = \frac{1}{N-1}\sum_{i=1}^{N}\left[H(x_i) - \hat{E}[H]\right]^2. \qquad \textbf{(2. 24)}$$

As shown in the equation above (2. 23), we can interpret the uncertainty in the $\hat{E}[H]$ estimate, reversely proportional to the sample dimension N. In order to limit this uncertainty, we can establish a convergence criterion to stop the MCS, through the definition of a relative uncertainty, based in the variation coefficient designated as ß, such that

$$\beta^2 = \frac{V(\hat{E}[H])}{(\hat{E}[H])^2}, \qquad \textbf{(2. 25)}$$

rearranging the equation, to putting N in evidence, and substituting $V(\hat{E}[H])$, we arrive to the following expression

$$N = \frac{V(H)}{\left[\beta \times \hat{E}[H]\right]^2}. \qquad \textbf{(2. 26)}$$

Through the above expression we can finally arrive to the conclusion that, for a given precision of the estimate's ß, to decrease the number of drawings N, or the size of the sample, we must first reduce $V(H)$.

This forms the conceptual basis of the variance reduction schemes which aim to reduce the computational effort involved in the calculation of an estimator, for a given predefined accuracy ß.

### 2.4.4. Confidence interval

Knowing the variance $V(E[H])$, allows us to easily estimate a confidence interval (CI) for $\hat{E}[H]$, and that means, there is a given probability the calculated interval contains the exact value we are looking for. Based in the central limit theorem [16], that states the sum of independent identically distributed variables

$$Z = \frac{\sqrt{N}}{\sigma}\left(\left(\sum_{i=1}^{N} H(\mathrm{x}_i)\right) - \mu\right), \qquad \textbf{(2. 27)}$$

tends towards the normal (Gaussian) distribution N (0,1) with average μ=0 and a variance $\sigma^2$=1, as it can be seen in figure (2.9), with a symmetric interval centered in 0 and with a half-width of two standard deviations, corresponding to a probability possible of calculating through the integral of the respective PDF:

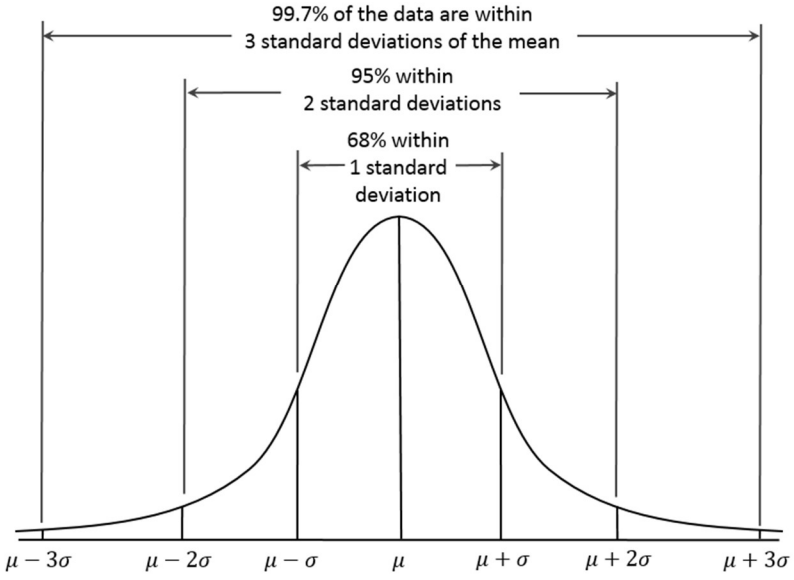


**Figure 2.9** - Normal Distribution N (0,1)

For any real positive value Z, it's possible to find the opposing values (+z) and (-z), between which Z lies with a certain probability 1-α,

$$P(-z \le Z \le z) = 1 - \alpha, \qquad \textbf{(2. 28)}$$

the number z can be obtained via the cumulative probability distribution as,

$$\Phi(z) = P(Z \le z) = 1 - \alpha/2 \Rightarrow z = \Phi^{-1}(1 - \alpha/2), \quad \textbf{(2. 29)}$$

therefore, determining a confidence interval CI for $\hat{E}[H]$, in a MCS method, originates:

$$CI(1-\alpha) = \left[ \hat{E}[H] - \Phi^{-1}(1-\alpha/2)\frac{\hat{\sigma}}{\sqrt{N}}, \hat{E}[H] + \Phi^{-1}(1-\alpha/2)\frac{\hat{\sigma}}{\sqrt{N}} \right]. \quad \textbf{(2. 30)}$$

For example, defining a variation coefficient ß=0,05 or 5%, and CI=95%, the confidence interval is:

$$CI(95\%) = \left[ \hat{E}[H] - 1{,}96\frac{\hat{\sigma}}{\sqrt{N}}, \hat{E}[H] + 1{,}96\frac{\hat{\sigma}}{\sqrt{N}} \right]. \quad \textbf{(2. 31)}$$

## 2.5. Modeling Generating System Components

### 2.5.1. Conventional Generating Units

Conventional generating units are still the more common source of energy, mostly composed of thermal energy conversion units, commonly based of fossil-fuel, such as petroleum, natural gas and charcoal, but also derived from nuclear sources conversion through thermodynamic cycle [14].

These unit's failure/repair state cycles can be easily represented by the Markov model for a two state component, with the enabled state representing the fully functional operating unit with maximum capacity, and the disabled sate as the opposite. However, there may be some cases in which a component might not be in any of those two states, but instead in a "partial damaged" state, in which the unit is operating at a percentage of its total capacity and therefore not fully operational neither disabled.

### 2.5.2. Hydro Generating Units

Hydro generating units nowadays occupy a considerable percentage of the any country's generating system. These units convert the potential energy of the water to electric energy, through controlling the volume of water and the fall distance that interact with the dam's generators, as such, they can also be modeled the same way as the conventional generating units,

However, the capacity time-dependent model for these units, is complex, due to the ties with the reservoir storage, weather, and the inflows. One simple yet crude approach, is to resort to hydrological series, historical recordings, in order to forecast the production each month. Doing this by capturing the proportional relation between the reservoir availability and the energy produced [17-18]. Therefore, modeling these units' in the sequential MCS can be easily done with the hydrological series, due to the chronological nature of the method.

### 2.5.3. Wind Farms

Wind farms consisting of an aggregation of multiple independent wind turbine generators, convert the kinetic energy of the wind to electricity. Assuming all the wind generators to be equal within a farm, allows us to model such power source using the multi-state Markov model, as pictured below, with each transition following an exponential distribution [14],

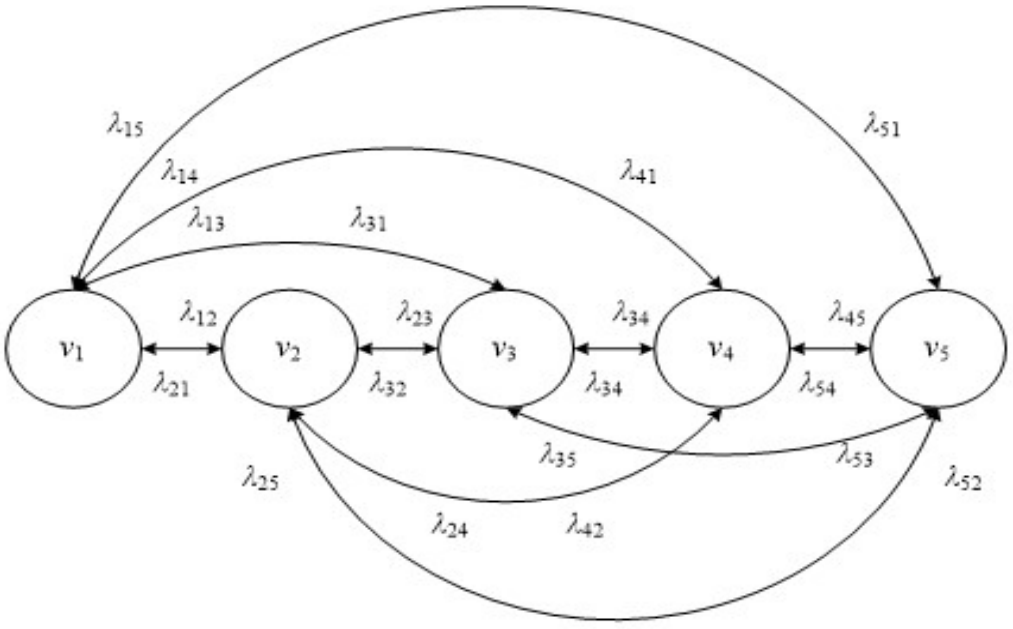


**Figure 2.10** - Multi-state Markov chain for modeling the wind speed with transitions between non-adjacent states [14].

As with the hydro generating units, these units follow a capacity time-dependent model, with the aid of the historical records for hourly wind series, which capture the hourly production in a percentage of the total capacity. It's possible to integrate them in the MCS method without any trouble, mainly, due to the needlessness to build spatial and time correlation models, since these correlations are included in the historical recordings, and naturally integrated in the simulation timeline.

### 2.5.4. Transmission Lines and Transformers

Assuming the operating limits are constant these components are also modeled by the Marko model for two state component with transitions that follow an exponential distribution [14].

### 2.5.5. Load

Loads are often modeled using a chronological representation with fluctuating load levels for every hour of the year, forecast uncertainties can also be introduced in the model through normal distribution [16], with a probability for each forecast scenario.

The chronological nature of the load, also allows for an easy integration with the sequential MCS, which follows the load level throughout the simulation period matching them with the respective available capacity to determine if the load shedding occurs, adding to this, each load bus has its own hourly load profile in percentage of its peak load, obtained by dividing the peak load of that hour by the peak load of the year.

## 2.6. Simulation Algorithm

The algorithm for the sequential MCS method for the HL1 reliability assessment follows the next few steps [14]:

1. Defining the initial parameters, maximum simulation period, $N_{MAX}$, the relative uncertainty ß, initialize the counters time, $h=0$, and $N_{YEAR}$ =1;
2. Update the simulation time: h: = h + 1;
3. Select a system state (select the availability of the components according to their stochastic failure/repair cycle model and the capacity time-dependent model, select the load level, etc.)
4. Evaluate the system state selected (compose the state and check if the load level can be supplied with the available generating and/or transmission capacity without violating

operating limits; If not, apply remedial actions, such as generation re-dispatch and/or load shedding)

5. Update the outcome of the test functions of the reliability and other indices
6. If $h$ = 8760, store the reliability indices, update their relative uncertainty ($\beta$), and advance, if not, go back to step 2
7. If $N_{YEAR}$ is equal to $N_{MAX}$ or if the relative uncertainties of the reliability indices are less than the specified tolerance, stop the simulation; otherwise, $N_{YEAR} = N_{YEAR} + 1$, $h$ = 0, and go back to step 2

## 2.7. Convergence Accelerators

As seen before, it's possible to decrease the computational effort and the number of samples, maintaining the same precision ß, and the expected value $\hat{E}[H]$, only by diminishing the variance $V(H)$. The following paragraphs describe two effective techniques to accelerate the MCS convergence [11].

### 2.7.1. Control Variable

This method assumes it's possible to calculate a value approximate to the real one which we wish determine, through an analytical method independent from the MCS. For instance, if we wish to determine the LOLP of a composite system, we can perceive that $LOLP_g$, calculated considering only the generating system, may be an approximation to the correct value of the compound system and even some well-correlated manner with him [11] [14].

The MCS will only be used to calculate the difference between both values. In order to insure that the convergence is effective, it's imperative, considering we wish to achieve a quick convergence speed, choosing a highly correlated value with the solution of the problem, a correct control variable, therefore.

Considering Z as a random variable with the result deriving from the approximate analytic model, and that is strongly correlated with H (LOLP), we may define this new auxiliary random variable Y as,

$$Y = H - r \times (Z - E[Z]), \qquad \textbf{(2. 32)}$$

where r is a real parameter, as said before it's easy to prove that Y and H have the same expected value, and the variance is as follows:

$$E[Y] = E[H] - r \times (E[Z] - E[E[Z]]) = E[H], \quad \textbf{(2. 33)}$$

$$V(Y) = V(H - rE(Z)), \quad \textbf{(2. 34)}$$

with $rE(Z)$ as a scalar,

$$V(Y) = V(H) - 2rC(H,Z) + r^2 V(Z), \quad \textbf{(2. 35)}$$

$C(H,Z)$ is the covariance between H and Z, the theoretical value of r that minimizes $V(Y)$ may be obtained with the derivative of the right member of equation (2.34) equating to zero,

$$2rV(Z) - 2C(H,Z) = 0. \quad \textbf{(2. 36)}$$

Substituting $r = \frac{C(H,Z)}{V(Z)}$ in the expression above we have,

$$V(Y) = V(H) - \frac{C^2(H,Z)}{V(Z)}, \quad \textbf{(2. 37)}$$

now $C^2(H,Z)$ is, by definition, equal to $\rho^2 V(H) V(Z)$, in which ρ is the correlation coefficient between H and Z, then

$$V(Y) = (1 - \rho^2) \times V(H). \quad \textbf{(2. 38)}$$

If Z and Y are correlated, $V(Y)$ will be less than $V(H)$, as Y and H have the same expected value, $E[H]$ may be estimated in a more efficient manner by sampling Y than F,

$$\hat{E}(H) = \frac{1}{N^*} \sum_{i=1}^{N^*} Y_i, \quad \textbf{(2. 39)}$$

in which N* is the new number of system state drawings, necessary and smaller than N, the reason between N/N* is the acceleration measure introduced by the control variable

$$\frac{N}{N^*} = \frac{1}{1-\rho^2}. \qquad \textbf{(2. 40)}$$

This result shows that the more correlated are the variable that is intended to estimate and the analytical value calculated, the greater the acceleration introduced by the method.

### 2.7.2. Importance Sampling

This technique is based in the distortion of the probability distribution of $x_i$, in turn distorting $H(x_i)$ and increasing the probability of occurrence of rare events, such as Loss of Load. Like the control variable this method aims to reduce the variance without perturbing the expected value.

Recalling that the probabilistic analysis of a power systems can be seen as determining the expected value of the analysis function of the system states, such that [11] [14],

$$E[H] = \frac{1}{N}\sum_{i=1}^{N} H(x_i) f(x_i), \qquad \textbf{(2. 41)}$$

where $f(x_i)$ is the probability distribution function, if we consider $g(x_i)$ the distorted PDF, calculated through the next expression,

$$g(x_i) = f(x_i) + k \cdot [1 - f(x_i)], \qquad \textbf{(2. 42)}$$

K represents the acceleration coefficient, and directly affects the method's efficiency, therefore is required to choose an adequate value. Now, multiplying and dividing the interior of the summation in equation (2. 40) by $p'(x_i)$ we can rewrite it as:

$$E[H] = \frac{1}{N}\sum_{i=1}^{N} H(x_i)\frac{f(x_i)}{g(x_i)} g(x_i). \qquad \textbf{(2. 43)}$$

Now the system state's sampling will follow the probabilistic distribution of $g(x_i)$, as previously mentioned this too doesn't affect the expected value however it can considerably reduce the variance,

$$V(H) = \frac{1}{N-1}\sum_{i=1}^{N}\left[H(x_i)\frac{f(x_i)}{g(x_i)} - E[H]\right]^2 . \quad \textbf{(2. 44)}$$

Theoretically speaking, there is a value of $g(X)$, that could render the variance as zero,

$$g^*(X) = \frac{H(X)}{LOLP} f(X), \quad \textbf{(2. 45)}$$

However, such value would require of us to know the exact value $LOLP = E[H]$ which we wish to estimate, creating a circular reference in the calculus, $E[H]$may now be estimated in a more efficient manner by sampling $g(x_i)$ than $f(x_i)$ resulting,

$$\hat{E}[H] = \frac{1}{N'}\sum_{i=1}^{N^*} H(x_i)\frac{f(x_i)}{g(x_i)}, \quad \textbf{(2. 46)}$$

in which N* is the new number of system state drawings, necessary and smaller than N, due to the acceleration introduced by the distorted distribution $g(x_i)$.

# Chapter 3

# Sequential Monte Carlo with Kullback-Leibler Cross-Entropy

This chapter introduces the Kullback-Leibler (KL) cross-entropy (CE) method currently used and its integration with the MCS method and importance sampling and the respective algorithms. Introduces the test systems used in the validation of the crude Monte Carlo estimates for different peak reductions factors as well as for the CE and finally offering an analysis and comparison between methodologies.

## 3.1. Kullback-Leibler Cross-Entropy

The cross-entropy (CE) method main algorithm is an alternative approach based on the Kullback-Leibler cross-entropy, that aims to find the "optimal" distribution distortion, known as g*(x), which derives from equations (3. 1) and (3. 2) as such [8] [19-20]:

$$g^*(X) = \frac{H(X) \times f(X)}{LOLP}, \tag{3. 1}$$

therefore, we have:

$$LOLP = H(X) \times \frac{f(X)}{g^*(X)}. \tag{3. 2}$$

As it stands, the obvious problem is that $g^*(X)$ depends on the same parameter we wish to estimate (LOLP), as so, if we consider $g(X) = f(X;v)$, the idea now would be to choose the reference parameter v such that the distance between densities $g^*(X)$ and $f(X;v)$ is minimal.

A particular measure of distances between two probability density functions (PDF), deriving from the Shannon entropy information theory, is the Kullback-Leibler Divergence, which can also be called the Cross-Entropy between two PDF [19]. The Kullback-Leibler Divergence is defined as:

$$D_{KL}(g^*,g) = E_f\left[\ln\frac{g^*(X)}{g(X)}\right], \quad \textbf{(3. 3)}$$

$$D_{KL}(g^*,g) = \int g^*(X)\ln g^*(X)dx - \int g^*(x)\ln g(x)dx\,. \quad \textbf{(3. 4)}$$

The Kullback-Leibler Divergence result cannot be perceived as a real "distance" in the formal sense, because it's not symmetric: $D_{KL}(g^*,g) \neq D_{KL}(g,g^*)$, even so recalling that, $D_{KL}(g^*,g) \geq 0$, with equality only possible with $g^* = g$.

Considering the minimization of the *Kullback-Leibler Divergence,* $\min_g D_{KL}(g^*,g)$ the problem should focus on the right branch of equation (3. 4), more specifically the second integral, which means, in order to minimize the "distance" we have to maximize the following integral:

$$\max_v \int g^*(x)\ln g(x)dx\,. \quad \textbf{(3. 5)}$$

Once again assuming our $g^*(x)$ as the optimal distortion and replacing it in equation (3. 5), we have:

$$\max_v \int \frac{H(x)\times f(x)}{LOLP}\ln g(x)dx\,, \quad \textbf{(3. 6)}$$

Substituting $f(x)$ with $f(x;u)$ and $g(x)$ with $f(x;v)$, which refer to the binomial probability density functions with the probability vectors **u** and **v**, we obtain the following maximization problem:

$$\max_v \int \frac{H(x)\times f(x;u)}{LOLP}\ln f(x;v)dx\,, \quad \textbf{(3. 7)}$$

which is equivalent to:

$$\max_{v} D_{KL}(v) = \max_{v} E_u\left[H(X)\ln f(X;v)\right]. \quad \textbf{(3. 8)}$$

Once again the rare nature of the event raises problems, in the drawings used in the CE Method, the instances where the load shedding occurs are still too few. Therefore, we use again importance sampling with a different distribution $f(x;w)$, equation (3. 8) can be rewritten as:

$$\max_{v} D_{KL}(v) = \max_{v} E_w\left[H(X)\frac{f(X;u)}{f(X;w)}\ln f(X;v)\right], \quad \textbf{(3. 9)}$$

and thus the solution to equation (3. 9) may readily be calculated as:

$$\frac{1}{N}\sum_{i=1}^{N} H(X_i)W(X;u,w)\nabla \ln f(X;v) = 0\,, \quad \textbf{(3. 10)}$$

with

$$W(X;u,w) = \frac{f(X;u)}{f(X;w)}. \quad \textbf{(3. 11)}$$

The obvious main advantage of this approach is that it provides us with a solution plausible to calculate analytically, which occurs in particular when the random variables distribution belongs to the natural exponential family (NEF) [8] [19].

If the rare event probability is too small, the program may present some difficulties, namely if said probability hits values below $10^{-5}$, therefore we must resort to a multi-level iterative algorithm in order to surpass this difficulty [20].

### 3.1.1. Main Kullback-Leibler CE Algorithm for Rare Event Simulation

The main CE algorithm for rare event simulation, is a multi-level algorithm developed to overcome the difficulty of rare event simulation, such as the case in study, the load shedding. The main idea behind this algorithm is to construct a sequence of reference parameters $\{v_t,\ \ t \geq 0\}$ and levels $\{\gamma_t,\ \ t \geq 1\}$ and iterating upon them [14] [8].

The algorithm's initialization starts by following the next steps:

1. Define a ρ = 10%, $v_0 = u$, the target load $\gamma = L_{peak}$ and set the iteration counter t = 1;
2. Generate a sample $\mathbf{X_i}$, …, $\mathbf{X_n}$ from the PDF $f(X_i; v_{t-1})$;
3. Evaluate $S_{(X_i)}$ for all samples, where $S_{(X_i)}$ is the total generating capacity of each Xi sample;
4. Compute the sample $(1-\rho)$-quantile $\hat{\gamma}_t$ of the performances according to:

$$\hat{\gamma}_t = \begin{cases} S_{\{(1-\rho)N\}} & if \quad \hat{\gamma}_t < \gamma \\ \gamma & if \quad \hat{\gamma}_t > \gamma \end{cases}. \qquad \textbf{(3. 12)}$$

5. Calculate the corresponding LOLP, $H(X_i)$;
6. Calculate $W(X_i; u; v_{t-1})$ with,

$$W_i(\mathrm{X}_i; u; v_{t-1}) = \frac{\prod_{j=1}^{N} \left(1-u_j\right)^{x_{ij}} u_j^{\,n_j - x_{ij}}}{\prod_{j=1}^{N} \left(1-v_{t-1,j}\right)^{x_{ij}} v_{t-1,j}^{\,n_j - x_{ij}}} \qquad \textbf{(3. 13)}$$

Assuming the algorithm was correctly initialized the following step would be to solve the stochastic program:

$$\max_v D_{KL}(v) = \max_v \frac{1}{N} \sum_{i=1}^{N} H(X) W(X; u; w) \ln f(X; v), \qquad \textbf{(3. 14)}$$

however, equation (3. 13) requires further simplification, starting by solving the derivate PDF, as shown in (3. 10), in this particular case, the reliability assessment of the generating system, the probability density function corresponding to the Binomial Distribution is:

$$f(x_i; n_i; u_i) = \binom{n_i}{x_i} \times \left( (1-u_i)^{x_i} \times u_i^{\,(n_i - x_i)} \right), \qquad \textbf{(3. 15)}$$

with $x_i$ following a binomial distribution with parameters $n_i \in \mathbb{N}$ and $u_i \in [0,1]$, in this case $n_i$ represents the number of units within a generating group, upon solving the derivative,

$$\frac{\partial}{\partial v_j}\ln f(x;v) = \frac{1}{f(x;v)} f(x;v) \times \left( \frac{x_j}{v_j - 1} + \frac{n_j}{v_j} + \frac{x_j}{v_j} \right), \qquad \textbf{(3. 16)}$$

and integrating it in (3. 13), we should arrive at the following expression,

$$\frac{1}{N}\sum_{i=1}^{N} H(X_i)\, W(X_i;u;w) \left( \frac{x_j}{v_j - 1} + \frac{n_j}{v_j} + \frac{x_j}{v_j} \right) = 0, \qquad \textbf{(3. 17)}$$

which in turn with further simplification should provide us with step 7. the updating expression:

7. Update vector **v**, using the sample $\mathbf{X_i}$, …, $\mathbf{X_n}$:

$$v_{tj} = 1 - \frac{1}{n_j} \frac{\sum_{i=1}^{N} H(X_i) W(X_i;u;v_{t-1}) X_{ij}}{\sum_{i=1}^{N} H(X_i) W(X_i;u;v_{t-1})}; \qquad \textbf{(3. 18)}$$

8. If $\hat{\gamma}_t < L_{peak}$ , set t = t +1 and reiterate from step 2., else close the algorithm and return the final values of vector **v.**

## 3.1.2. Cross-Entropy Integration with the Sequential Monte Carlo

The MCS method can be easily depicted, through a block diagram, along with its integrated mechanics such as the variance reduction methods, control variable or importance sampling, and the Kullback-Leibler cross-entropy algorithm. The following picture depicts such diagram:

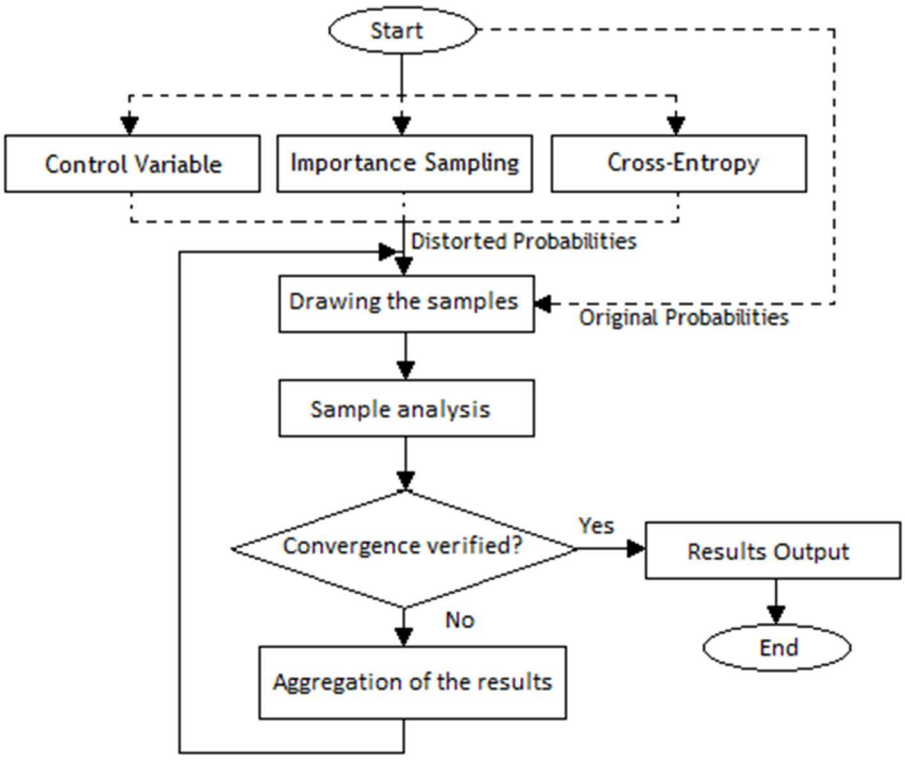


**Figure 3.1** – Block Diagram representing the Sequential Monte Carlo method, with the alternative integrated techniques for variance reduction, depicted with dashed lines.

## 3.2. Validation of the Sequential Monte Carlo Simulation

The accuracy of the MCS method was attained by assessment of the reliability for a generating system (HL1) for the test system IEEE RTS 79 [20]. The main aim of these experiments is to determine the proximity between the estimates of the reliability indices and the scientifically published results in the current literature.

### 3.2.1. Test System

The IEEE-RTS 79 was developed to fulfill the need for a standardized database to test and compare results between different adequacy assessment methods. This test system is composed of 24 buses, 32 generating units, 33 transmission lines and 5 transformers, with a total installed capacity is 3405 MW [14] [21].

The system load model consists of 8736 hourly peaks with an annual peak load of 2850 MW. The hourly system load is distributed among the respective load buses according to fixed percentages. The following figure depicts IEEE-RTS 79 single-line diagram.

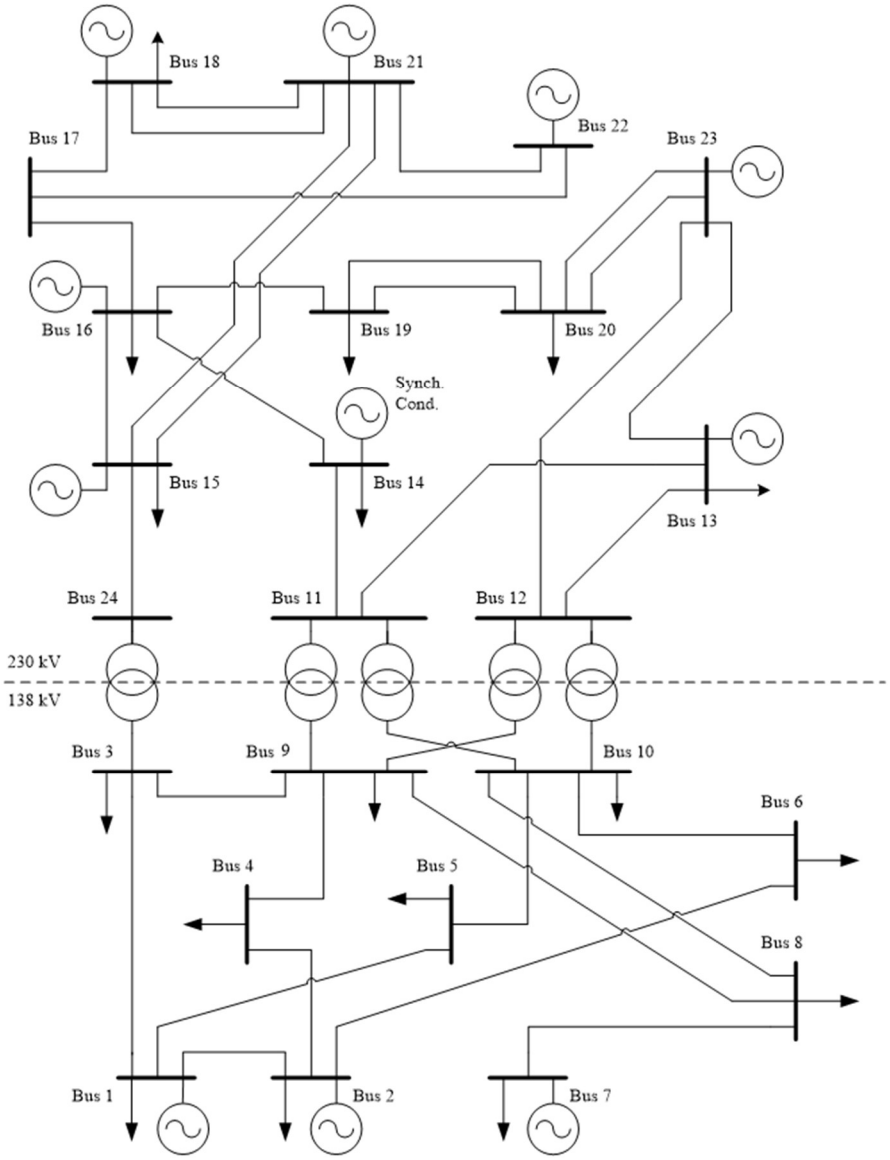


**Figure 3.2** - Single-Line diagram for the test system IEEE-RTS 79 [14]

Other test systems are available, such as the IEE-RTS 96 [22] which consists of three interconnected areas, each of them composed of a IEEE-RTS 79 system, with equal configuration, which in turn helps compose the IEEE-RTS 96 with a 10 215 MW total installed capacity distributed by 96 generating units, interconnected by 104 transmission lines and 16 transformers with an annual peak demand of 8550 MW [22]. Although all of this works tests have been conducted with the IEEE-RTS 79 system, the algorithm should function properly for all systems depending on a few adjustments.

### 3.2.2. IEEE-RTS 79 Generating System

The IEEE-RTS 79 consists of 32 units totalizing an installed capacity of 3405 MW. The load model consists of 8736 hourly levels with a peak load of 2850 MW. Table 3.1 shows the different generation groups that can be formed along with their respective capacities and unavailability.

**Table 3.1** – IEEE-RTS 79 generating system [14].

| Group | Unit Size (MW) | $u_i$ | No. of Units |
|---|---|---|---|
| | | | IEEE-RTS 79 |
| 1 | 12 | 0.02 | 5 |
| 2 | 20 | 0.10 | 4 |
| 3 | 50 | 0.01 | 6 |
| 4 | 76 | 0.02 | 4 |
| 5 | 100 | 0.04 | 3 |
| 6 | 155 | 0.04 | 4 |
| 7 | 197 | 0.05 | 3 |
| 8 | 350 | 0.08 | 1 |
| 9 | 400 | 0.12 | 2 |
| Total | | | 32 |

As it can be seen above, the groups represent a well distributed generation, with multiples generating units in each groups with small capacity and small unavailability's, with the exception for group 7, 8 and 9 which consist of bigger units with bigger capacities, representing approximately 50% of the total installed capacity, as a result the MCS will be facing a diverse and well composed generating system.

### 3.2.3. Generating System Results

Integrating test system IEEE-RTS 79 in to the sequential MCS in order to test its efficiency resulted in the following estimates of the LOLE, EENS and the LOLF as the simulation's outcome, as can be seen in Table 3.2:

**Table 3.2** – Crude Sequential MCS (SMCS) Generating System Reliability Indices Results for IEEE-RTS 79 [14]

| IEEE-RTS 79 | LOLE (h/year) | EENS (MWh/year) | LOLF (occ./year) |
|---|---|---|---|
| Analytical | 9.394 | 1176.30 | 2.025 |
| Crude Sequential MCS | 9.370 | 1163.00 | 2.024 |
| Β (%) | 0.70 | 1.00 | 0.56 |
| 99% Interval of Confidence | [9.201, 9.538] | [1132.99, 1193.00] | [1.994, 2.053] |

The results provided by an analytical method [9], were assumed as a basis for comparison of the SMCS method estimates. Contrarily to the SMCS, enumeration methods calculate the exact value of the reliability indices, however as show in Table 3.2 the estimates almost equal to the reliability indices analytically calculated, with all three within their respective confidence interval and respecting their coefficient of variation. These results prove that the SMCS can accurately assess the reliability of small size generating systems.

## 3.3. Crude Sequential Monte Carlo Simulation Results

The Sequential Monte Carlo Simulation Method can be dubbed crude, due to the lack of any variance reduction mechanism integrated within the method. Therefore, number of iterations (simulated years) and time it takes to converge can be frustratingly too much and too slow. The following table presents the results obtained with the crude SMCS for different values of peak reduction factor, what this does is regulate the simulations peak demand by a percentage of its maximum peak.

**Table 3.3** – Crude SMCS results for IEEE-RTS 79 with different peak reduction factors.

| Peak Reduction | Peak Demand MW | Simulated Years | LOLE (h/year) | EENS (MWh/year) | LOLF (occ./year) |
|---|---|---|---|---|---|
| 0.6 | 1710 | 10 000 + | 0 | 0 | 0 |
| | β (%) | | 100 | 100 | 100 |
| 0.7 | 1995 | 10 000 + | 0.0023 | 0.0915 | 0.0008 |
| | β (%) | | 39.37 | 41.39 | 35.34 |
| 0.8 | 2280 | 10 000 + | 0.0848 | 6.0577 | 0.0259 |
| | β (%) | | 11.15 | 15.49 | 9.12 |
| 0.9 | 2565 | 10 000 + | 1.3285 | 131.31 | 0.3145 |
| | β (%) | | 3.89 | 5.34 | 3.24 |
| 1 | 2850 | 2133 | 9.0734 | 1099.3 | 1.9816 |
| | β (%) | | 4.99 | 3.65 | 2.99 |

As shown in the table above, the values were calculated for a max of 10 000 simulated years or a coefficient of variation of 5%. It's possible to observe the presence of a dependency between the peak reduction factors and the number of simulated years in order for the crude sequential MCS to converge, which takes a considerable number of years for smaller values of peak demand.

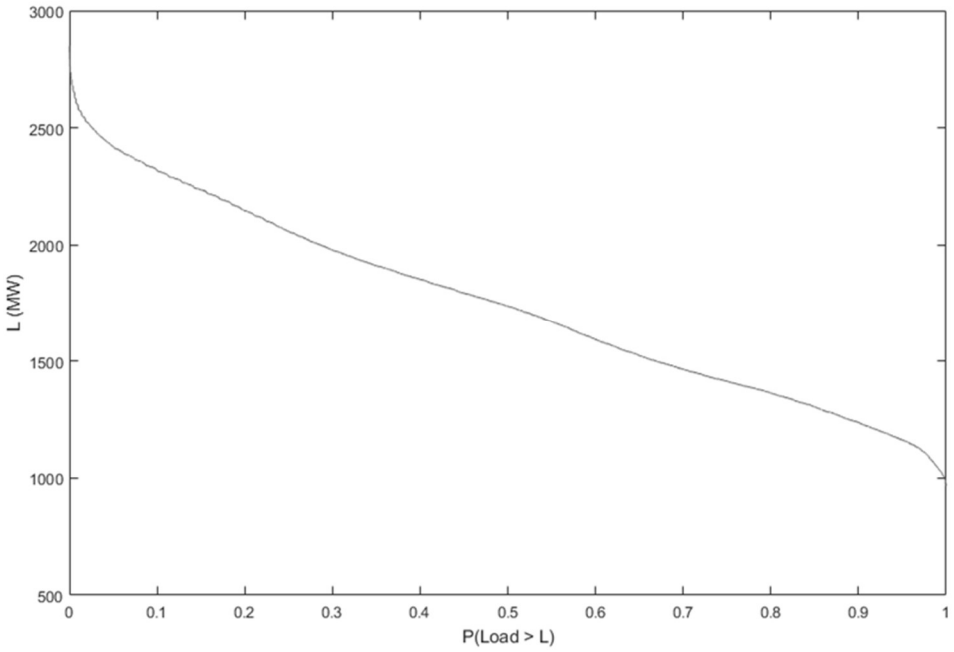


**Figure 3.3** – Load cumulative distribution diagram

Although we will mostly be using the targeted peak demand to calculate the distortions due to the different peak reduction factors, figure 3.3 clearly shows that the load is annual

The smaller values of peak reduction, result in lower values for peak demand, as such the load shedding occurrences drop, as such the method requires more years simulated with load shedding to estimate the indices with the required accuracy. This happens because the variance of each iteration is too high. Therefore, the need for variance reduction mechanism such as the control variable, importance sampling or even the cross-entropy method.

## 3.4. Sequential MCS with Kullback-Leibler Cross-Entropy

As seen in Table 3.3 the crude sequential MCS is able to accurately estimate the reliability indices for different peak reduction factors. However, the number of simulated years required to achieve the intend precision and converge is considerable, thus the necessity for introducing variance reduction techniques, in this case the Kullback-Leibler cross-entropy method will be the choice due to the nature of this work revolving around it.

Similar setup as the one used for the simulations in Table 3.3 was followed, however more new parameters were chosen for the cross-entropy, mainly the number of samples fixed at 10 000 which was deemed enough, and an often used quantile value of $\rho$=0.1, to control the CE's convergence, as such the following results were obtained.

**Table 3.4 -** SMCS with CE results for IEEE-RTS 79 with different peak reduction factors.

| Peak Reduction | Peak Demand MW | Simulated Years | LOLE (h/year) | EENS (MWh/year) | LOLF (occ./year) |
|---|---|---|---|---|---|
| 0.6 | 1710 | 55 | 0.0001 | 0.0029 | 1.8E-05 |
| | β (%) | | 4.33 | 4.37 | 4.84 |
| 0.7 | 1995 | 45 | 0.0034 | 0.2291 | 0.0010 |
| | β (%) | | 4.69 | 4.93 | 4.84 |
| 0.8 | 2280 | 2 | 0.1184 | 9.4375 | 0.0276 |
| | β (%) | | 2.75 | 1.97 | 4.67 |
| 0.9 | 2565 | 37 | 1.2373 | 124.70 | 0.2972 |
| | β (%) | | 4.01 | 4.21 | 4.99 |
| 1 | 2850 | 38 | 8.7496 | 1097.0 | 1.8555 |
| | β (%) | | 4.53 | 4.98 | 4.07 |

Once again it's possible to observe that the sequential MCS was able to accurately estimate the reliability indices for the preset coefficient of variation of 5%. However, its most noticeable change resides in the number of simulated years towards convergence, which reduced drastically compared to the crude SMCS. Nonetheless, keeping the estimate reliability indices intact, this results from the distortion calculated in the cross-entropy, which allows for more load shedding occurrences.

**Table 3.5** - Distorted availability introduced by the cross-entropy for different peak reduction factors

| | Group | Peak Reduction Factor | | | | | Original |
|---|---|---|---|---|---|---|---|
| | | 0.6 | 0.7 | 0.8 | 0.9 | 1 | $u_i$ |
| Distortion $v_i$ | 1 | 0.02 | 0.03 | 0.02 | 0.02 | 0.02 | 0.02 |
| | 2 | 0.13 | 0.12 | 0.12 | 0.11 | 0.12 | 0.10 |
| | 4 | 0.05 | 0.06 | 0.03 | 0.04 | 0.03 | 0.02 |
| | 5 | 0.12 | 0.13 | 0.06 | 0.10 | 0.06 | 0.04 |
| | 6 | 0.29 | 0.19 | 0.10 | 0.11 | 0.09 | 0.04 |
| | 7 | 0.56 | 0.31 | 0.19 | 0.16 | 0.16 | 0.05 |
| | 8 | 0.98 | 0.90 | 0.71 | 0.51 | 0.31 | 0.08 |
| | 9 | 0.99 | 0.97 | 0.87 | 0.69 | 0.52 | 0.12 |
| | 3 | 0.02 | 0.02 | 0.01 | 0.02 | 0.01 | 0.01 |

Table 3.5 shows the distortion calculated using the Kullback-Leibler cross-entropy method, this distortion allows us to observe more load shedding occurrences, by adjusting the unavailability of each group. Having in consideration that this distortion must maintain a certain correlation with the original distribution in order to avoid changes in the estimates.

As it can be seen the distortion values are different for each peak reduction factor, this is because with smaller load peaks we must introduce more frequent failures or a bigger number of units failing to cause fail load shedding. Further analysis shows that the groups assigned with higher values of distortion for most cases are groups 7, 8 and 9 this can be easily attributed to them being the bigger

units, which, as said before represent approximately half of the total generating capacity, therefore raising their unavailability should result in more frequent load shedding occurrences.

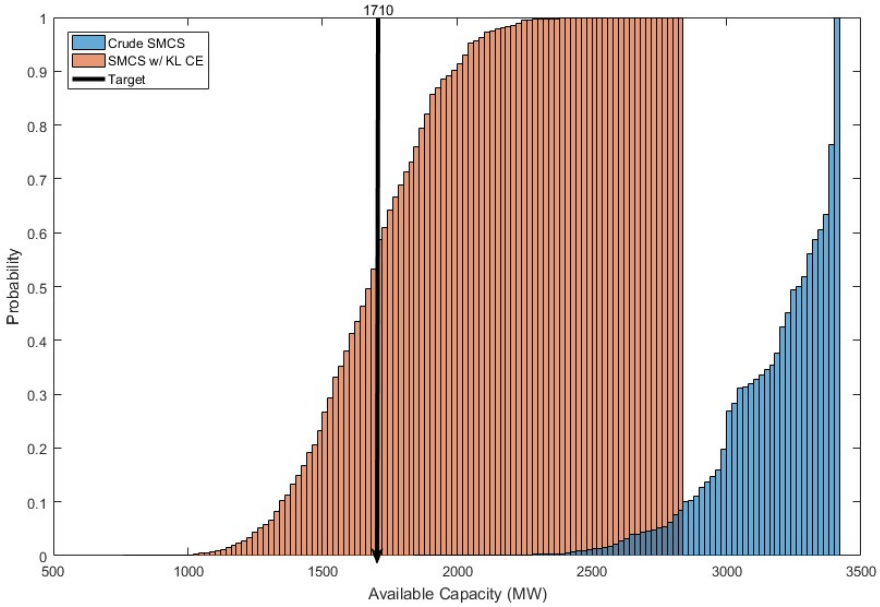


**Figure 3.4** – Capacity Outage Probability Table (COPT) histogram for 50 000 samples obtained the original FOR and the FOR with Kullback-Leibler distortion for a peak reduction factor of 0.6

Figure 3.3 shows the frequency of the available capacities for the SMCS with the Kullback-Leibler CE and with the crude SMCS. Contrary to the crude SMCS the distribution has more probability of being near the peak demand target of 1710, allowing for more load shedding occurrences, thus, reducing the variance of each iteration and accelerating the convergence, which in this case with a peak reduction factor of 0.6 and cross-entropy distortion takes precisely 38 simulated years to converge with a coefficient of variation of 5%. This represents approximately 1.78% of the original simulated years with the crude SMCS, and therefore an acceleration of the sequential MCS by approximately 5613.16%.

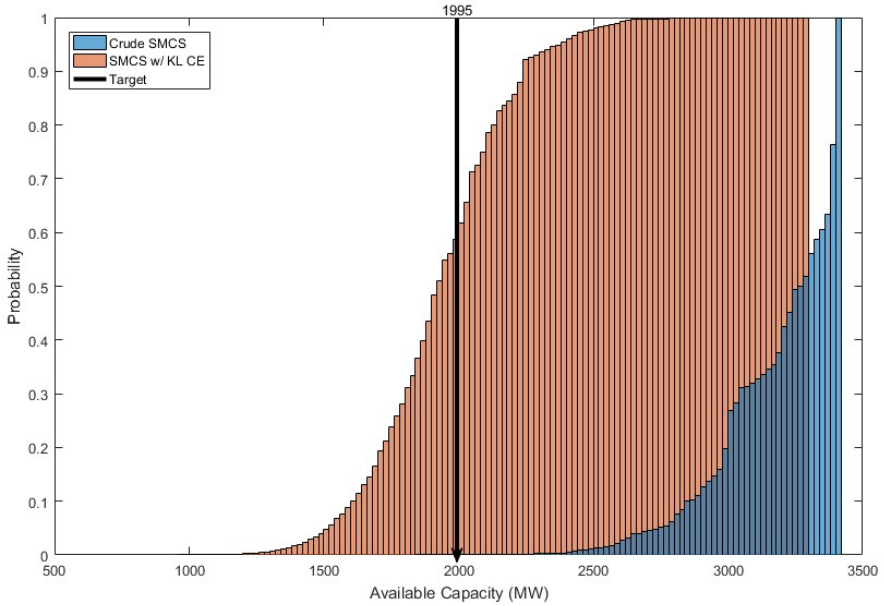


**Figure 3.5** - COPT histogram for 50 000 samples obtained the original FOR and the FOR with Kullback-Leibler distortion for a peak reduction factor of 0.7

Closer analysis of these figures frequency of available capacities with the original distribution, clearly shows most cases would never result in a load shedding due to approximately half of the available capacities being equal or higher than 3000, thus surpassing the maximum peak demand of 2850 with a peak reduction factor of 1. This explains the considerable number of simulated years needed by the crude SMCS in order to converge.

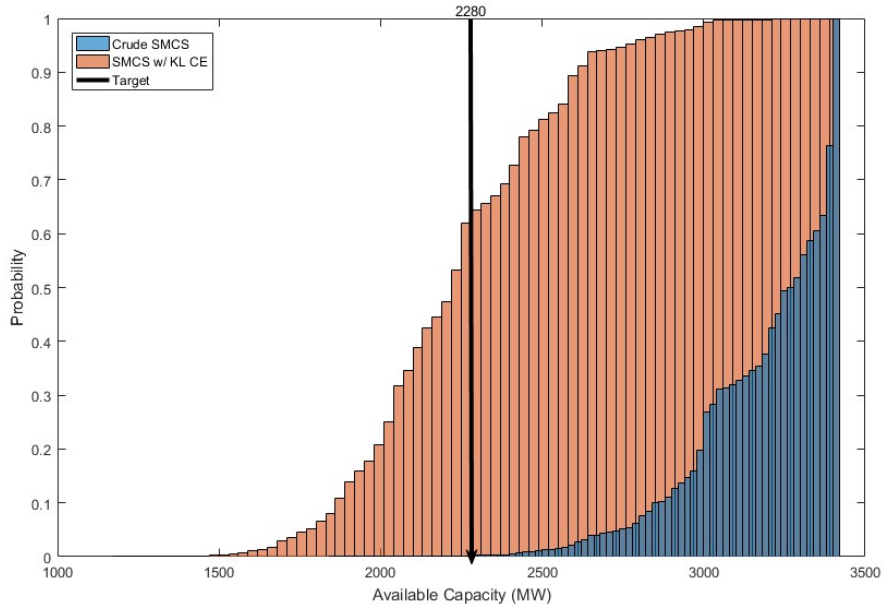


**Figure 3.6** - COPT histogram for 50 000 samples obtained the original FOR and the FOR with Kullback-Leibler distortion for a peak reduction factor of 0.8

Another closer inspection of figure 3.3, 3.4 and 3.5 shows that observing load shedding occurrences with peak reduction factors of 0.8 or smaller, corresponding to peak demands of ≤2280 it's nearly impossible for the original distribution.

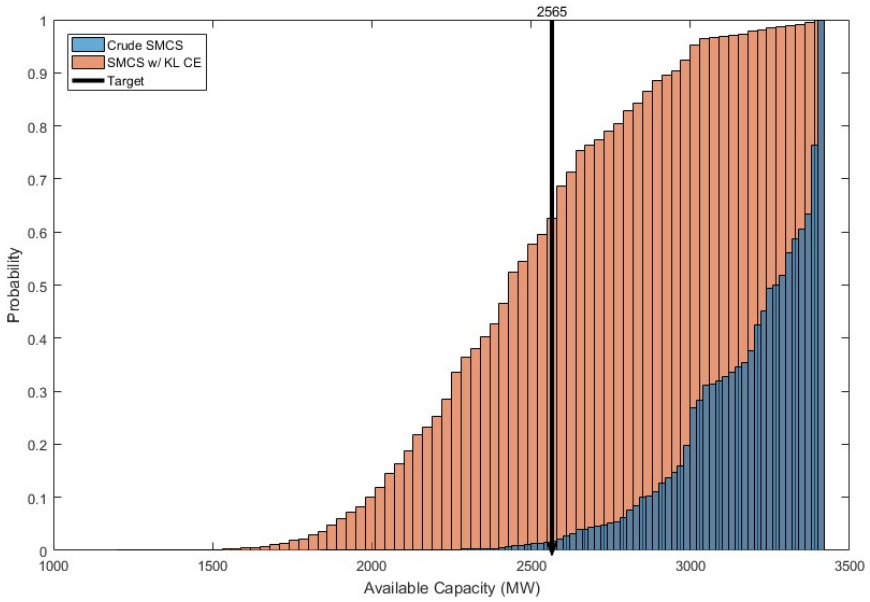


**Figure 3.7 -** COPT histogram for 50 000 samples obtained the original FOR and the FOR with Kullback-Leibler distortion for a peak reduction factor of 0.9

The distortion introduced by the Kullback-Leibler raises the probability of load shedding occurrences for all the different peak reduction factors to at least 50-60%, near the target load.

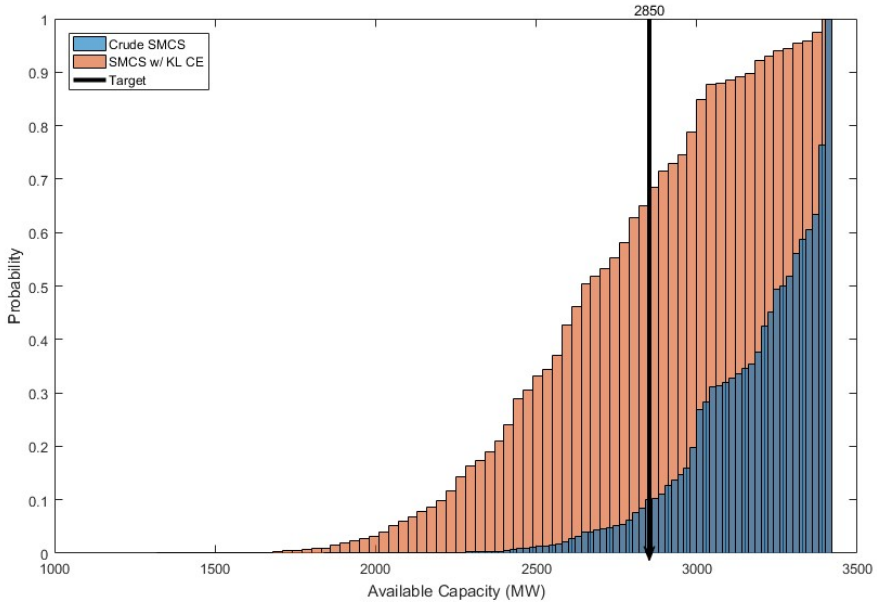


**Figure 3.8 -** COPT histogram for 50 000 samples obtained the original FOR and the FOR with Kullback-Leibler distortion for a peak reduction factor of 1.0

Although these particular figures were obtained for 50 000 samples, the sequential MCS draws each state in a continuous and alternate timeline simulation, which means the number of samples grows with the elapsing simulation. The following Table 3.6 shows the number of load shedding for each peak reduction factor with crescent numbers of samples.

**Table 3.6** – Number of load shedding occurrences for different peak reduction values and different number of samples for the original unavailability values

| Number of samples | Load shedding Occurrences for different Peak Reduction Values for the crude SMCS | | | | |
|---|---|---|---|---|---|
| | 0.6 | 0.7 | 0.8 | 0.9 | 1 |
| 10 000 | 0 | 0 | 17 | 152 | 812 |
| 25 000 | 0 | 0 | 47 | 386 | 2 100 |
| 50 000 | 0 | 8 | 86 | 790 | 4 260 |
| 100 000 | 0 | 8 | 185 | 1 496 | 8 412 |
| 250 000 | 0 | 15 | 453 | 3 705 | 21 215 |
| 500 000 | 0 | 34 | 937 | 7 489 | 42 325 |
| 1 000 000 | 3 | 100 | 1 993 | 15 298 | 84 696 |

Looking at the above Table 3.6, it's clear that without the distortion introduced by the CE method, it takes an almost immeasurable number of samples to observe load shedding occurrences for small values of peak reduction factor. Contrariwise to the distortion calculated for each peak reduction factor, the required number of samples in order to observe load shedding occurrences reduces drastically, with the distorted unavailability values insuring that at least approximately half of the samples result in load shedding.

**Table 3.7 -** Number of load shedding occurrences for different peak reduction values and different number of samples for the unavailability values with the distortion introduced by the CE method

| Number of samples | Load shedding Occurrences for different Peak Reduction Values for the SMCS w/ CE | | | | |
|---|---|---|---|---|---|
| | 0.6 | 0.7 | 0.8 | 0.9 | 1 |
| 10 000 | 5 721 | 5 825 | 6 206 | 6 061 | 6 472 |
| 25 000 | 14 309 | 14 472 | 15 563 | 15 319 | 16 350 |
| 50 000 | 28 809 | 29 396 | 31 040 | 30 654 | 32 927 |
| 100 000 | 57 568 | 58 375 | 62 195 | 61 564 | 65 265 |

# Chapter 4

# Sequential Monte Carlo with Cauchy-Schwarz Cross-Entropy

This chapter introduces an original contribution, in the form of a new Cauchy-Schwarz (CS) cross-entropy (CE) method. It discusses the parallelism between CS and KL, the respective developed algorithms for the Cauchy-Schwarz CE and finishes with a comparison between the two methodologies.

## 4.1. Cauchy-Schwarz Divergence

The Cauchy-Schwarz PDF divergence is another particular measure of distances between two probability density functions (PDF), and a possible alternative to the Kullback-Leibler divergence in finding the "optimal" distribution distortion. It derives from the Rényi entropy, which in information theory, generalizes other entropies such as the Shannon entropy. Like the Kullback-Leibler can also be called a Cross-Entropy between two PDF [23]. The Cauchy-Schwarz PDF divergence measure is given by:

$$D_{CS}(q,p) = -\ln \frac{\int q(x)p(x)dx}{\sqrt{\int q(x)^2 dx \int p(x)^2 dx}}. \qquad (4.\ 1)$$

Deriving from equations (3. 1) and (3. 2), we find an optimal distribution $g*(X)$. Like before, it still depends on the parameter we wish to estimate (LOLP). Thus considering $g(X) = f(X;v)$, the main aim remains: choose the reference parameter v such that the following distance between densities $g*(X)$ and $g(X)$ is minimal [23-24],

$$D_{CS}(g^*, g) = -\ln \frac{\int g^*(x) g(x) dx}{\sqrt{\int g^*(x)^2 dx \int g(x)^2 dx}}. \quad \textbf{(4. 2)}$$

Taking any $g^*(X)$ and $f(X;v)$ such that $0 \le D_{CS}(g^*, g) < \infty$, this may be considered a symmetric measure. Like in the Kullback-Leibler divergence, the minimum is obtained if and only if $g^*(X) = g(X)$ [24].

Equation (4.2) may be expanded, by distributing the integral into the weighted summation of Gaussian components, given the terms inside the natural logarithm. Therefore, we arrive at the following expression,

$$D_{CS}(g^*, g) = -\ln \int g^*(x) g(x) dx + \frac{1}{2} \ln \int g^*(x)^2 dx + \frac{1}{2} \ln \int g(x)^2 dx, \quad \textbf{(4. 3)}$$

thus, substituting $g^*(X)$ and $g(X)$ with $H(x) f(x;u)$ and $f(x;v)$ respectively, we have,

$$\begin{aligned} D_{CS}(g^*, f(x;v)) = &-\ln \int H(x) f(x;u) f(x;v) dx \\ &+ \frac{1}{2} \ln \int f(x;u)^2 dx + \frac{1}{2} \ln \int f(x;v)^2 dx \end{aligned}. \quad \textbf{(4. 4)}$$

Acknowledging that the integral of the product of two Gaussians is the Gaussian in the space of mean parameters *μ*, such that,

$$\begin{aligned} D_{CS}(g^*, f(x;v)) = &-\ln E_v[H(X) f(X;u)] \\ &+ \frac{1}{2} \ln E_v\left[\frac{f(X;u)^2}{f(X;v)}\right] + \frac{1}{2} E_v[f(X;v)], \end{aligned} \quad \textbf{(4. 5)}$$

we finally arrive to a simplified expression plausible to optimize, in function of the parameter we wish to find *v*, and that way serve as a proof of concept. Therefore, we must resort to an optimization method, which in this case will be the evolutionary particle swarm optimization (EPSO).

## 4.2. Metaheuristics

A metaheuristic is a mathematical optimization procedure, aiming to find a heuristic that may provide us with an acceptable solution to an optimization problem with limited information. This is done by sampling a large set of solutions which is too large to be completely sampled. The main disadvantage is that compared to most optimization algorithms and iterative methods, metaheuristics don't guarantee that a globally optimal solution can be achieved [25-29].

### 4.2.1. Evolutionary Particle Swarm Optimization

The evolutionary particle swarm optimization (EPSO) is a hybrid method based on evolutionary computing and particle swarm optimization, two optimization techniques belonging to the metaheuristic family [26-27].

Given a set of particles, which may be referred as a set of chromosomes, the general EPSO algorithm follows this scheme [26-29]:

I. Replication – each particle is replicated (cloned) r-1 times;
II. Mutation - each clone suffers a mutation in its strategic parameters;
III. Reproduction – each particle generates 1 descendant according to the particle movement equation;
IV. Evaluation – each descendant has its fitness evaluated;
V. Selection - by stochastic tournament, the best particle of each group of r descendants of the previous generation, survives to form a new generation;

### 4.2.2. Particle Movement Equation

The particle movement equation of EPSO, is the following [26-27]:

$$X_i^{(k+1)} = X_i + V_i^{(k+1)}, \quad \textbf{(4. 6)}$$

that is, given a particle $X_i$ a new particle arises from equation (4.6) where $V_i^{(k+1)}$ is calculated as shown below,

$$V_i^{(k+1)} = w_{i1}V_i^{(k)} + w_{i2}m_i\left(b_i - X_i\right) + w_{i3}\left(b_G - X_i\right)P, \quad \textbf{(4. 7)}$$

where:

- $X_i$ - location of particle i;
- $V_i$ - velocity of particle i;
- $b_i$ - best point found by particle i in its past life up until the current generation;
- $b_G$ - best overall point found by the swarm of particles up to the current generation;
- $w_{i1}$ - weight conditioning the inertia term;
- $w_{i2}$ - weight conditioning the *memory* term;
- $w_{i3}$ - weight conditioning the *cooperation* or *information exchange* term;
- P – communication factor matrix;

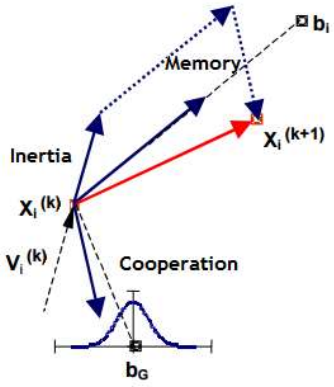


**Figure 4.1 -** Illustration of the EPSO movement rule [27].

The communication factor **P** is a diagonal matrix with diagonal elements 0 or 1 depending on a threshold communication probability, each time an element is needed, this threshold is compared against a random number, uniform distribution, and the value of 0 or 1 is selected, depends on such random number being smaller or greater than the fixed threshold [27].

In the most effective EPSO variant, not only the weights affecting the components of movement are mutated but also the global best is randomly disturbed to give,

$$b_G^* = b_G + w_{i4} N(0,1), \qquad \textbf{(4. 8)}$$

where $w_{i4}$ is the forth strategic parameter associated with particle i, controlling the "size" of the neighborhood of $b_G$ where it is more likely to find the real global best solution.

### 4.2.3. The mutation scheme

The mutation of a parameter W into W* is controlled by multiplicative lognormal random numbers such as [26-28]:

$$\widetilde{w}_{ik} = w_{ik}\left[\log N(0,1)\right]^{\sigma}, \quad \textbf{(4. 9)}$$

multiplicative Gaussian numbers such,

$$\widetilde{w}_{ik} = w_{ik}\left[1 + \sigma N(0,1)\right], \quad \textbf{(4. 10)}$$

or additive Gaussian distributed random numbers as

$$\widetilde{w}_{ik} = w_{ik} + \sigma N(0,1), \quad \textbf{(4. 11)}$$

where σ, the learning parameter, must be externally defined.

### 4.2.4. Cauchy-Schwarz CE EPSO parameter tests

After adopting EPSO, as our optimization method, equation (4.5) will be set as the fitness function. However, more parameters must be chosen, such as the solution's lower and upper bounds, the number of samples, the size of the population and the maximum number of generations in order to find an acceptably consistent solution, therefore the following tests were conducted:

The solutions lower bound was set to 0.01 with the upper bound set as 0.99, for the first tests the number of samples will be trialed, with the following results obtained for a population size of 50, a mutation rate of 0.4, a communication probability of 0.7, a max generation of 25 and a peak reduction factor of 0.6:

**Table 4.1** - EPSO test results for Cauchy-Schwarz fitness function with different numbers of samples

| Group | Kullback-Leibler CE $v_i$ | Cauchy-Schwarz CE EPSO $v_i$ | | | |
|---|---|---|---|---|---|
| | 10 000 samples | 10 000 samples | 15 000 samples | 20 000 samples | 25 000 samples |
| 1 | 0.9781 | 0.9852 | 0.9896 | 0.9814 | 0.9807 |
| 2 | 0.8742 | 0.8896 | 0.9012 | 0.8977 | 0.9023 |
| 4 | 0.9463 | 0.9772 | 0.9587 | 0.9645 | 0.9723 |
| 5 | 0.8750 | 0.9422 | 0.9677 | 0.9445 | 0.9899 |
| 6 | 0.7069 | 0.7111 | 0.7107 | 0.7043 | 0.7158 |
| 7 | 0.4359 | 0.3844 | 0.3542 | 0.3615 | 0.3538 |
| 8 | 0.0167 | 0.1786 | 0.0103 | 0.0196 | 0.0602 |
| 9 | 0.0054 | 0.0228 | 0.0288 | 0.0859 | 0.0487 |
| 3 | 0.9820 | 0.9862 | 0.9678 | 0.9818 | 0.9851 |

As shown in the table above, the EPSO best fitness, provides us with a solution very similar to the Kullback-Leibler CE distortion. With the exception of group 5 and 7, which present slight deviations in the distortion value, 15 000 samples seem so far the best option, mainly due to proximity between the Kullback-Leibler distortion values for group 8 and 9, with a smaller number of samples, and therefore less computational time

The second test will be performed for different values of population size, however previous parameters are kept constant, with the exception of the numbers of samples now set to 15 000:

**Table 4.2** - EPSO test results for Cauchy-Schwarz fitness function with different population sizes

| Group | Kullback-Leibler CE $v_i$ | Cauchy-Schwarz CE EPSO $v_i$ | | | | | |
|---|---|---|---|---|---|---|---|
| | | PopSize 25 | PopSize 35 | PopSize 45 | PopSize 50 | PopSize 75 | PopSize 100 |
| 1 | 0.9781 | 0.9900 | 0.9705 | 0.9613 | 0.9896 | 0.9878 | 0.9650 |
| 2 | 0.8742 | 0.8986 | 0.8976 | 0.9051 | 0.9012 | 0.9006 | 0.9018 |
| 4 | 0.9463 | 0.9745 | 0.9697 | 0.9715 | 0.9587 | 0.9772 | 0.9685 |
| 5 | 0.8750 | 0.9419 | 0.9300 | 0.9709 | 0.9677 | 0.9400 | 0.9414 |
| 6 | 0.7069 | 0.7073 | 0.7124 | 0.7263 | 0.7107 | 0.7301 | 0.7073 |
| 7 | 0.4359 | 0.4055 | 0.3565 | 0.3515 | 0.3542 | 0.3398 | 0.3576 |
| 8 | 0.0167 | 0.1607 | 0.0442 | 0.0520 | 0.0103 | 0.0660 | 0.0142 |
| 9 | 0.0054 | 0.0622 | 0.0556 | 0.0551 | 0.0288 | 0.0163 | 0.0190 |
| 3 | 0.9820 | 0.9837 | 0.9900 | 0.9900 | 0.9678 | 0.9892 | 0.9728 |

As shown in the table above, the EPSO best fitness, seems more stable for a population size of 100, mainly because of the proximity between the Kullback-Leibler distortion values for group 8 and 9. The third and final test will be performed for different values of max generation, once again previous parameters are kept constant, with the exception of the population size now set to 100:

**Table 4.3** - EPSO test results for Cauchy-Schwarz fitness function for values of max generation

| Group | Kullback-Leibler CE $v_i$ | Cauchy-Schwarz CE EPSO $v_i$ | |
|---|---|---|---|
| | | MaxGen 25 | MaxGen 50 |
| 1 | 0.9781 | 0.9852 | 0.9896 |
| 2 | 0.8742 | 0.8896 | 0.9012 |
| 4 | 0.9463 | 0.9772 | 0.9587 |
| 5 | 0.8750 | 0.9422 | 0.9677 |
| 6 | 0.7069 | 0.7111 | 0.7107 |
| 7 | 0.4359 | 0.3844 | 0.3542 |
| 8 | 0.0167 | 0.1786 | 0.0103 |
| 9 | 0.0054 | 0.0228 | 0.0288 |
| 3 | 0.9820 | 0.9862 | 0.9678 |

The difference between the two test seems negligible with both options viable differentiating only in the computational time for this instance.

### 4.2.5. Cauchy-Schwarz CE EPSO results

Given the conclusions obtained in the previous tests, a baseline for the parameters was set, lower bound = 0.01, upper bound = 0.99, number of samples = 15 000, population size of 100, a mutation rate of 0.4, a communication probability of 0.7, a max generation of 25 and a peak reduction factor of 0.6. Due to the nature of the optimization method EPSO, not guaranteeing the global optimal, the program will run 30 trials, each with a different MATLAB seed, in order to obtain the mean distortion values for each group. The results are:

**Table 4.4 -** Cauchy-Schwarz CE EPSO results for peak reduction factor 0.6

| Group | Kullback-Leibler CE $v_i$ | Cauchy-Schwarz CE EPSO $v_i$ |
|---|---|---|
| | | Mean values |
| 1 | 0.9781 | 0.9784 |
| 2 | 0.8742 | 0.8984 |
| 4 | 0.9463 | 0.9741 |
| 5 | 0.8750 | 0.9546 |
| 6 | 0.7069 | 0.7154 |
| 7 | 0.4359 | 0.3497 |
| 8 | 0.0167 | 0.0476 |
| 9 | 0.0054 | 0.0174 |
| 3 | 0.9820 | 0.9857 |
| Mean Computational time (s) | 0.19 | 802.98 |

Table 4.4 presents us with the mean values for the EPSO after 30 trials with different seeds, but also shows the computational time (effort) required to achieve them, which shows an immediate disadvantage in comparison with the Kullback-Leibler CE method. However, the main objective still remains, verifying if the Cauchy-Schwarz PDF divergence offers a better distortion than the current CE method. In order to test the Cauchy-Schwarz distortion values effectiveness, comparison of the mean number of years simulated to converge was necessary. Therefore, the sequential MCS was tested for 30 trials, again with random seeds each and with a peak reduction factor of 0.6. The results are:

**Table 4.5** - Mean years simulated in SMCS to achieve convergence, for the KL and CS distortions

| | | Years simulated | Years simulated |
|---|---|---|---|
| Seed | Trial | Kullback-Leibler | Cauchy-Schwarz |
| 34563457 | 1 | 76 | 192 |
| 45667 | 2 | 65 | 295 |
| 64356345 | 3 | 59 | 172 |
| ... | ... | ... | ... |
| 39047589 | 16 | 52 | 2 |
| ... | ... | ... | ... |
| 538754 | 28 | 57 | 234 |
| 38975983 | 29 | 76 | 148 |
| 908734 | 30 | 84 | 181 |
| Mean Values | | 64.50 | 185.17 |

Despite the obvious unfavorable aspects of the Cauchy-Schwarz distortions, mainly due to the lack of guarantees from the EPSO solutions being the global optimal, trial 16 proves that there is in fact a better possible distortion and the Cauchy-Schwarz may yet prove as an alternative to the Kullback-Leibler CE method, and overall both distortion allow for a quicker convergence than the crude SMCS.

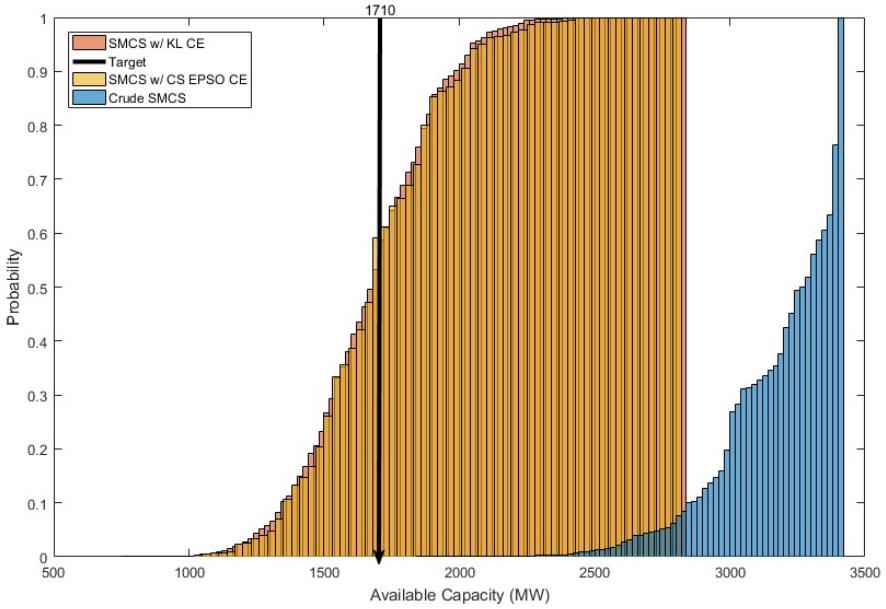


**Figure 4.2 -** Capacity Outage Probability Table (COPT) histogram for 50 000 samples obtained the original FOR, the FOR with Kullback-Leibler distortion and the FOR with Cauchy-Schwarz EPSO CE distortion for a peak reduction factor of 0.6

Figure 4.2 shows the frequency of the available capacities for 50 000 samples with the Cauchy-Schwarz distortion values, this explains the slight difficulty for the SMCS to converge as fast as with the Kullback-Leibler distortion, in comparison with the histogram in figure 3.3, where the values are concentrated around the target value for the demand, facilitating more load shedding occurrences this one is more dispersed.

Further tests were conducted for the EPSO with different parameters, namely with 50 000 and max number of generations of 50, with a considerable bigger mean calculation time of 5012.04 seconds. However, the distortion obtained was similar, which in turn resulted in a negligible difference in the simulated years required to converge the MCS, of 180.43 years, all the tests above mentioned can be analyzed with more detail by consulting attachments.

## 4.3. Cauchy-Schwarz Cross-Entropy

Given the observations made with the previous tests, presented motivation to continue exploring the Cauchy-Schwarz PDF divergence measure expression (4.2), however simplifying it in function of ***u*** instead of ***v***, which resulted in the following expression,

$$D_{CS}\left(g^{*}, f\left(x;v\right)\right) = -\ln E_u\left[H\left(X\right)f\left(X;v\right)\right] + \frac{1}{2}\ln E_u\left[f\left(X;u\right)\right] + \frac{1}{2}\ln E_u\left[\frac{f\left(X;v\right)^2}{f\left(X;u\right)}\right], \quad \textbf{(4. 12)}$$

following the same logic as with the Kullback-Leibler divergence, we wish to minimize the distance between PDF, $\min_v D_{CS}(g^*, f(x;v)) = 0 \leftrightarrow \nabla D_{CS}(g^*, f(x;v))$,

$$\min_v D_{CS} = \min_v \left\{ -\ln E_u\left[H(X) f(X;v)\right] + \frac{1}{2}\ln E_u\left[f(X;u)\right] + \frac{1}{2}\ln E_u\left[\frac{f(X;v)^2}{f(X;u)}\right] \right\}, \quad \textbf{(4. 13)}$$

considering that, only the 1st and the 3rd terms of equation (4.13) depend on ***v***, the 2nd is zero, which is equivalent to

$$\nabla\left\{ -\ln E_u\left[H(X) f(X;v)\right] \right\} + \nabla\left\{ \frac{1}{2}\ln E_u\left[\frac{f(X;v)^2}{f(X;u)}\right] \right\} = 0. \quad \textbf{(4. 14)}$$

Following the derivate rules for natural logarithm $\frac{\partial}{\partial x}\ln(u) = \frac{1}{u}\frac{\partial u}{\partial x}$, we have

$$\min_v D_{CS}(v) = -\frac{E_u\left[H(X)\nabla f(X;v)\right]}{E_u\left[H(X) f(X;v)\right]} + \frac{1}{2}\frac{E_u\left[\frac{\nabla f(X;v)^2}{f(X;u)}\right]}{E_u\left[\frac{f(X;v)^2}{f(X;u)}\right]}, \quad \textbf{(4. 15)}$$

as it stands, we are left with the derivatives of the binomial functions $f(X;v)$ and $f(X;v)^2$

$$-\frac{\frac{1}{N}\sum_{i=0}^{N} H(X)\nabla f(X;v)}{\frac{1}{N}\sum_{i=0}^{N} H(X) f(X;v)} + \frac{1}{2}\frac{\frac{1}{N}\sum_{i=0}^{N}\frac{\nabla f(X;v)^2}{f(X;u)}}{\frac{1}{N}\sum_{i=0}^{N}\frac{f(X;v)^2}{f(X;u)}} = 0, \quad \textbf{(4. 16)}$$

which, upon expansion, the derivatives of $f(X;v)$ and $f(X;v)^2$ result in,

$$\frac{\partial}{\partial v_j} f(x;v) = f(x;v) \times \left( \frac{x_j}{v_j - 1} + \frac{n}{v_j} - \frac{x_j}{v_j} \right), \qquad \textbf{(4. 17)}$$

$$\frac{\partial}{\partial v_j} f(x;v)^2 = f(x;v)^2 \times 2\left( \frac{x_j}{v_j - 1} + \frac{n}{v_j} - \frac{x_j}{v_j} \right), \qquad \textbf{(4. 18)}$$

replacing in equation (4.16) $f(X;v)$ and $f(X;v)^2$ , by (4.17) and (4.18) respectively, we and simplifying the expressions we have

$$\begin{gathered} -\frac{\frac{1}{N}\sum_{i=0}^{N} H(X) f(X;v) \times \left( \frac{x_{ij}}{v_j - 1} + \frac{n}{v_j} - \frac{x_{ij}}{v_j} \right)}{\frac{1}{N}\sum_{i=0}^{N} H(X) f(X;v)} \\ +\frac{1}{2}\frac{\frac{1}{N}\sum_{i=0}^{N} \frac{f(X;v)^2}{f(X;u)} \times 2\left( \frac{x_{ij}}{v_j - 1} + \frac{n}{v_j} - \frac{x_{ij}}{v_j} \right)}{\frac{1}{N}\sum_{i=0}^{N} \frac{f(X;v)^2}{f(X;u)}} = 0 \end{gathered}, \qquad \textbf{(4. 19)}$$

$$\frac{\frac{1}{N}\sum_{i=0}^{N} H(X) f(X;v) x_{ij}}{\frac{1}{N}\sum_{i=0}^{N} H(X) f(X;v)} \left( \frac{1}{v_j (v_j - 1)} \right) = \frac{\frac{1}{N}\sum_{i=0}^{N} \frac{f(X;v)^2}{f(X;u)} x_{ij}}{\frac{1}{N}\sum_{i=0}^{N} \frac{f(X;v)^2}{f(X;u)}} \left( \frac{1}{v_j (v_j - 1)} \right), \qquad \textbf{(4. 20)}$$

$$\frac{\frac{1}{N}\sum_{i=0}^{N} H(X) f(X;v) x_{ij}}{\frac{1}{N}\sum_{i=0}^{N} H(X) f(X;v)} = \frac{\frac{1}{N}\sum_{i=0}^{N} \frac{f(X;v)^2}{f(X;u)} x_{ij}}{\frac{1}{N}\sum_{i=0}^{N} \frac{f(X;v)^2}{f(X;u)}}. \qquad \textbf{(4. 21)}$$

Finally, we arrive at equation (4.21) which can be considered simpler than the equation (4.5) used as fitness function in the EPSO. However, it still can't be analytically solved as the updating equation (3.18), therefore we must resort to a solver algorithm in order to obtain a solution (distortion).

### 4.3.1. Simple Analytic Example

In order to test this new equation and to illustrate the proposed approach, we are going to consider a small generating system with 20 small units, each with a 10 MW capacity totalizing an installed capacity of 200 MW, consider also the unavailability (F.O.R.) is the same for all units and equal to 0.01, the peak demand is 120 with a peak reduction factor of 0.6.

To find the exact value for LOLP we calculated and constructed the table for out of service capacities as shown below:

**Table 4.6 – Table for out of service capacities for a small generating system described above**

| Available Capacity (MW) | $H(X)$ | $f(X;u)$ |
|---|---|---|
| 0 | 1 | 1E-40 |
| 10 | 1 | 1.98E-37 |
| 20 | 1 | 1.86219E-34 |
| 30 | 1 | 1.10614E-31 |
| 40 | 1 | 4.65409E-29 |
| 50 | 1 | 1.47441E-26 |
| 60 | 1 | 3.64918E-24 |
| 70 | 1 | 7.22537E-22 |
| 80 | 1 | 1.16238E-19 |
| 90 | 1 | 1.53434E-17 |
| 100 | 1 | 1.6709E-15 |
| 110 | 1 | 1.50381E-13 |
| 120 | 0 | 1.11658E-11 |
| 130 | 0 | 6.80254E-10 |
| 140 | 0 | 3.36726E-08 |
| 150 | 0 | 1.33343E-06 |
| 160 | 0 | 4.12531E-05 |
| 170 | 0 | 0.000960955 |
| 180 | 0 | 0.015855761 |
| 190 | 0 | 0.165233725 |
| 200 | 0 | 0.817906938 |
| Load of Loss Probability (LOLP) | | 1.5207E-13 |

**Table 4.7 – Distortion obtained with the Kullback-Leibler CE and the Cauchy-Schwarz CE**

| Kullback-Leibler Distortion $v$ | Cauchy-Schwarz Distortion $v$ |
|---|---|
| 0.45055960 | 0.45174306 |

As shown in Table 4.7 the distortion can be considered equal for both methods, with the KL being analytically calculated and the CS obtained through the use of a simple solver. Proving again the

similarity between methods and helping strengthen previous observations, such as: Cauchy-Schwarz being an acceptable alternative to the Kullback-Leibler CE

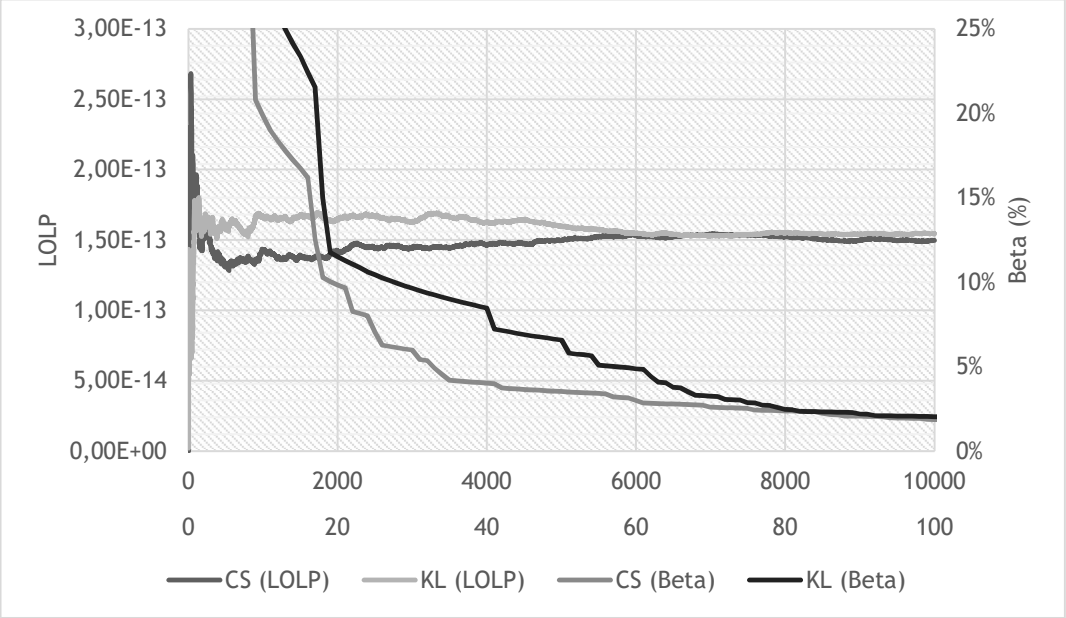


**Figure 4.3 – Chart depicting a possible LOLP and respective Beta evolutions throughout the SMCS for both distortions KL and CS**

In this particular case depicted in figure 4.3 we can observe that in fact the distortion introduced by the CS cross-entropy, can result in a SMCS that converges with a 5% beta earlier than the one with the Kullback-Leibler distortion.

However, this is the same situation observed for other tests, changing the sample, might result in slightly different behaviors, such as, better with KL or even equal with the KL and the CS.

### 4.3.2. Cauchy-Schwarz CE Method Algorithm for Rare Event Simulation

Similarly, to the Kullback-Leibler CE algorithm, the Cauchy-Schwarz Cross-Entropy algorithm for rare event simulation, we must introduce importance sampling through the use of the parameter $W(X_i;u;v_{t-1})$, in order to raise the number of rare occurrences we observe, is a multi-level algorithm as well, with slight differences, mainly in the updating equation.

The algorithm's initialization starts by following the same steps as before:

1. Define a ρ = 10%, $v_0 = u$, the target load $\gamma = L_{peak}$ and set the iteration counter t = 1;
2. Generate a sample $\mathbf{X_i}, \ldots, \mathbf{X_n}$ from the PDF $f(X_i;v_{t-1})$;

3. Evaluate $S_{(X_i)}$ for all samples, where $S_{(X_i)}$ is the total generating capacity of each Xi sample;
4. Compute the sample $(1-\rho)$-quantile $\hat{\gamma}_t$ of the performances according to equation (3.12)
5. Calculate the corresponding LOLP, $H(X_i)$;
6. Calculate $W(X_i;u;v_{t-1})$ with equation (3.13);
7. Update vector **v**, using the sample $\mathbf{X_i}$, …, $\mathbf{X_n}$ and running a minimization solver for the following equation

$$\frac{E_u\left[H(X)W(X_i;u;v_{t-1})f(X;v)x_{ij}\right]}{E_u\left[H(X)W(X_i;u;v_{t-1})f(X;v)\right]} = \frac{E_u\left[W(X_i;u;v_{t-1})\frac{f(X;v)^2}{f(X;u)}x_{ij}\right]}{E_u\left[W(X_i;u;v_{t-1})\frac{f(X;v)^2}{f(X;u)}\right]} \quad \textbf{(4. 22)}$$

8. If $\hat{\gamma}_t < L_{peak}$, set t = t +1 and reiterate from step 2., else close the algorithm and return the final values of vector **v.**

### 4.3.3. Solver LSQNONLIN

LSQNONLIN is a pre-implemented solver algorithm available in MATLAB, basically it solves nonlinear least-squares curve fitting problems such as:

$$\min_x \|f(x)\|_2^2 = \min_x \left(f_1(x)^2 + f_2(x)^2 + \ldots + f_n(x)^2\right). \quad \textbf{(4. 23)}$$

Its maim advantage in relation to other algorithms such as FSOLVE, is the possibility to set constraints for the outcome solution with optional lower bounds (lb) and upper bounds (ub) on the variables that compose x which the program accepts as vectors or matrices [30].

Instead of computing the value $\|f(x)\|_2^2$, which represents the sum of the squares, it requires the user-defined function to compute the vector-valued function.

$$f(x)=\begin{bmatrix} f_1(x) \\ f_2(x) \\ \vdots \\ f_n(x) \end{bmatrix} \quad \textbf{(4. 24)}$$

LSQNONLIN implements two different algorithms: trust-region-reflective and the Levenberg-Marquardt, both algorithms were tested in this work. However, the one chosen was the default, trust-region-reflective, due to the better results obtained with it [30].

#### 4.3.3.1. Trust Region Reflective Algorithm

For the trust region reflective algorithm, the nonlinear system of equations can't be undermined, in other words, the number of equations must match at least the number of variables of x.

In order to better comprehend the trust region approach, we are going to consider an unconstrained minimization problem, minimize $f(x)$, with the function receiving vectors as arguments, and returning scalars [31].

Supposing we have a point x located in n-space and we wish to improve upon it, the basic idea is to approximate f with a simpler function q, which reasonably reflects the behavior of function f in a neighborhood N around point x, this neighborhood is the so called, trust region.

A trial step s is computed by minimizing over N. This is the trust-region sub problem,

$$\min_S \{q(s), s \in N\}. \quad \textbf{(4. 25)}$$

The current point x updates to x+s if $f(x+s) < f(x)$, otherwise the point remains unchanged and the region of trust N, shrinks, repeating the trial step, with the maim questions being, how to choose and compute q and how to choose and modify N, with what precision.

Standard trust-region method, q is defined by the first two terms of the Taylor approximation to F at x, with the neighborhood N usually spherical or ellipsoidal, mathematically the sub problem is stated [30-31]

$$\min\left\{\frac{1}{2}s^T Hs + s^T g \ such \ \text{that} \ \|Ds\| \le \Delta\right\}, \quad \textbf{(4. 26)}$$

where g is the gradient of $f(x)$, H is the hessian matrix, D is a diagonal scaling matrix and $\Delta$ is a positive scalar.

The philosophy behind this choice of S is to force global convergence and achieve fast local convergence, a sketch of unconstrained minimization using trust-region ideas is easy to give:

I. Formulate the two-dimensional trust-region sub problem;
II. Solve equation (4.26) to determine the trial step *s*;
III. If $f(x+s) < f(x)$, then *x* = *x* + *s*;
IV. Adjust Δ;

These four steps are repeated until convergence. The trust-region dimension Δ is adjusted according to standard rules, being in particular decreased if the trial step is not accepted.

## 4.4. Sequential MCS with Cauchy-Schwarz Cross-Entropy

Given the breakthroughs with the Cauchy-Schwarz PDF distance measure equation, and the formulation of the multi-level algorithm for CS cross-entropy, we implement a program similar to the Kullback-Leibler, integrating it with the sequential MCS and the respective test system IEEE-RTS 79.

### 4.4.1. Cauchy-Schwarz Cross-Entropy Tests

In order to increase the method's robustness some initial tests were made by changing some of the parameters such as the number of samples, the constraints, and the solver's max number of evaluations, taking in consideration all test were conducted with a peak reduction factor of 0.6 the test results are as follows:

**Table 4.8** – Cauchy-Schwarz CE tests for 10 000 samples with lower bound lb = 0.01 and upper bound ub = 0.99

| Group | Kullback-Leibler CE $v_i$ | Cauchy-Schwarz CE EPSO $v_i$ 10 000 samples | | | | |
|---|---|---|---|---|---|---|
| | | Seed 156412 | Seed 348568 | Seed 456737 | Seed 690896 | Seed 324684 |
| 1 | 0.9781 | 0.9822 | 0.9799 | 0.9900 | 0.9900 | 0.9766 |
| 2 | 0.8742 | 0.9900 | 0.8997 | 0.8975 | 0.9507 | 0.9024 |
| 4 | 0.9463 | 0.9682 | 0.9717 | 0.1685 | 0.1488 | 0.9642 |
| 5 | 0.8750 | 0.9456 | 0.9538 | 0.3694 | 0.0100 | 0.9366 |
| 6 | 0.7069 | 0.7144 | 0.7156 | 0.0100 | 0.2857 | 0.7132 |
| 7 | 0.4359 | 0.3462 | 0.3490 | 0.9900 | 0.1695 | 0.3539 |
| 8 | 0.0167 | 0.0100 | 0.0135 | 0.9900 | 0.6913 | 0.0100 |
| 9 | 0.0054 | 0.0100 | 0.0117 | 0.1735 | 0.0100 | 0.0100 |
| 3 | 0.9820 | 0.9865 | 0.9862 | 0.9900 | 0.0996 | 0.9838 |

As shown in table 4.8 10 000 samples doesn't offer much stability, with the exception of groups 1 and 2, the remaining ones present themselves with oscillating results in the distortion.

**Table 4.9** – Cauchy-Schwarz CE tests for 25 000 samples with lower bound lb = 0.01 and upper bound ub = 0.99

| Group | Kullback-Leibler CE $v_i$ | Cauchy-Schwarz CE EPSO $v_i$ 25 000 samples | | | | |
|---|---|---|---|---|---|---|
| | | Seed 156412 | Seed 348568 | Seed 456737 | Seed 690896 | Seed 324684 |
| 1 | 0.9781 | 0.9786 | 0.9804 | 0.9816 | 0.9827 | 0.9827 |
| 2 | 0.8742 | 0.9003 | 0.8960 | 0.8999 | 0.8928 | 0.8973 |
| 4 | 0.9463 | 0.9660 | 0.9708 | 0.9697 | 0.9750 | 0.9690 |
| 5 | 0.8750 | 0.9421 | 0.9388 | 0.9429 | 0.9416 | 0.9376 |
| 6 | 0.7069 | 0.7112 | 0.7097 | 0.7009 | 0.7143 | 0.7081 |
| 7 | 0.4359 | 0.3459 | 0.3448 | 0.3513 | 0.3569 | 0.3531 |
| 8 | 0.0167 | 0.0100 | 0.0123 | 0.0216 | 0.0100 | 0.0100 |
| 9 | 0.0054 | 0.0218 | 0.0100 | 0.0100 | 0.0100 | 0.0100 |
| 3 | 0.9820 | 0.9845 | 0.9869 | 0.9882 | 0.9859 | 0.9856 |

With 25 000 samples the distorted distribution stability seems to increase, which so far indicates the stability might be related with the number of samples, leaving group 8 with negligible instability

**Table 4.10** – Cauchy-Schwarz CE tests for 50 000 samples with lower bound lb = 0.01 and upper bound ub = 0.99

| Group | Kullback-Leibler CE $v_i$ | Cauchy-Schwarz CE EPSO $v_i$ 50 000 samples | | | | |
|---|---|---|---|---|---|---|
| | | Seed 156412 | Seed 348568 | Seed 456737 | Seed 690896 | Seed 324684 |
| 1 | 0.9781 | 0.9802 | 0.9762 | 0.9801 | 0.9811 | 0.9796 |
| 2 | 0.8742 | 0.8979 | 0.8966 | 0.8952 | 0.9014 | 0.9016 |
| 4 | 0.9463 | 0.9707 | 0.9709 | 0.9713 | 0.9670 | 0.9717 |
| 5 | 0.8750 | 0.9407 | 0.9502 | 0.9428 | 0.9424 | 0.9459 |
| 6 | 0.7069 | 0.7111 | 0.5192 | 0.7151 | 0.7149 | 0.7095 |
| 7 | 0.4359 | 0.3558 | 0.0100 | 0.3499 | 0.3564 | 0.3483 |
| 8 | 0.0167 | 0.0100 | 0.9900 | 0.0100 | 0.0100 | 0.0100 |
| 9 | 0.0054 | 0.0100 | 0.0100 | 0.0100 | 0.0100 | 0.0100 |
| 3 | 0.9820 | 0.9850 | 0.9861 | 0.9868 | 0.9857 | 0.9871 |

Table 4.10 shows most groups with stable distortions, with the exception of groups 7 and 8 showing instability again. However, now it seems to have more relation with the constraints instead of the number of samples. Therefore, we will conduct a new test with the upper bound equal to $v_{t-1}$ and changing with each iteration of the multi-level algorithm. The results are:

**Table 4.11** – Cauchy-Schwarz CE tests for 50 000 samples with lower bound lb = 0.01 and upper bound ub = $v_{t-1}$

| Group | Kullback-Leibler CE $v_i$ | Cauchy-Schwarz CE EPSO $v_i$ 50 000 samples | | | | |
|---|---|---|---|---|---|---|
| | | Seed 156412 | Seed 348568 | Seed 456737 | Seed 690896 | Seed 324684 |
| 1 | 0.9781 | 0.9780 | 0.9692 | 0.9788 | 0.9604 | 0.9560 |
| 2 | 0.8742 | 0.8967 | 0.8497 | 0.8951 | 0.8499 | 0.8509 |
| 4 | 0.9463 | 0.9712 | 0.9146 | 0.9712 | 0.9617 | 0.9567 |
| 5 | 0.8750 | 0.9404 | 0.8201 | 0.9417 | 0.9227 | 0.9262 |
| 6 | 0.7069 | 0.7113 | 0.7070 | 0.7147 | 0.7149 | 0.7070 |
| 7 | 0.4359 | 0.3552 | 0.3708 | 0.3500 | 0.3584 | 0.3584 |
| 8 | 0.0167 | 0.0100 | 0.0456 | 0.0100 | 0.0100 | 0.0322 |
| 9 | 0.0054 | 0.0100 | 0.0330 | 0.0100 | 0.0100 | 0.0174 |
| 3 | 0.9820 | 0.9849 | 0.9680 | 0.9865 | 0.9736 | 0.9760 |

With the values observed in the above table 4.11, stability seems to have been achieved due to the high number of samples and the robust constraints implemented

### 4.4.2. SMCS with Cauchy-Schwarz CE results

Given the test results and the conclusions obtained about the studied parameters, we will finally test the overall efficiency of the new Cauchy-Schwarz cross-entropy method, with the current iteration.

Each test was conducted with the multi-level algorithm previously describe with 50 000 samples and the constraints lb=0.01 and ub= $v_{t-1}$. The following tables and figures depict the results for different values of peak reduction factor, which were compared with the respective values for the Kullback-Leibler CE.

**Table 4.12** - Cauchy-Schwarz CE EPSO results for peak reduction factor 0.6

| Group | Kullback-Leibler CE $v_i$ | Cauchy-Schwarz CE EPSO $v_i$ |
|---|---|---|
| | | Mean values |
| 1 | 0.9781 | 0.9613 |
| 2 | 0.8742 | 0.8535 |
| 4 | 0.9463 | 0.9514 |
| 5 | 0.8750 | 0.8995 |
| 6 | 0.7069 | 0.7053 |
| 7 | 0.4359 | 0.3584 |
| 8 | 0.0167 | 0.0188 |
| 9 | 0.0054 | 0.0124 |
| 3 | 0.9820 | 0.9738 |
| Mean Computational time (s) | 0.19 | 70.81 |

The first and most noticeable improvement in relation to the EPSO CS is the computational time and effort, which decreased drastically. In this case with a peak reduction factor of 0.6 the computational time decreased approximately 91.18% in comparison with the CS EPSO.

**Table 4.13** - Mean years simulated in SMCS to achieve convergence, for the KL and CS distortions for a peak reduction factor of 0.6

| | | Years simulated | Years simulated |
|---|---|---|---|
| Seed | Trial | Kullback-Leibler | Cauchy-Schwarz |
| 34563457 | 1 | 76 | 61 |
| 45667 | 2 | 65 | 65 |
| 64356345 | 3 | 59 | 78 |
| ... | ... | ... | ... |
| 538754 | 28 | 57 | 85 |
| 38975983 | 29 | 76 | 2 |
| 908734 | 30 | 84 | 69 |
| Mean Values | | 64.50 | 81.67 |

Despite the mean years simulated towards the MCS convergence with the CS cross-entropy distortion, still being slightly higher than with the Kullback-Leibler CE, again represents a major reduction from the values obtained with the EPSO

This can be attributed to the similarity between the two distorted distributions, observed in the following figure 4.4

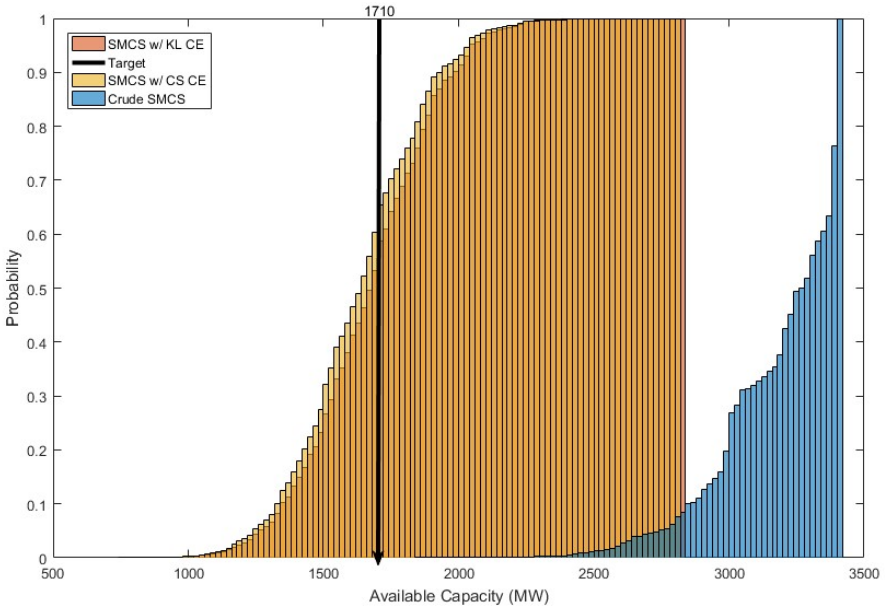


**Figure 4.4 -** Capacity Outage Probability Table (COPT) histogram for 50 000 samples obtained the original FOR, the FOR with Kullback-Leibler distortion and the FOR with Cauchy-Schwarz CE distortion for a peak reduction factor of 0.6

**Table 4.14** - Cauchy-Schwarz CE EPSO results for peak reduction factor 0.7

| Group | Kullback-Leibler CE $v_i$ | Cauchy-Schwarz CE EPSO $v_i$ |
|---|---|---|
| | | Mean values |
| 1 | 0.9736 | 0.9695 |
| 2 | 0.8791 | 0.8713 |
| 4 | 0.9447 | 0.9274 |
| 5 | 0.8695 | 0.8745 |
| 6 | 0.8124 | 0.7596 |
| 7 | 0.6859 | 0.6332 |
| 8 | 0.0963 | 0.0560 |
| 9 | 0.0324 | 0.0179 |
| 3 | 0.9845 | 0.9797 |
| Mean Computational time (s) | 0.62 | 50.38 |

Again, the Cauchy-Schwarz distortion shows a considerable relation with the Kullback-Leibler, with the main differences only observed in groups 6 and 8.

**Table 4.15** - Mean years simulated in SMCS to achieve convergence, for the KL and CS distortions for a peak reduction factor of 0.7

| | | Years simulated | Years simulated |
|---|---|---|---|
| Seed | Trial | Kullback-Leibler | Cauchy-Schwarz |
| 34563457 | 1 | 53 | 35 |
| 45667 | 2 | 57 | 41 |
| 64356345 | 3 | 37 | 31 |
| ... | ... | ... | ... |
| 538754 | 28 | 43 | 54 |
| 38975983 | 29 | 38 | 45 |
| 908734 | 30 | 47 | 29 |
| Mean Values | | 45.20 | 37.23 |

Now these are interesting results, with the mean simulated years for the CS distortion smaller than with the Kullback-Leibler distribution. The main reason for this can be explained by taking a close look at the following figure 4.5.

The Cauchy-Schwarz distorted distribution, introduces a higher chance for load shedding, through the increase in probability for cases around the targeted demand of 1995 MW.

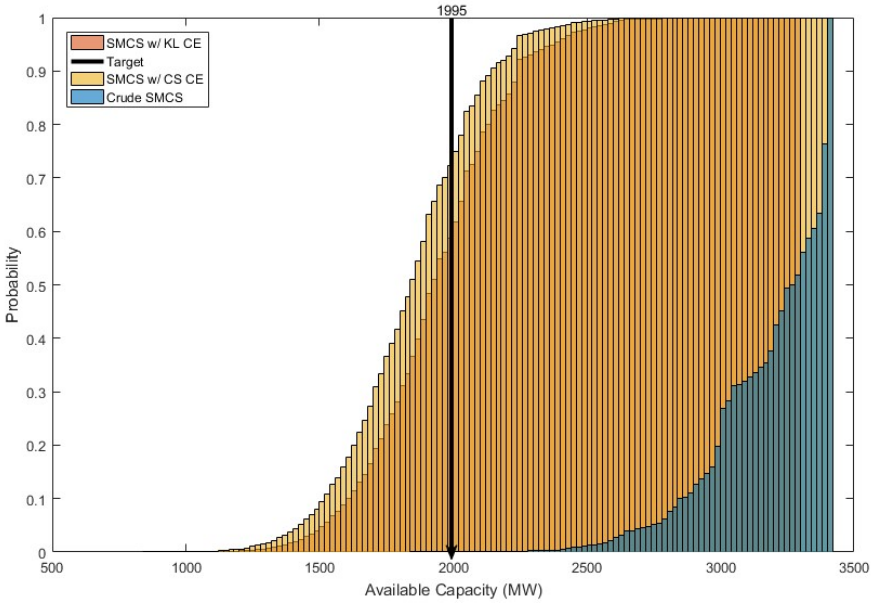


**Figure 4.5 -** COPT histogram for 50 000 samples obtained the original FOR, the FOR with Kullback-Leibler distortion and the FOR with Cauchy-Schwarz CE distortion for a peak reduction factor of 0.7

For a peak reduction value of 0.8, we observe the worst values so far, with more differences between distortions, resulting in the high values presented in tables 4.17.

**Table 4.16** - Cauchy-Schwarz CE EPSO results for peak reduction factor 0.8

| Group | Kullback-Leibler CE $v_i$ | Cauchy-Schwarz CE EPSO $v_i$ |
|---|---|---|
| | | Mean values |
| 1 | 0.9793 | 0.9739 |
| 2 | 0.8821 | 0.8897 |
| 4 | 0.9716 | 0.9629 |
| 5 | 0.9363 | 0.9361 |
| 6 | 0.8968 | 0.7724 |
| 7 | 0.8111 | 0.6672 |
| 8 | 0.2944 | 0.7227 |
| 9 | 0.1295 | 0.0520 |
| 3 | 0.9876 | 0.9828 |
| Mean Computational time (s) | 0.42 | 49.11 |

**Table 4.17** - Mean years simulated in SMCS to achieve convergence, for the KL and CS distortions for a peak reduction factor of 0.8

| | | Years simulated | Years simulated |
|---|---|---|---|
| Seed | Trial | Kullback-Leibler | Cauchy-Schwarz |
| 34563457 | 1 | 54 | 133 |
| 45667 | 2 | 37 | 137 |
| 64356345 | 3 | 68 | 110 |
| ... | ... | ... | ... |
| 538754 | 28 | 32 | 167 |
| 38975983 | 29 | 43 | 186 |
| 908734 | 30 | 59 | 180 |
| Mean Values | | 48.87 | 155.37 |

Closer inspection of figure 4.6, may provide a better understanding of what cause such a difference between the mean simulated years towards convergence. The two distributions look identical, with approximately the same probability near the targeted load. However, the Cauchy-Schwarz distribution delivers less stability than the previous two cases.

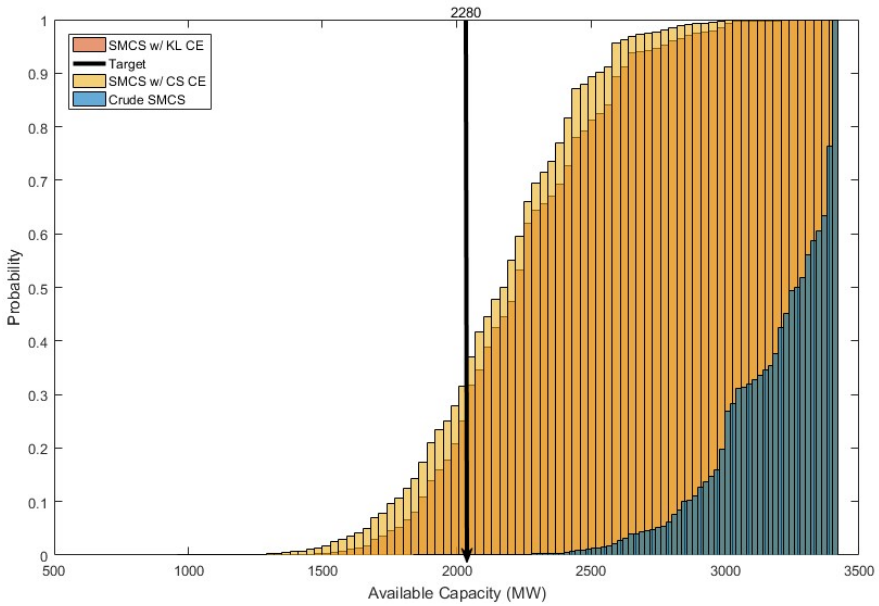


**Figure 4.6 -** COPT histogram for 50 000 samples obtained the original FOR, the FOR with Kullback-Leibler distortion and the FOR with Cauchy-Schwarz CE distortion for a peak reduction factor of 0.8

**Table 4.18** - Cauchy-Schwarz CE EPSO results for peak reduction factor 0.9

| Group | Kullback-Leibler CE $v_i$ | Cauchy-Schwarz CE EPSO $v_i$ |
|---|---|---|
| | | Mean values |
| 1 | 0.9782 | 0.9787 |
| 2 | 0.8939 | 0.8969 |
| 4 | 0.9636 | 0.9582 |
| 5 | 0.9026 | 0.9572 |
| 6 | 0.8879 | 0.8278 |
| 7 | 0.8425 | 0.7882 |
| 8 | 0.4882 | 0.3978 |
| 9 | 0.3121 | 0.3378 |
| 3 | 0.9841 | 0.9813 |
| Mean Computational time (s) | 0.43 | 34.28 |

These last two cases, show the same behavior, slight similarity between the two distortions (CS and KL), less than with the two first peak reduction factors, but much more than with the last case.

**Table 4.19** - Mean years simulated in SMCS to achieve convergence, for the KL and CS distortions for a peak reduction factor of 0.9

| | | Years simulated | Years simulated |
|---|---|---|---|
| Seed | Trial | Kullback-Leibler | Cauchy-Schwarz |
| 34563457 | 1 | 33 | 52 |
| 45667 | 2 | 43 | 41 |
| 64356345 | 3 | 32 | 47 |
| ... | ... | ... | ... |
| 538754 | 28 | 33 | 51 |
| 38975983 | 29 | 34 | 53 |
| 908734 | 30 | 2 | 44 |
| Mean Values | | 33.00 | 49.63 |

Such similarity results in closer mean convergence values, that keep pointing towards the global resemblance between methodologies, with a potential for better results with the Cauchy-Schwarz entropy as it happens for a peak reduction factor of 0.7.

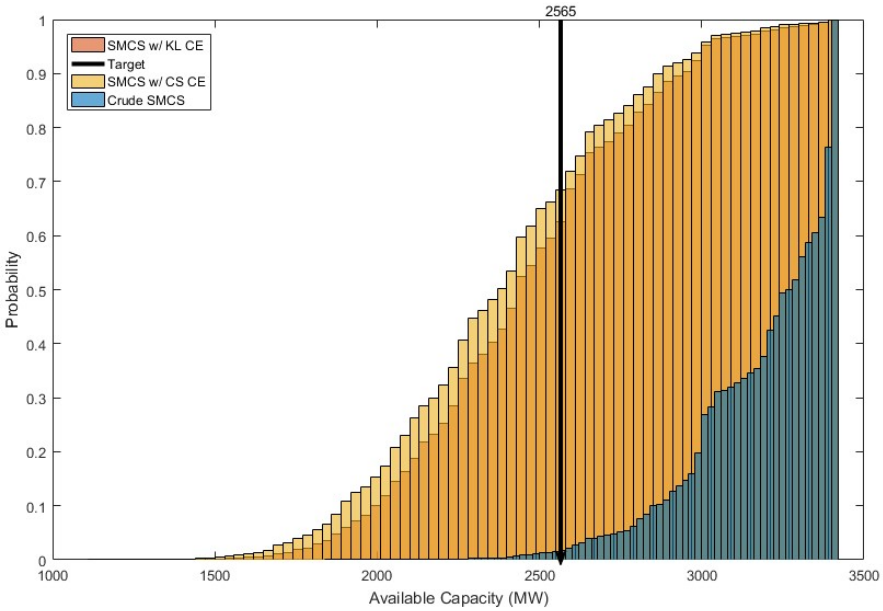


**Figure 4.7 -** COPT histogram for 50 000 samples obtained the original FOR, the FOR with Kullback-Leibler distortion and the FOR with Cauchy-Schwarz CE distortion for a peak reduction factor of 0.9

Again with the relation of similarity between the two distributions, which extends to the last case.

**Table 4.20** - Cauchy-Schwarz CE EPSO results for peak reduction factor 1.0

| Group | Kullback-Leibler CE $v_i$ | Cauchy-Schwarz CE EPSO $v_i$ |
|---|---|---|
| | | Mean values |
| 1 | 0.9756 | 0.9598 |
| 2 | 0.8824 | 0.8496 |
| 4 | 0.9709 | 0.9545 |
| 5 | 0.9398 | 0.9226 |
| 6 | 0.9061 | 0.8336 |
| 7 | 0.8386 | 0.7532 |
| 8 | 0.6878 | 0.6989 |
| 9 | 0.4765 | 0.4413 |
| 3 | 0.9869 | 0.9750 |
| Mean Computational time (s) | 0.43 | 40.40 |

Once more the two distortions only differentiating in groups 6 and 7, with the remaining values presenting difference's smaller than approximately 5%.

**Table 4.21** - Mean years simulated in SMCS to achieve convergence, for the KL and CS distortions for a peak reduction factor of 1.0

| | | Years simulated | Years simulated |
|---|---|---|---|
| Seed | Trial | Kullback-Leibler | Cauchy-Schwarz |
| 34563457 | 1 | 29 | 60 |
| 45667 | 2 | 37 | 43 |
| 64356345 | 3 | 59 | 44 |
| ... | ... | ... | ... |
| 538754 | 28 | 24 | 65 |
| 38975983 | 29 | 33 | 52 |
| 908734 | 30 | 42 | 56 |
| Mean Values | | 37.23 | 52.53 |

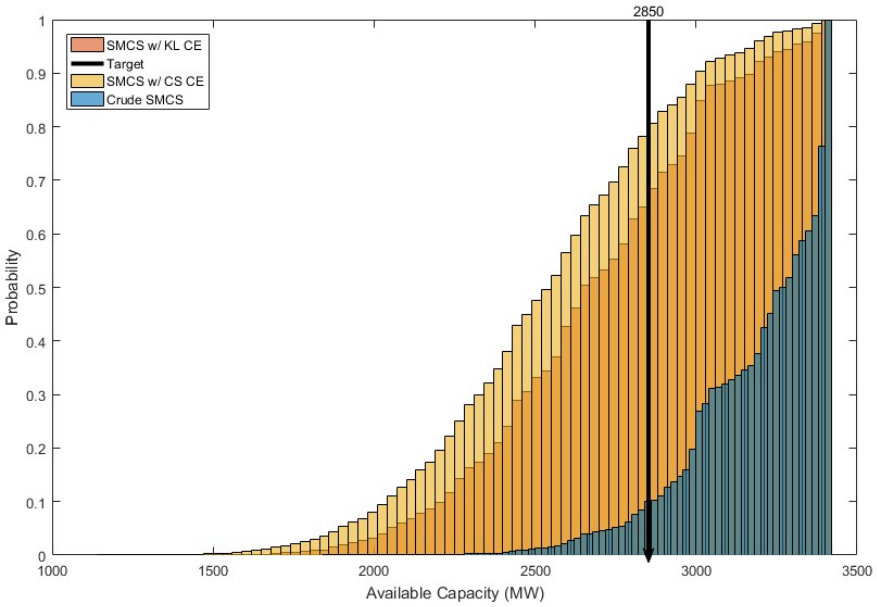


**Figure 4.8 -** COPT histogram for 50 000 samples obtained the original FOR, the FOR with Kullback-Leibler distortion and the FOR with Cauchy-Schwarz CE distortion for a peak reduction factor of 1.0

Observing the figure above show that the Kullback-Leibler distribution in most cases being more concentrated around the targeted peak demand than the Cauchy-Schwarz. As it stands the MCS estimates the following three indices the LOLE (hours/year), the EENS (MWh/year) and the LOLF (occurrences/year), figure 4.9 helps understand the MCS behavior with the two distortions

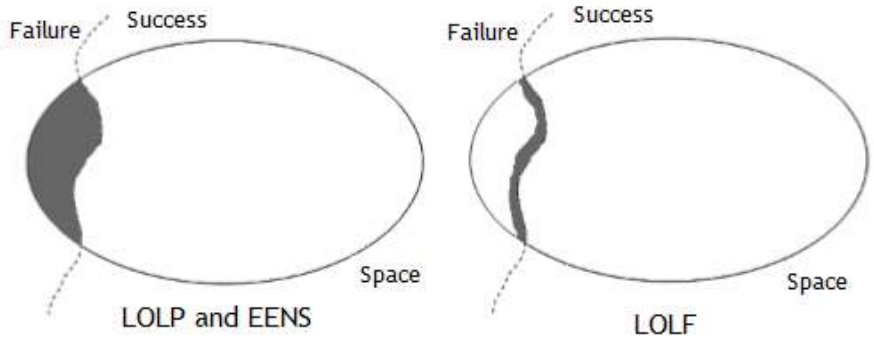


**Figure 4.9 – Failure states with contribution to the reliability indices [30]**

The first two indices benefit from a distribution with more load shedding occurrences for any available capacity. The LOLF benefits from available capacities with a distribution more concentrated around the target peak demand. And that may be one of the reasons preventing the SMCS with the CS distortion from converging before the one with the KL distortion. However, further tests are required to prove this claim and to better compare the two methods.

# Chapter 5

# Conclusions

This chapter summarizes this document's previous observations and analysis, offering a closer inspection of the main ideas gained throughout chapter 3 and 4, and analyzing them in a bigger spectrum. It also concludes if the previously proposed objectives for this dissertation in chapter 1 are achieved. Finishing with some proposals for the future horizon and possible improvements for this work.

## 5.1. General Conclusions

This dissertation started by offering the context and complexity of the problem in hand, which, with the expansion and modernization of the ever-growing power systems is undeniably growing in complexity, increasing the difficulties in properly modeling these systems and assess their reliability.

The research started the basic notions of reliability assessment, followed by a progressive structure of ideas that led us to the Monte Carlo methods and its integrated mechanisms for variance reduction.

From these mechanisms, the Cross-Entropy stands out due to its high efficiency and autonomy compared to the Control Variable and Importance Sampling. Nonetheless the Cross-Entropy method does this not only by introducing new ideas but also borrows from the other two methods to create an overall efficient variance reduction mechanism.

It does so by adopting a different approach to the problem using the Kullback-Leibler divergence which as previously stated derives from the Shannon Entropy and the Cross-Entropy notions from information theory. It perceives each PDF as a string of information and by calculating a measure of "distance" between them, tries to minimize it, leaving us with two different distributions but highly correlated.

Comparisons between the crude SMCS and the SMCS with cross-entropy left no doubts. Despite the obvious advantages of using the MCS to estimate the reliability indices, without any variance reduction mechanism is a sluggish method in the computational time and effort departments. With the CE distortion the quickness of the MCS is considerable.

Seeing that the Kullback-Leibler is not the only formula capable of calculating this measure of information, we opted for the Cauchy-Schwarz divergence, which belongs to the Rényi entropy a more generalized entropy, with the Shannon entropy as particular case of it.

Theoretically the "optimal" distortion should only require an iteration of the MCS to converge, which may prove that other methods might find a better distortion. With this in mind, this dissertation presented a new method for calculating the distribution distortion needed to accelerate the SMCS, based on the Cauchy-Schwarz PDF distance equation (4.1).

However, the Cauchy-Schwarz equation is not as easy to simplify as the Kullback-Leibler, and we had to resort to an optimization method, such as the EPSO, to test if it really resulted in acceptable distortion values compared to Kullback-Leibler distortion.

First tests began to show similarity between each methods values with consistent results from the EPSO. The next step was to saturate it with 30 runs with different MATLAB seeds and using the mean values of the resulting distortions in the SMCS to compare its effectiveness with the KL CE.

After another 30 runs with different seeds this time of the SMCS with the new distortion and despite the considerable difference in years simulated to converge between the two methods, which were still less with the KL distortion. The Cauchy-Schwarz still proved beneficial in comparison to the crude SMCS, even with the values obtained from the EPSO which does not guarantee the global optimal.

With these results instigating further research, upon closer inspection of equation (4.5), the binomial derivatives and after a few simplifications, we arrived at a simpler equation (4.21), yet still not a close-form expression.

Firstly, we opted to test this new update expression with a simple numeric example which led to some interesting observations. Namely with multiple cases in which the CS distortion was beneficial in comparison to the KL distortion. However, these conclusions also depend on the characteristics of the system under analysis and its load diagram.

Adapting the Kullback-Leibler cross-entropy multi-level algorithm to our updating expression (4.22) and using the previous explained solver algorithm, LSQNONLIN available in MATLAB, allowed for further testing.

The new test results kept tending to the same similarity relations observed before with the CS EPSO distortion. Again saturating the new method with 30 runs each with different seeds and using the mean values in the SMCS, showed an increase in efficiency compared to the CS EPSO distortion. However closer to the Kullback-Leibler mean simulated years are, with the exception of the test with a 0.7 peak reduction factor, the other tests result kept being worse than with the KL distortion.

Through chart analyses, we really can observe the similarity between the two method's distorted distributions, with the Kullback-Leibler distribution in most cases being more concentrated around the targeted peak demand than the Cauchy-Schwarz. This might help shed a light in previous results, the MCS estimates three important indices the LOLE (hours/year), the EENS (MWh/year) and the LOLF

(occurrences/year). The first two indices benefit from a distribution with more load shedding occurrences for any available capacity, the LOLF benefits from available capacities more concentrated around the target peak demand.

Seeing that all three indices must achieve the same coefficient of variation in order for the SMCS to converge, this explains the particular advantage of the Kullback-Leibler in these studied cases which offers a middle ground between the three.

To claim the Cauchy-Schwarz CE method as superior alternative to the Kullback-Leibler CE, we would require more tests with more systems, for different load diagrams and with multiple and varied generating system compositions. Therefore, more time and further tests may prove advantageous to better define the two methodologies. Mainly by comparing them with a SMCS estimating only the LOLE and the EENS, and observing what are the implications from that.

The main conclusion to this work, is that it shows that we can use other cross-entropy formulas in trying to achieve the "optimal" distortion, such as the Cauchy-Schwarz CE which yet may prove as a viable alternative to the Kullback-Leibler, opening path for other alternatives which may prove advantageous or not depending on the geometry of the problem.

The SMCS obviously stands to gain from further research in this area, with the results of the work developed in this dissertation serving as possible inspiration for other research studies branching from the notions of cross-entropy.

# References


[1] The Basics of Grid Security, Available “http://securethegrid.com/the-basics-of-grid-security/”. Accessed 15-March-2016

[2] R. N. Allan and R. Billinton, *Reliability Evaluation of Power Systems*, 2nd ed. Plenum Press, 1996.

[3] M. V. F. Pereira and N. J. Balu, “Composite generation/transmission reliability evaluation,” *Proceedings of the IEEE*, vol. 80, no. 4, pp. 470–491, Apr. 1992.

[4] A. M. Leite da Silva, L. A. F. Manso, and G. J. Anders, “Composite reliability evaluation for large-scale power systems,” *Proceedings of the IEEE Power Tech Conference*, 2003.

[5] A. M. Leite da Silva, R. A. González-Fernández, and C. Singh, “Generating capacity reliability evaluation based on Monte Carlo simulation and Cross-Entropy methods,” *IEEE Transactions on Power Systems*, vol. 25, no. 1, pp. 129–137, Feb. 2010.

[6] R. A. González-Fernández and A. M. Leite da Silva, “Reliability assessment of time-dependent systems via sequential Cross-Entropy Monte Carlo simulation,” *IEEE Transactions on Power Systems*, vol. 26, no. 4, pp. 2381–2389, Nov. 2011.

[7] R. Billinton and W. Li, *Reliability Assessment of Electric Power Systems using Monte Carlo Methods*. New York: Plenum Press, 1994.

[8] R. Y. Rubinstein and D. P. Kroese, *Simulation and the Monte Carlo method*, 2nd ed. John Wiley & Sons, Inc., 2008.

[9] A. M. Leite da Silva, A. C. G. Melo, and S. H. F. Cunha, “Frequency and duration method for reliability evaluation of large-scale hydrothermal generating systems,” *IEE Proceedings Generation, Transmission and Distribution*, vol. 138, no. 1, pp. 94–102, Jan. 1991.

[10] A. Sankarakrishnan and R. Billinton, “Sequential Monte Carlo simulation for composite power system reliability analysis with time varying loads,” *IEEE Transactions on Power Systems*, vol. 10, no. 3, pp. 1540–1545, Aug. 1995.

[11] V. Miranda, "Fiabilidade em Sistemas de Potencia", Version 3.2, Oporto, September 2015

[12] L. V. Lobo, "Determinacao de Indices de Fiabilidade em Sistemas Electricos Utilizando o Metodo de Monte Carlo", Oporto, September 2000

[13] A. Teixeira de Sousa, "Estudos de Fiabilidade Utilizando o Metodo de Simulacao de Monte Carlo Integrando Informacao Expressa sob a Forma de Numeros Imprecisos", Oporto, September 1997

[14] Leonel Carvalho, "Advances on the Sequential Monte Carlo Reliability Assessment of Generation-Transmission Systems using Cross-Entropy and Population-based Methods", PhD Thesis, FUP, University of Porto, Portugal, March 2013

[15] W.LI, and Billinton R., "Reliability Assessment of Electric Power Systems Using Monte Carlo Methods", 1st Edition, Plenum Press, 1994

[16] S. M. Ross, *Introduction to Probability Models*, 10th ed. Academic Press, Inc., 2006.

[17] M. A. Matos, J. A. Peças Lopes, M. A. da Rosa, R. Ferreira, A. M. Leite da Silva, W. Sales, L. Resende, L. A. . . Manso, P. Cabral, M. Ferreira, N. Martins, C. Artaiz, F. Soto, and R. López, "Probabilistic evaluation of reserve requirements of generating systems with renewable power sources: the Portuguese and Spanish cases," *International Journal of Electrical Power & Energy Systems*, vol. 31, no. 9, pp. 562–569, Oct. 2009.

[18] A. M. Leite da Silva, W. S. Sales, L. A. F. Manso, and R. Billinton, "Long-term probabilistic evaluation of operating reserve requirements with renewable sources," *IEEE Transactions on Power Systems*, vol. 25, no. 1, pp. 106–116, Feb. 2010.

[19] P.T. De Boer, D.P. Kroese, S. Mannor, and R.Y. Rubinstein, "A Tutorial on the Cross-Entropy Method", *Annals of Operations Research*, vol. 134, pp. 19-67, 2005.

[20] Leonel Magalhães Carvalho, Reinaldo Andrés González-Fernández, Armando Martins Leite da Silva, Mauro Augusto da Rosa and Vladimiro Miranda, "Simplified Cross-Entropy Based Approach for Generating Capacity Reliability Assessment", IEEE Transactions on Power Systems, vol.28, no.2, pp.1609-1616, May 2013, doi: 10.1109/TPWRS.2012.2213618

[21] P. M. Subcommittee, "IEEE Reliability Test System," *IEEE Transactions on Power Apparatus and Systems*, vol. PAS-98, no. 6, pp. 2047–2054, Nov. 1979.

[22] C. Grigg, P. Wong, P. Albrecht, R. Allan, M. Bhavaraju, R. Billinton, Q. Chen, C. Fong, S. Haddad, S. Kuruganty, W. Li, R. Mukerji, D. Patton, N. Rau, D. Reppen, A. Schneider, M. Shahidehpour, and C. Singh, "The IEEE reliability test system-1996. A report prepared by the reliability test system task force of the application of probability methods subcommittee," *IEEE Transctions on Power Systems*, vol. 14, no. 3, pp. 1010–1020, Aug. 1999.

[23] R. Jenssen, D. Erdogmus, K.E. Hill, J.C. Principe, and T. Eltoft, "Optimizing the Cauchy-Schwarz PDF Distance for Information Theoretic, Non-Parametric Clustering", 2005

[24] J. Principe, D. X, and J. Fisher, "Information Theoretic Learning", in *Unsupervised Adaptive Filter*, S. Haykin (Ed.), John Wiley & Sons, New York, 2000, vol. I, Chapter 7

[25] Blum, C, and Roli, A. "Metaheuristics in combinatorial optimization: Overview and conceptual comparison", *ACM Computing Surveys*: 268–308, 2003.

[26] V. Miranda, "Computação Evolucionaria: Uma Introdução", Version 2.1, pp. 26-28, FEUP, Oporto, 2005

[27] About EPSO. Available: "http://epso.inescporto.pt/". Accessed 20-April-2016

[28] Vladimiro Miranda, Leonel Magalhães Carvalho, Mauro Augusto da Rosa, Armando Martins Leite da Silva and Chanan Singh, "Improving Power System Reliability Calculation Efficiency With EPSO Variants", IEEE Transactions on Power Systems, vol.24, no.4, pp.1772-1779, November 2009, doi: 10.1109/TPWRS.2009.2030397

[29] Leonel Magalhães Carvalho, Diego Issicaba, Mauro Augusto da Rosa, Joel Veiga Ramos and Vladimiro Miranda, "Reliability Evaluation of Generation Systems via Sequential Population-Based Monte Carlo Simulation", Proceedings of PMAPS 2012 - International Conference on Probabilistic Methods Applied to Power Systems, Istanbul, Turkey, June 2012.

[30] LSQNONLIN. Available: “http://www.mathworks.com/help/optim/ug/lsqnonlin.html”. Acessed 10-June-2016

[31] Equation Solving Algorithms. Available: “http://www.mathworks.com/help/optim/ug/equation-solving-algorithms.html” . Accessed 10-June-2016

# Annex A – Cauchy-Schwarz EPSO CE parameters tests

**Table A. 1** – Test results for CS EPSO distortion with 10 000 sample for different EPSO max generations with a peak reduction factor of 0.6 and the common parameters: mutation rate 0.4, communication probability of 0.7 and a population size of 50

| Group | $v_i$ | 10 000 Samples | | | |
|---|---|---|---|---|---|
| | Kullback-Leibler CE | Cauchy-Schwarz CE | | | |
| 1 | 0.9781 | 0.9900 | 0.9826 | 0.9838 | 0.9852 |
| 2 | 0.8742 | 0.8928 | 0.9028 | 0.8918 | 0.8896 |
| 4 | 0.9463 | 0.9900 | 0.9836 | 0.9610 | 0.9772 |
| 5 | 0.8750 | 0.9250 | 0.9382 | 0.9446 | 0.9422 |
| 6 | 0.7069 | 0.7179 | 0.7032 | 0.7008 | 0.7111 |
| 7 | 0.4359 | 0.4647 | 0.4415 | 0.3885 | 0.3844 |
| 8 | 0.0167 | 0.1551 | 0.1690 | 0.1842 | 0.1786 |
| 9 | 0.0054 | 0.0718 | 0.0190 | 0.0257 | 0.0228 |
| 3 | 0.9820 | 0.9900 | 0.9836 | 0.9852 | 0.9862 |
| EPSO Max Generation | | 10 | 15 | 20 | 25 |

**Table A. 2** – Test results for CS EPSO distortion with 15 000 sample for different EPSO max generations with a peak reduction factor of 0.6 and the common parameters: mutation rate 0.4, communication probability of 0.7 and a population size of 50

| Group | $v_i$ | 15 000 Samples | | | |
|---|---|---|---|---|---|
| | Kullback-Leibler CE | Cauchy-Schwarz CE | | | |
| 1 | 0.9781 | 0.9871 | 0.9900 | 0.9900 | 0.9896 |
| 2 | 0.8742 | 0.9266 | 0.9117 | 0.9061 | 0.9012 |
| 4 | 0.9463 | 0.9765 | 0.9900 | 0.9832 | 0.9587 |
| 5 | 0.8750 | 0.9818 | 0.9891 | 0.9900 | 0.9677 |
| 6 | 0.7069 | 0.6586 | 0.6969 | 0.7160 | 0.7107 |
| 7 | 0.4359 | 0.4242 | 0.3703 | 0.3610 | 0.3542 |
| 8 | 0.0167 | 0.2924 | 0.2964 | 0.1200 | 0.0103 |
| 9 | 0.0054 | 0.2154 | 0.1368 | 0.0711 | 0.0288 |
| 3 | 0.9820 | 0.9787 | 0.9900 | 0.9766 | 0.9678 |
| EPSO Max Generation | | 10 | 15 | 20 | 25 |

**Table A. 3** – Test results for CS EPSO distortion with 20 000 sample for different EPSO max generations with a peak reduction factor of 0.6 and the common parameters: mutation rate 0.4, communication probability of 0.7 and a population size of 50

| Group | $v_i$ | 20 000 Samples | | | |
|---|---|---|---|---|---|
| | Kullback-Leibler CE | Cauchy-Schwarz CE | | | |
| 1 | 0.9781 | 0.9774 | 0.9900 | 0.9812 | 0.9814 |
| 2 | 0.8742 | 0.9900 | 0.9141 | 0.8927 | 0.8977 |
| 4 | 0.9463 | 0.9277 | 0.9803 | 0.9580 | 0.9645 |
| 5 | 0.8750 | 0.9461 | 0.9436 | 0.9433 | 0.9445 |
| 6 | 0.7069 | 0.7177 | 0.7203 | 0.7047 | 0.7043 |
| 7 | 0.4359 | 0.3984 | 0.3702 | 0.3637 | 0.3615 |
| 8 | 0.0167 | 0.2267 | 0.0115 | 0.0320 | 0.0196 |
| 9 | 0.0054 | 0.1481 | 0.1123 | 0.0952 | 0.0859 |
| 3 | 0.9820 | 0.9755 | 0.9721 | 0.9712 | 0.9818 |
| EPSO Max Generation | | 10 | 15 | 20 | 25 |

**Table A. 4** – Test results for CS EPSO distortion with 25 000 sample for different EPSO max generations with a peak reduction factor of 0.6 and the common parameters: mutation rate 0.4, communication probability of 0.7 and a population size of 50

| Group | $v_i$ | 25 000 Samples | | | |
|---|---|---|---|---|---|
| | Kullback-Leibler CE | Cauchy-Schwarz CE | | | |
| 1 | 0.9781 | 0.9900 | 0.9900 | 0.9806 | 0.9807 |
| 2 | 0.8742 | 0.9417 | 0.9229 | 0.9018 | 0.9023 |
| 4 | 0.9463 | 0.9443 | 0.9653 | 0.9723 | 0.9723 |
| 5 | 0.8750 | 0.9719 | 0.9699 | 0.9900 | 0.9899 |
| 6 | 0.7069 | 0.7306 | 0.7195 | 0.7147 | 0.7158 |
| 7 | 0.4359 | 0.2679 | 0.3568 | 0.3388 | 0.3538 |
| 8 | 0.0167 | 0.1533 | 0.0814 | 0.0600 | 0.0602 |
| 9 | 0.0054 | 0.1119 | 0.0892 | 0.0491 | 0.0487 |
| 3 | 0.9820 | 0.9594 | 0.9842 | 0.9850 | 0.9851 |
| EPSO Max Generation | | 10 | 15 | 20 | 25 |

**Table A. 5** – Test results for CS EPSO distortion with 15 000 sample for different EPSO Population sizes with a peak reduction factor of 0.6 and the common parameters: mutation rate 0.4, communication probability of 0.7 and max generation of 50

| Group | $v_i$ | 15 000 Samples | | | | | |
|---|---|---|---|---|---|---|---|
| | Kullback-Leibler CE | Cauchy-Schwarz CE | | | | | |
| 1 | 0.9781 | 0.9900 | 0.9705 | 0.9613 | 0.9896 | 0.9878 | 0.9650 |
| 2 | 0.8742 | 0.8986 | 0.8976 | 0.9051 | 0.9012 | 0.9006 | 0.9018 |
| 4 | 0.9463 | 0.9745 | 0.9697 | 0.9715 | 0.9587 | 0.9772 | 0.9685 |
| 5 | 0.8750 | 0.9419 | 0.9300 | 0.9709 | 0.9677 | 0.9400 | 0.9414 |
| 6 | 0.7069 | 0.7073 | 0.7124 | 0.7263 | 0.7107 | 0.7301 | 0.7073 |
| 7 | 0.4359 | 0.4055 | 0.3565 | 0.3515 | 0.3542 | 0.3398 | 0.3576 |
| 8 | 0.0167 | 0.1607 | 0.0442 | 0.0520 | 0.0103 | 0.0660 | 0.0142 |
| 9 | 0.0054 | 0.0622 | 0.0556 | 0.0551 | 0.0288 | 0.0163 | 0.0190 |
| 3 | 0.9820 | 0.9837 | 0.9900 | 0.9900 | 0.9678 | 0.9892 | 0.9728 |
| EPSO Population Size | | 25 | 35 | 45 | 50 | 75 | 100 |

**Table A. 6** – Test results for CS EPSO distortion with 15 000 sample for different EPSO Max generations with a peak reduction factor of 0.6 and the common parameters: mutation rate 0.4, communication probability of 0.7 and a population size of 100

| Group | $v_i$ | 15 000 Samples | |
|---|---|---|---|
| | Kullback-Leibler CE | Cauchy-Schwarz CE | |
| 1 | 0.9781 | 0.9650 | 0.9650 |
| 2 | 0.8742 | 0.9018 | 0.8976 |
| 4 | 0.9463 | 0.9685 | 0.9586 |
| 5 | 0.8750 | 0.9414 | 0.9397 |
| 6 | 0.7069 | 0.7073 | 0.7072 |
| 7 | 0.4359 | 0.3576 | 0.3579 |
| 8 | 0.0167 | 0.0142 | 0.0442 |
| 9 | 0.0054 | 0.0190 | 0.0192 |
| 3 | 0.9820 | 0.9728 | 0.9819 |
| Max Generation | | 25 | 35 |

# Annex B – Cauchy-Schwarz EPSO CE test results

**Table B. 1** – Test results for 30 runs of the CS EPSO with different MATLAB seeds and with the common parameters: number of samples 15 000, peak reduction factor of 0.6, mutation rate 0.4, communication probability 0.6, max generation 25, population size 100.

| Cauchy-Schwarz EPSO Cross-Entropy distortion $v_i$ | | | | | | | | | | | |
|---|---|---|---|---|---|---|---|---|---|---|---|
| Seed | Time (s) | Group 1 | Group 2 | Group 4 | Group 5 | Group 6 | Group 7 | Group 8 | Group 9 | Group 3 | BestFit |
| 156412 | 804.94 | 0.9746 | 0.8969 | 0.9818 | 0.9412 | 0.7100 | 0.3373 | 0.0449 | 0.0184 | 0.9894 | 4.80E-01 |
| 348568 | 805.41 | 0.9659 | 0.8999 | 0.9605 | 0.9480 | 0.7048 | 0.3476 | 0.0444 | 0.0135 | 0.9834 | 4.80E-01 |
| 456737 | 791.00 | 0.9809 | 0.8967 | 0.9696 | 0.9399 | 0.7314 | 0.3465 | 0.0695 | 0.0192 | 0.9892 | 4.81E-01 |
| 690896 | 792.04 | 0.9878 | 0.8975 | 0.9770 | 0.9691 | 0.7069 | 0.3469 | 0.0450 | 0.0100 | 0.9900 | 4.76E-01 |
| 324684 | 806.11 | 0.9877 | 0.8976 | 0.9818 | 0.9653 | 0.7302 | 0.3445 | 0.0508 | 0.0190 | 0.9890 | 4.78E-01 |
| 735676 | 796.15 | 0.9629 | 0.9009 | 0.9818 | 0.9653 | 0.7048 | 0.3469 | 0.0818 | 0.0172 | 0.9810 | 4.81E-01 |
| 634235 | 790.63 | 0.9649 | 0.8999 | 0.9708 | 0.9411 | 0.7301 | 0.3575 | 0.0441 | 0.0192 | 0.9860 | 4.75E-01 |
| 978559 | 802.14 | 0.9748 | 0.8978 | 0.9711 | 0.9675 | 0.7051 | 0.3374 | 0.0298 | 0.0190 | 0.9883 | 4.78E-01 |
| 235456 | 823.43 | 0.9648 | 0.9016 | 0.9588 | 0.9669 | 0.7051 | 0.3466 | 0.0525 | 0.0100 | 0.9828 | 4.77E-01 |
| 764868 | 866.71 | 0.9878 | 0.8976 | 0.9567 | 0.9678 | 0.7052 | 0.3468 | 0.0257 | 0.0156 | 0.9888 | 4.78E-01 |
| 542475 | 837.97 | 0.9650 | 0.9011 | 0.9708 | 0.9655 | 0.7305 | 0.3577 | 0.0271 | 0.0192 | 0.9884 | 4.78E-01 |
| 525463 | 854.90 | 0.9688 | 0.8975 | 0.9758 | 0.9701 | 0.7302 | 0.3363 | 0.0322 | 0.0107 | 0.9849 | 4.80E-01 |
| 446367 | 804.15 | 0.9900 | 0.8961 | 0.9818 | 0.9411 | 0.7073 | 0.3550 | 0.1105 | 0.0166 | 0.9855 | 4.82E-01 |
| 895673 | 799.00 | 0.9709 | 0.8953 | 0.9821 | 0.9380 | 0.7069 | 0.3565 | 0.0273 | 0.0160 | 0.9842 | 4.77E-01 |
| 655358 | 791.16 | 0.9871 | 0.9030 | 0.9764 | 0.9690 | 0.7055 | 0.3422 | 0.0450 | 0.0100 | 0.9843 | 4.79E-01 |
| 245365 | 793.90 | 0.9710 | 0.8965 | 0.9756 | 0.9639 | 0.7052 | 0.3549 | 0.0450 | 0.0165 | 0.9850 | 4.78E-01 |
| 213125 | 789.32 | 0.9876 | 0.8868 | 0.9754 | 0.9417 | 0.7299 | 0.3468 | 0.0721 | 0.0279 | 0.9836 | 4.83E-01 |
| 326685 | 786.74 | 0.9900 | 0.8978 | 0.9818 | 0.9675 | 0.7096 | 0.3571 | 0.0430 | 0.0101 | 0.9900 | 4.78E-01 |
| 244765 | 788.94 | 0.9642 | 0.9057 | 0.9589 | 0.9297 | 0.7050 | 0.3582 | 0.0321 | 0.0539 | 0.9730 | 4.87E-01 |
| 425465 | 791.60 | 0.9900 | 0.9009 | 0.9770 | 0.9672 | 0.7302 | 0.3468 | 0.0973 | 0.0171 | 0.9844 | 4.82E-01 |
| 344536 | 795.62 | 0.9650 | 0.8977 | 0.9817 | 0.9370 | 0.7302 | 0.3469 | 0.0499 | 0.0192 | 0.9838 | 4.77E-01 |
| 965734 | 811.16 | 0.9900 | 0.9053 | 0.9587 | 0.9476 | 0.7073 | 0.3570 | 0.0526 | 0.0154 | 0.9808 | 4.80E-01 |
| 907745 | 793.61 | 0.9900 | 0.8970 | 0.9764 | 0.9694 | 0.7072 | 0.3565 | 0.0433 | 0.0100 | 0.9892 | 4.77E-01 |
| 435275 | 800.73 | 0.9875 | 0.8968 | 0.9825 | 0.9672 | 0.7086 | 0.3470 | 0.0455 | 0.0130 | 0.9875 | 4.77E-01 |
| 345546 | 793.33 | 0.9881 | 0.8981 | 0.9817 | 0.9673 | 0.7051 | 0.3469 | 0.0524 | 0.0172 | 0.9849 | 4.76E-01 |
| 423454 | 793.63 | 0.9643 | 0.8978 | 0.9569 | 0.9422 | 0.7320 | 0.3675 | 0.0279 | 0.0296 | 0.9863 | 4.82E-01 |
| 786423 | 799.56 | 0.9899 | 0.8975 | 0.9779 | 0.9673 | 0.7126 | 0.3467 | 0.0471 | 0.0151 | 0.9886 | 4.78E-01 |
| 675678 | 790.17 | 0.9667 | 0.8974 | 0.9845 | 0.9301 | 0.7302 | 0.3572 | 0.0261 | 0.0101 | 0.9857 | 4.79E-01 |
| 453456 | 795.77 | 0.9877 | 0.8987 | 0.9819 | 0.9399 | 0.7265 | 0.3398 | 0.0245 | 0.0191 | 0.9851 | 4.80E-01 |
| 890678 | 799.65 | 0.9877 | 0.8976 | 0.9754 | 0.9452 | 0.7073 | 0.3550 | 0.0381 | 0.0154 | 0.9884 | 4.78E-01 |
| Mean | 802.98 | 0.9784 | 0.8984 | 0.9741 | 0.9546 | 0.7154 | 0.3497 | 0.0476 | 0.0174 | 0.9857 | 0.4790 |

**Table B. 2** – Test results for 30 runs of the CS EPSO with different MATLAB seeds and with the common parameters: number of samples 50 000, peak reduction factor of 0.6, mutation rate 0.4, communication probability 0.6, max generation 50, population size 100.

| Cauchy-Schwarz EPSO Cross-Entropy distortion $v_i$ | | | | | | | | | | | |
|---|---|---|---|---|---|---|---|---|---|---|---|
| Seed | Time (s) | Group 1 | Group 2 | Group 4 | Group 5 | Group 6 | Group 7 | Group 8 | Group 9 | Group 3 | BestFit |
| 156412 | 5254.96 | 0.9799 | 0.8964 | 0.9725 | 0.9465 | 0.7173 | 0.3490 | 0.0208 | 0.0121 | 0.9847 | 4.78E-01 |
| 348568 | 4899.02 | 0.9802 | 0.9024 | 0.9599 | 0.9434 | 0.7098 | 0.3490 | 0.0361 | 0.0130 | 0.9818 | 4.77E-01 |
| 456737 | 5205.16 | 0.9817 | 0.9024 | 0.9725 | 0.9460 | 0.7105 | 0.3492 | 0.0382 | 0.0109 | 0.9784 | 4.77E-01 |
| 690896 | 5141.10 | 0.9889 | 0.8955 | 0.9607 | 0.9392 | 0.7098 | 0.3490 | 0.0284 | 0.0113 | 0.9822 | 4.78E-01 |
| 324684 | 4798.02 | 0.9800 | 0.8942 | 0.9594 | 0.9474 | 0.7107 | 0.3488 | 0.0208 | 0.0130 | 0.9818 | 4.77E-01 |
| 735676 | 5105.93 | 0.9802 | 0.8943 | 0.9606 | 0.9475 | 0.7098 | 0.3488 | 0.0470 | 0.0133 | 0.9819 | 4.77E-01 |
| 634235 | 4784.85 | 0.9802 | 0.8955 | 0.9692 | 0.9441 | 0.7141 | 0.3488 | 0.0165 | 0.0269 | 0.9830 | 4.78E-01 |
| 978559 | 5065.33 | 0.9709 | 0.8953 | 0.9821 | 0.9380 | 0.7069 | 0.3565 | 0.0273 | 0.0160 | 0.9842 | 4.77E-01 |
| 235456 | 5248.24 | 0.9811 | 0.9026 | 0.9599 | 0.9464 | 0.7098 | 0.3488 | 0.0386 | 0.0113 | 0.9820 | 4.77E-01 |
| 764868 | 4798.84 | 0.9802 | 0.9025 | 0.9720 | 0.9438 | 0.7106 | 0.3487 | 0.0234 | 0.0271 | 0.9822 | 4.77E-01 |
| 542475 | 5114.29 | 0.9812 | 0.9015 | 0.9716 | 0.9464 | 0.7098 | 0.3491 | 0.0208 | 0.0122 | 0.9818 | 4.77E-01 |
| 525463 | 5423.59 | 0.9811 | 0.8942 | 0.9722 | 0.9512 | 0.7106 | 0.3488 | 0.0293 | 0.0130 | 0.9820 | 4.77E-01 |
| 446367 | 5196.26 | 0.9779 | 0.9024 | 0.9686 | 0.9439 | 0.7174 | 0.3476 | 0.0193 | 0.0122 | 0.9812 | 4.77E-01 |
| 895673 | 4922.03 | 0.9802 | 0.9025 | 0.9715 | 0.9457 | 0.7098 | 0.3476 | 0.0362 | 0.0133 | 0.9784 | 4.77E-01 |
| 655358 | 4908.62 | 0.9812 | 0.8959 | 0.9686 | 0.9441 | 0.7171 | 0.3488 | 0.0208 | 0.0122 | 0.9818 | 4.77E-01 |
| 245365 | 4958.66 | 0.9802 | 0.8956 | 0.9686 | 0.9475 | 0.7174 | 0.3476 | 0.0275 | 0.0192 | 0.9814 | 4.77E-01 |
| 213125 | 5266.05 | 0.9796 | 0.8944 | 0.9620 | 0.9434 | 0.7104 | 0.3542 | 0.0294 | 0.0133 | 0.9888 | 4.79E-01 |
| 326685 | 5072.23 | 0.9802 | 0.8934 | 0.9607 | 0.9460 | 0.7105 | 0.3542 | 0.0361 | 0.0271 | 0.9819 | 4.78E-01 |
| 244765 | 4739.23 | 0.9891 | 0.8961 | 0.9687 | 0.9475 | 0.7105 | 0.3488 | 0.0370 | 0.0130 | 0.9784 | 4.78E-01 |
| 425465 | 4778.76 | 0.9802 | 0.9097 | 0.9727 | 0.9881 | 0.7173 | 0.3460 | 0.0204 | 0.0269 | 0.9791 | 4.83E-01 |
| 344536 | 4926.85 | 0.9811 | 0.8959 | 0.9606 | 0.9439 | 0.7105 | 0.3488 | 0.0193 | 0.0130 | 0.9814 | 4.77E-01 |
| 965734 | 4874.26 | 0.9802 | 0.8959 | 0.9611 | 0.9392 | 0.7105 | 0.3460 | 0.0376 | 0.0134 | 0.9825 | 4.77E-01 |
| 907745 | 4754.27 | 0.9802 | 0.9041 | 0.9725 | 0.9392 | 0.7171 | 0.3551 | 0.0364 | 0.0129 | 0.9791 | 4.77E-01 |
| 435275 | 4756.64 | 0.9811 | 0.8942 | 0.9692 | 0.9464 | 0.7103 | 0.3488 | 0.0386 | 0.0266 | 0.9814 | 4.77E-01 |
| 345546 | 4856.57 | 0.9802 | 0.8955 | 0.9686 | 0.9434 | 0.7174 | 0.3490 | 0.0327 | 0.0133 | 0.9785 | 4.77E-01 |
| 423454 | 5142.46 | 0.9802 | 0.9030 | 0.9606 | 0.9460 | 0.7099 | 0.3541 | 0.0283 | 0.0271 | 0.9825 | 4.78E-01 |
| 786423 | 4990.81 | 0.9802 | 0.9016 | 0.9613 | 0.9460 | 0.7100 | 0.3541 | 0.0297 | 0.0122 | 0.9821 | 4.77E-01 |
| 675678 | 5119.61 | 0.9802 | 0.8953 | 0.9685 | 0.9460 | 0.7098 | 0.3490 | 0.0208 | 0.0269 | 0.9818 | 4.78E-01 |
| 453456 | 5202.06 | 0.9817 | 0.8955 | 0.9725 | 0.9426 | 0.7174 | 0.3552 | 0.0386 | 0.0121 | 0.9809 | 4.77E-01 |
| 890678 | 5056.55 | 0.9802 | 0.9031 | 0.9614 | 0.9434 | 0.7084 | 0.3458 | 0.0284 | 0.0119 | 0.9810 | 4.77E-01 |
| Mean | 5012.04 | 0.9806 | 0.8984 | 0.9670 | 0.9461 | 0.7120 | 0.3498 | 0.0295 | 0.0162 | 0.9816 | 0.4775 |

**Table B. 3** - SMCS test results obtained with the Kullback-Leibler distortion and the CE EPSO distortions for 15 000 samples and 50 000 samples

| SMCS Simulated years towards converge | | | |
|---|---|---|---|
| Seed | SMCS w/ KL $v_i$ | SMCS w/ CS EPSO 15k samples $v_i$ | SMCS w/ CS EPSO 50k samples $v_i$ |
| 34563457 | 76 | 192 | 177 |
| 45667 | 65 | 295 | 120 |
| 64356345 | 59 | 172 | 221 |
| 562434 | 67 | 137 | 131 |
| 45645634 | 67 | 153 | 280 |
| 673456586 | 69 | 176 | 262 |
| 6574564 | 56 | 143 | 246 |
| 6767867 | 77 | 161 | 151 |
| 467467 | 62 | 165 | 329 |
| 645645664 | 64 | 134 | 98 |
| 3635643 | 79 | 189 | 339 |
| 363543453 | 66 | 143 | 129 |
| 3636 | 79 | 234 | 108 |
| 435687 | 70 | 203 | 150 |
| 9078345 | 43 | 178 | 157 |
| 39047589 | 52 | 2 | 98 |
| 507858936 | 69 | 148 | 185 |
| 8973478 | 58 | 175 | 192 |
| 97345873 | 65 | 141 | 201 |
| 893246583 | 67 | 138 | 104 |
| 86345873 | 67 | 425 | 190 |
| 21763 | 52 | 159 | 120 |
| 3456789 | 53 | 213 | 146 |
| 5636 | 51 | 126 | 156 |
| 90854902 | 65 | 355 | 226 |
| 87539 | 49 | 178 | 175 |
| 35773456 | 71 | 257 | 275 |
| 538754 | 57 | 234 | 156 |
| 38975983 | 76 | 148 | 161 |
| 908734 | 84 | 181 | 130 |
| Mean | 64.50 | 185.17 | 180.43 |

# Annex C – Cauchy-Schwarz CE parameter tests

**Table C. 1** – Test results for the Cauchy-Schwarz CE distortion with different number of samples and lb = 0.01 and ub = 0.99 for a peak reduction factor of 0.6

| Constraints | Samples | Cauchy-Schwarz EPSO Cross-Entropy distortion $v_i$ | | | | | | | | |
|---|---|---|---|---|---|---|---|---|---|---|
| | | Seed | Group 1 | Group 2 | Group 4 | Group 5 | Group 6 | Group 7 | Group 8 | Group 9 | Group 3 |
| Lower Bound = 0.01 Upper Bound = 0.99 | 10 000 | 156412 | 0.9822 | 0.9900 | 0.9682 | 0.9456 | 0.7144 | 0.3462 | 0.0100 | 0.0100 | 0.9865 |
| | | 348568 | 0.9799 | 0.8997 | 0.9717 | 0.9538 | 0.7156 | 0.3490 | 0.0135 | 0.0117 | 0.9862 |
| | | 456737 | 0.9900 | 0.8975 | 0.1685 | 0.3694 | 0.0100 | 0.9900 | 0.9900 | 0.1735 | 0.9900 |
| | | 690896 | 0.9900 | 0.9507 | 0.1488 | 0.0100 | 0.2857 | 0.1695 | 0.6913 | 0.0100 | 0.0996 |
| | | 324684 | 0.9766 | 0.9024 | 0.9642 | 0.9366 | 0.7132 | 0.3539 | 0.0100 | 0.0100 | 0.9838 |
| | 25 000 | 156412 | 0.9786 | 0.9003 | 0.9660 | 0.9421 | 0.7112 | 0.3459 | 0.0100 | 0.0218 | 0.9845 |
| | | 348568 | 0.9804 | 0.8960 | 0.9708 | 0.9388 | 0.7097 | 0.3448 | 0.0123 | 0.0100 | 0.9869 |
| | | 456737 | 0.9816 | 0.8999 | 0.9697 | 0.9429 | 0.7009 | 0.3513 | 0.0216 | 0.0100 | 0.9882 |
| | | 690896 | 0.9827 | 0.8928 | 0.9750 | 0.9416 | 0.7143 | 0.3569 | 0.0100 | 0.0100 | 0.9859 |
| | | 324684 | 0.9827 | 0.8973 | 0.9690 | 0.9376 | 0.7081 | 0.3531 | 0.0100 | 0.0100 | 0.9856 |
| | 50 000 | 156412 | 0.9802 | 0.8979 | 0.9707 | 0.9407 | 0.7111 | 0.3558 | 0.0100 | 0.0100 | 0.9850 |
| | | 348568 | 0.9762 | 0.8966 | 0.9709 | 0.9502 | 0.5192 | 0.0100 | 0.9900 | 0.0100 | 0.9861 |
| | | 456737 | 0.9801 | 0.8952 | 0.9713 | 0.9428 | 0.7151 | 0.3499 | 0.0100 | 0.0100 | 0.9868 |
| | | 690896 | 0.9811 | 0.9014 | 0.9670 | 0.9424 | 0.7149 | 0.3564 | 0.0100 | 0.0100 | 0.9857 |
| | | 324684 | 0.9796 | 0.9016 | 0.9717 | 0.9459 | 0.7095 | 0.3483 | 0.0100 | 0.0100 | 0.9871 |

**Table C. 2** – Test results for the Cauchy-Schwarz CE distortion with different number of samples and lb = 0.001 and ub = 0.999 for a peak reduction factor of 0.6

| Constraints | Samples | Cauchy-Schwarz EPSO Cross-Entropy distortion $v_i$ | | | | | | | | |
|---|---|---|---|---|---|---|---|---|---|---|
| | | Seed | Group 1 | Group 2 | Group 4 | Group 5 | Group 6 | Group 7 | Group 8 | Group 9 | Group 3 |
| Lower Bound = 0.001 Upper Bound = 0.999 | 10 000 | 156412 | 0.9820 | 0.9990 | 0.9682 | 0.9450 | 0.7136 | 0.3484 | 0.0010 | 0.0010 | 0.9862 |
| | | 348568 | 0.9798 | 0.9002 | 0.9719 | 0.9560 | 0.7135 | 0.3488 | 0.0136 | 0.0010 | 0.9862 |
| | | 456737 | 0.9692 | 0.9988 | 0.9840 | 0.8437 | 0.1927 | 0.7784 | 0.0010 | 0.6687 | 0.8991 |
| | | 690896 | 0.7836 | 0.8816 | 0.3318 | 0.0072 | 0.1998 | 0.1150 | 0.4978 | 0.0010 | 0.2582 |
| | | 324684 | 0.9767 | 0.9046 | 0.9639 | 0.9366 | 0.7138 | 0.3534 | 0.0010 | 0.0010 | 0.9830 |
| | 25 000 | 156412 | 0.9805 | 0.9007 | 0.9709 | 0.9437 | 0.7109 | 0.3441 | 0.0017 | 0.0010 | 0.9855 |
| | | 348568 | 0.9796 | 0.8945 | 0.9705 | 0.9384 | 0.7104 | 0.3447 | 0.0125 | 0.0010 | 0.9871 |
| | | 456737 | 0.9814 | 0.9004 | 0.9697 | 0.9431 | 0.7005 | 0.3514 | 0.0010 | 0.0010 | 0.9881 |
| | | 690896 | 0.9833 | 0.8920 | 0.9751 | 0.9430 | 0.7133 | 0.3565 | 0.0010 | 0.0010 | 0.9866 |
| | | 324684 | 0.9826 | 0.8965 | 0.9683 | 0.9378 | 0.7081 | 0.3532 | 0.0010 | 0.0010 | 0.9857 |
| | 50 000 | 156412 | 0.9800 | 0.8975 | 0.9708 | 0.9406 | 0.7110 | 0.3555 | 0.0010 | 0.0016 | 0.9850 |
| | | 348568 | 0.9809 | 0.8957 | 0.9744 | 0.9527 | 0.5017 | 0.0010 | 0.9990 | 0.0032 | 0.9882 |
| | | 456737 | 0.9780 | 0.8971 | 0.9719 | 0.9440 | 0.7151 | 0.3511 | 0.0030 | 0.0010 | 0.9867 |
| | | 690896 | 0.9810 | 0.9013 | 0.9667 | 0.9422 | 0.7151 | 0.3565 | 0.0018 | 0.0010 | 0.9859 |
| | | 324684 | 0.9795 | 0.9018 | 0.9717 | 0.9458 | 0.7103 | 0.3490 | 0.0010 | 0.0010 | 0.9871 |

**Table C. 3** – Test results for the Cauchy-Schwarz CE distortion with different number of samples and lb = 0.001 and ub = 0.999 for a peak reduction factor of 0.6

| Constraints | Samples | Cauchy-Schwarz EPSO Cross-Entropy distortion $v_i$ | | | | | | | | | |
|---|---|---|---|---|---|---|---|---|---|---|---|
| | | Seed | Group 1 | Group 2 | Group 4 | Group 5 | Group 6 | Group 7 | Group 8 | Group 9 | Group 3 |
| $v_{t-1}$ Lower Bound = 0.001 Upper Bound = | 10 000 | 156412 | 0.9770 | 0.8927 | 0.9717 | 0.9412 | 0.7155 | 0.3488 | 0.0177 | 0.0100 | 0.9833 |
| | | 348568 | 0.9592 | 0.8517 | 0.9612 | 0.9207 | 0.7099 | 0.3448 | 0.0206 | 0.0100 | 0.9698 |
| | | 456737 | 0.9456 | 0.8879 | 0.5750 | 0.7662 | 0.7555 | 0.4197 | 0.0286 | 0.0126 | 0.7271 |
| | | 690896 | 0.9800 | 0.9000 | 0.2609 | 0.0100 | 0.3726 | 0.1521 | 0.0275 | 0.0100 | 0.1263 |
| | | 324684 | 0.9560 | 0.8577 | 0.9520 | 0.9331 | 0.7148 | 0.3600 | 0.0410 | 0.0100 | 0.9687 |
| | 25 000 | 156412 | 0.9636 | 0.8506 | 0.9559 | 0.9281 | 0.7105 | 0.3556 | 0.0556 | 0.0312 | 0.9666 |
| | | 348568 | 0.0534 | 0.8282 | 0.0102 | 0.0207 | 0.0147 | 0.0183 | 0.0100 | 0.0113 | 0.0100 |
| | | 456737 | 0.9559 | 0.8564 | 0.9581 | 0.9307 | 0.7076 | 0.3543 | 0.0369 | 0.0145 | 0.9818 |
| | | 690896 | 0.9626 | 0.8419 | 0.9456 | 0.9051 | 0.7068 | 0.3624 | 0.0100 | 0.0178 | 0.9757 |
| | | 324684 | 0.9600 | 0.8524 | 0.9584 | 0.9224 | 0.7111 | 0.3611 | 0.0485 | 0.0156 | 0.9777 |
| | 50 000 | 156412 | 0.9780 | 0.8967 | 0.9712 | 0.9404 | 0.7113 | 0.3552 | 0.0100 | 0.0100 | 0.9849 |
| | | 348568 | 0.9692 | 0.8497 | 0.9146 | 0.8201 | 0.7070 | 0.3708 | 0.0456 | 0.0330 | 0.9680 |
| | | 456737 | 0.9788 | 0.8951 | 0.9712 | 0.9417 | 0.7147 | 0.3500 | 0.0100 | 0.0100 | 0.9865 |
| | | 690896 | 0.9604 | 0.8499 | 0.9617 | 0.9227 | 0.7149 | 0.3584 | 0.0100 | 0.0100 | 0.9736 |
| | | 324684 | 0.9560 | 0.8509 | 0.9567 | 0.9262 | 0.7070 | 0.3584 | 0.0322 | 0.0174 | 0.9760 |

# Annex D – Cauchy-Schwarz CE test results

**Table D. 1 -** Test results for 30 runs of the Cauchy-Schwarz CE with different MATLAB seeds and with the common parameters: number of samples 50 000, lb = 0.01 and ub = $v_{t-1}$ for a peak reduction factor of 0.6

| Cauchy-Schwarz EPSO Cross-Entropy distortion $v_i$ | | | | | | | | | | |
|---|---|---|---|---|---|---|---|---|---|---|
| Seed | Time (s) | Group 1 | Group 2 | Group 4 | Group 5 | Group 6 | Group 7 | Group 8 | Group 9 | Group 3 |
| 156412 | 303.36 | 0.9780 | 0.8967 | 0.9712 | 0.9404 | 0.7113 | 0.3552 | 0.0100 | 0.0100 | 0.9849 |
| 348568 | 43.90 | 0.9692 | 0.8497 | 0.9146 | 0.8201 | 0.7070 | 0.3708 | 0.0456 | 0.0330 | 0.9680 |
| 456737 | 49.74 | 0.9788 | 0.8951 | 0.9712 | 0.9417 | 0.7147 | 0.3500 | 0.0100 | 0.0100 | 0.9865 |
| 690896 | 48.32 | 0.9604 | 0.8499 | 0.9617 | 0.9227 | 0.7149 | 0.3584 | 0.0100 | 0.0100 | 0.9736 |
| 324684 | 44.54 | 0.9560 | 0.8509 | 0.9567 | 0.9262 | 0.7070 | 0.3584 | 0.0322 | 0.0174 | 0.9760 |
| 735676 | 42.82 | 0.9601 | 0.8401 | 0.9553 | 0.9173 | 0.7131 | 0.3587 | 0.0622 | 0.0100 | 0.9741 |
| 634235 | 52.37 | 0.9789 | 0.8949 | 0.9719 | 0.9396 | 0.7128 | 0.3532 | 0.0100 | 0.0100 | 0.9874 |
| 978559 | 54.69 | 0.9782 | 0.8964 | 0.9700 | 0.9418 | 0.7120 | 0.3532 | 0.0100 | 0.0100 | 0.9865 |
| 235456 | 65.45 | 0.9784 | 0.8939 | 0.9687 | 0.9408 | 0.7150 | 0.3518 | 0.0100 | 0.0100 | 0.9859 |
| 764868 | 42.86 | 0.9621 | 0.8477 | 0.9603 | 0.9312 | 0.7119 | 0.3620 | 0.0482 | 0.0245 | 0.9754 |
| 542475 | 46.31 | 0.9585 | 0.8401 | 0.9441 | 0.9150 | 0.7084 | 0.3566 | 0.0366 | 0.0100 | 0.9779 |
| 525463 | 122.55 | 0.7260 | 0.3159 | 0.6342 | 0.0100 | 0.5156 | 0.4326 | 0.0100 | 0.0126 | 0.7716 |
| 446367 | 66.75 | 0.9782 | 0.8959 | 0.9716 | 0.9448 | 0.7126 | 0.3551 | 0.0100 | 0.0100 | 0.9853 |
| 895673 | 42.11 | 0.9619 | 0.8443 | 0.9573 | 0.9228 | 0.7090 | 0.3544 | 0.0100 | 0.0100 | 0.9786 |
| 655358 | 46.90 | 0.9770 | 0.9000 | 0.9684 | 0.9475 | 0.7140 | 0.3510 | 0.0191 | 0.0100 | 0.9870 |
| 245365 | 50.75 | 0.9579 | 0.8483 | 0.9624 | 0.9246 | 0.7105 | 0.3610 | 0.0432 | 0.0203 | 0.9696 |
| 213125 | 54.63 | 0.9622 | 0.8491 | 0.9518 | 0.9230 | 0.7110 | 0.3615 | 0.0144 | 0.0100 | 0.9744 |
| 326685 | 297.38 | 0.9774 | 0.8986 | 0.9703 | 0.9417 | 0.7157 | 0.3539 | 0.0100 | 0.0100 | 0.9870 |
| 244765 | 50.16 | 0.9651 | 0.8466 | 0.9538 | 0.9352 | 0.7082 | 0.3535 | 0.0100 | 0.0100 | 0.9729 |
| 425465 | 51.87 | 0.9578 | 0.8395 | 0.9605 | 0.9177 | 0.7118 | 0.3551 | 0.0169 | 0.0212 | 0.9808 |
| 344536 | 42.27 | 0.9566 | 0.8500 | 0.9623 | 0.9293 | 0.7112 | 0.3605 | 0.0182 | 0.0104 | 0.9670 |
| 965734 | 50.43 | 0.9778 | 0.8965 | 0.9703 | 0.9381 | 0.7135 | 0.3503 | 0.0125 | 0.0100 | 0.9861 |
| 907745 | 55.05 | 0.9780 | 0.8956 | 0.9726 | 0.9442 | 0.7124 | 0.3519 | 0.0100 | 0.0100 | 0.9859 |
| 435275 | 56.59 | 0.9775 | 0.8907 | 0.9719 | 0.9450 | 0.7117 | 0.3475 | 0.0228 | 0.0100 | 0.9851 |
| 345546 | 58.28 | 0.9786 | 0.8991 | 0.9702 | 0.9408 | 0.7119 | 0.3507 | 0.0100 | 0.0100 | 0.9875 |
| 423454 | 58.12 | 0.9784 | 0.8968 | 0.9718 | 0.9421 | 0.7152 | 0.3496 | 0.0100 | 0.0100 | 0.9871 |
| 786423 | 59.87 | 0.9778 | 0.8951 | 0.9727 | 0.9465 | 0.7108 | 0.3562 | 0.0100 | 0.0100 | 0.9860 |
| 675678 | 43.86 | 0.9565 | 0.8492 | 0.9510 | 0.9201 | 0.7113 | 0.3612 | 0.0100 | 0.0100 | 0.9750 |
| 453456 | 53.73 | 0.9576 | 0.8432 | 0.9517 | 0.9327 | 0.7108 | 0.3552 | 0.0214 | 0.0118 | 0.9860 |
| 890678 | 68.70 | 0.9783 | 0.8965 | 0.9723 | 0.9413 | 0.7132 | 0.3610 | 0.0100 | 0.0100 | 0.9855 |
| Mean | 70.81 | 0.9613 | 0.8535 | 0.9514 | 0.8995 | 0.7053 | 0.3584 | 0.0188 | 0.0124 | 0.9738 |

**Table D. 2 -** Test results for 30 runs of the Cauchy-Schwarz CE with different MATLAB seeds and with the common parameters: number of samples 50 000, lb = 0.01 and ub = $v_{t-1}$ for a peak reduction factor of 0.7

| Cauchy-Schwarz EPSO Cross-Entropy distortion $v_i$ | | | | | | | | | | |
|---|---|---|---|---|---|---|---|---|---|---|
| Seed | Time (s) | Group 1 | Group 2 | Group 4 | Group 5 | Group 6 | Group 7 | Group 8 | Group 9 | Group 3 |
| 156412 | 58.83 | 0.9780 | 0.8967 | 0.9263 | 0.9584 | 0.7333 | 0.6324 | 0.0100 | 0.0100 | 0.9893 |
| 348568 | 39.07 | 0.9659 | 0.8497 | 0.9049 | 0.7964 | 0.7356 | 0.5464 | 0.7841 | 0.0557 | 0.9673 |
| 456737 | 52.22 | 0.9788 | 0.8967 | 0.9275 | 0.9538 | 0.7342 | 0.6354 | 0.0100 | 0.0121 | 0.9882 |
| 690896 | 46.17 | 0.9604 | 0.8499 | 0.9276 | 0.8286 | 0.7773 | 0.6387 | 0.0596 | 0.0246 | 0.9720 |
| 324684 | 44.76 | 0.9560 | 0.8509 | 0.9327 | 0.8237 | 0.7741 | 0.6412 | 0.0545 | 0.0271 | 0.9729 |
| 735676 | 42.57 | 0.9601 | 0.8401 | 0.9361 | 0.8190 | 0.7796 | 0.6406 | 0.0543 | 0.0243 | 0.9716 |
| 634235 | 53.87 | 0.9772 | 0.8878 | 0.9272 | 0.8368 | 0.7721 | 0.6339 | 0.0100 | 0.0100 | 0.9838 |
| 978559 | 54.06 | 0.9782 | 0.8964 | 0.9220 | 0.9520 | 0.7406 | 0.6325 | 0.0100 | 0.0100 | 0.9895 |
| 235456 | 57.48 | 0.9784 | 0.8939 | 0.9238 | 0.9561 | 0.7385 | 0.6326 | 0.0100 | 0.0138 | 0.9833 |
| 764868 | 38.66 | 0.9621 | 0.8477 | 0.9330 | 0.8258 | 0.7750 | 0.6401 | 0.0530 | 0.0192 | 0.9736 |
| 542475 | 46.90 | 0.9585 | 0.8401 | 0.9329 | 0.8267 | 0.7768 | 0.6377 | 0.0397 | 0.0266 | 0.9733 |
| 525463 | 50.43 | 0.9779 | 0.8961 | 0.9296 | 0.9532 | 0.7362 | 0.6336 | 0.0100 | 0.0110 | 0.9886 |
| 446367 | 65.27 | 0.9782 | 0.8945 | 0.9252 | 0.9568 | 0.7372 | 0.6344 | 0.0100 | 0.0100 | 0.9858 |
| 895673 | 42.93 | 0.9619 | 0.8443 | 0.9342 | 0.8279 | 0.7708 | 0.6391 | 0.0651 | 0.0224 | 0.9718 |
| 655358 | 55.05 | 0.9770 | 0.8951 | 0.9265 | 0.9572 | 0.7341 | 0.6347 | 0.0100 | 0.0100 | 0.9897 |
| 245365 | 46.39 | 0.9579 | 0.8483 | 0.9312 | 0.8252 | 0.7751 | 0.6410 | 0.0556 | 0.0334 | 0.9696 |
| 213125 | 52.02 | 0.9622 | 0.8491 | 0.9285 | 0.8234 | 0.7792 | 0.6401 | 0.0481 | 0.0235 | 0.9725 |
| 326685 | 51.65 | 0.9774 | 0.8967 | 0.9221 | 0.9585 | 0.7388 | 0.6340 | 0.0100 | 0.0100 | 0.9890 |
| 244765 | 46.41 | 0.9651 | 0.8466 | 0.9321 | 0.8296 | 0.7714 | 0.6396 | 0.0386 | 0.0251 | 0.9729 |
| 425465 | 45.17 | 0.9578 | 0.8395 | 0.9355 | 0.8222 | 0.7748 | 0.6393 | 0.0504 | 0.0240 | 0.9715 |
| 344536 | 39.63 | 0.9566 | 0.8500 | 0.9283 | 0.8269 | 0.7772 | 0.6375 | 0.0536 | 0.0203 | 0.9670 |
| 965734 | 51.21 | 0.9768 | 0.8872 | 0.9237 | 0.8372 | 0.7741 | 0.6325 | 0.0286 | 0.0100 | 0.9842 |
| 907745 | 57.97 | 0.9780 | 0.8877 | 0.9292 | 0.8380 | 0.7717 | 0.6341 | 0.0231 | 0.0100 | 0.9843 |
| 435275 | 58.77 | 0.9775 | 0.8880 | 0.9250 | 0.8327 | 0.7792 | 0.6320 | 0.0329 | 0.0100 | 0.9842 |
| 345546 | 61.13 | 0.9777 | 0.8877 | 0.9238 | 0.8383 | 0.7752 | 0.6307 | 0.0100 | 0.0100 | 0.9840 |
| 423454 | 57.30 | 0.9784 | 0.8942 | 0.9268 | 0.9566 | 0.7366 | 0.6350 | 0.0100 | 0.0159 | 0.9895 |
| 786423 | 50.37 | 0.9778 | 0.8949 | 0.9248 | 0.9575 | 0.7349 | 0.6345 | 0.0100 | 0.0100 | 0.9898 |
| 675678 | 41.48 | 0.9565 | 0.8492 | 0.9279 | 0.8318 | 0.7727 | 0.6382 | 0.0542 | 0.0219 | 0.9728 |
| 453456 | 51.99 | 0.9576 | 0.8432 | 0.9293 | 0.8269 | 0.7763 | 0.6391 | 0.0537 | 0.0161 | 0.9728 |
| 890678 | 51.52 | 0.9783 | 0.8971 | 0.9237 | 0.9574 | 0.7358 | 0.6344 | 0.0100 | 0.0104 | 0.9855 |
| Mean | 50.38 | 0.9695 | 0.8713 | 0.9274 | 0.8745 | 0.7596 | 0.6332 | 0.0560 | 0.0179 | 0.9797 |

**Table D. 3 -** Test results for 30 runs of the Cauchy-Schwarz CE with different MATLAB seeds and with the common parameters: number of samples 50 000, lb = 0.01 and ub = $v_{t-1}$ for a peak reduction factor of 0.8

| Cauchy-Schwarz EPSO Cross-Entropy distortion $v_i$ | | | | | | | | | | |
|---|---|---|---|---|---|---|---|---|---|---|
| Seed | Time (s) | Group 1 | Group 2 | Group 4 | Group 5 | Group 6 | Group 7 | Group 8 | Group 9 | Group 3 |
| 156412 | 32.26 | 0.9656 | 0.8942 | 0.9481 | 0.9400 | 0.7693 | 0.6606 | 0.7444 | 0.0335 | 0.9758 |
| 348568 | 35.99 | 0.9701 | 0.8922 | 0.9713 | 0.9387 | 0.7652 | 0.6587 | 0.7841 | 0.0100 | 0.9893 |
| 456737 | 33.74 | 0.9663 | 0.8881 | 0.9655 | 0.9322 | 0.7677 | 0.6605 | 0.7522 | 0.0105 | 0.9882 |
| 690896 | 30.42 | 0.9693 | 0.8871 | 0.9546 | 0.9464 | 0.7755 | 0.6676 | 0.7297 | 0.0615 | 0.9792 |
| 324684 | 28.20 | 0.9800 | 0.8860 | 0.9631 | 0.9443 | 0.7749 | 0.6688 | 0.6971 | 0.0690 | 0.9900 |
| 735676 | 296.21 | 0.9711 | 0.8880 | 0.9581 | 0.9337 | 0.7754 | 0.6742 | 0.7069 | 0.0683 | 0.9846 |
| 634235 | 29.61 | 0.9701 | 0.8851 | 0.9548 | 0.9240 | 0.7708 | 0.6611 | 0.7453 | 0.0480 | 0.9888 |
| 978559 | 26.92 | 0.9633 | 0.8916 | 0.9640 | 0.9199 | 0.7726 | 0.6718 | 0.7210 | 0.0570 | 0.9827 |
| 235456 | 36.20 | 0.9785 | 0.8849 | 0.9659 | 0.9294 | 0.7721 | 0.6617 | 0.7365 | 0.0508 | 0.9893 |
| 764868 | 25.73 | 0.9782 | 0.8905 | 0.9657 | 0.9385 | 0.7739 | 0.6680 | 0.7026 | 0.0525 | 0.9826 |
| 542475 | 29.61 | 0.9794 | 0.8961 | 0.9778 | 0.9424 | 0.7787 | 0.6722 | 0.6973 | 0.0678 | 0.9775 |
| 525463 | 30.19 | 0.9779 | 0.8912 | 0.9757 | 0.9406 | 0.7695 | 0.6667 | 0.7340 | 0.0531 | 0.9831 |
| 446367 | 37.02 | 0.9677 | 0.8902 | 0.9787 | 0.9496 | 0.7696 | 0.6618 | 0.7306 | 0.0494 | 0.9775 |
| 895673 | 26.63 | 0.9745 | 0.8893 | 0.9791 | 0.9434 | 0.7728 | 0.6689 | 0.7133 | 0.0569 | 0.9900 |
| 655358 | 25.84 | 0.9770 | 0.8919 | 0.9587 | 0.9371 | 0.7708 | 0.6655 | 0.7148 | 0.0670 | 0.9897 |
| 245365 | 33.77 | 0.9792 | 0.8958 | 0.9543 | 0.9350 | 0.7757 | 0.6710 | 0.7143 | 0.0580 | 0.9750 |
| 213125 | 35.30 | 0.9741 | 0.8807 | 0.9650 | 0.9405 | 0.7718 | 0.6682 | 0.7173 | 0.0541 | 0.9796 |
| 326685 | 27.81 | 0.9682 | 0.8887 | 0.9515 | 0.9253 | 0.7746 | 0.6710 | 0.7046 | 0.0764 | 0.9762 |
| 244765 | 31.63 | 0.9785 | 0.8904 | 0.9547 | 0.9275 | 0.7725 | 0.6729 | 0.7234 | 0.0620 | 0.9742 |
| 425465 | 27.61 | 0.9800 | 0.8859 | 0.9541 | 0.9350 | 0.7754 | 0.6677 | 0.7243 | 0.0574 | 0.9898 |
| 344536 | 24.96 | 0.9640 | 0.8865 | 0.9653 | 0.9445 | 0.7746 | 0.6758 | 0.6949 | 0.0740 | 0.9783 |
| 965734 | 26.80 | 0.9778 | 0.8874 | 0.9586 | 0.9236 | 0.7753 | 0.6690 | 0.7105 | 0.0719 | 0.9785 |
| 907745 | 39.49 | 0.9786 | 0.8850 | 0.9553 | 0.9308 | 0.7705 | 0.6646 | 0.7351 | 0.0100 | 0.9826 |
| 435275 | 299.31 | 0.9775 | 0.8907 | 0.9777 | 0.9399 | 0.7708 | 0.6593 | 0.7340 | 0.0279 | 0.9843 |
| 345546 | 35.59 | 0.9786 | 0.8985 | 0.9548 | 0.9214 | 0.7726 | 0.6727 | 0.7051 | 0.0601 | 0.9813 |
| 423454 | 43.63 | 0.9787 | 0.8931 | 0.9553 | 0.9271 | 0.7689 | 0.6683 | 0.7197 | 0.0500 | 0.9877 |
| 786423 | 32.56 | 0.9778 | 0.8917 | 0.9661 | 0.9525 | 0.7752 | 0.6694 | 0.7134 | 0.0669 | 0.9898 |
| 675678 | 30.51 | 0.9800 | 0.8920 | 0.9631 | 0.9302 | 0.7733 | 0.6666 | 0.7099 | 0.0474 | 0.9888 |
| 453456 | 32.94 | 0.9669 | 0.8918 | 0.9610 | 0.9576 | 0.7702 | 0.6657 | 0.7326 | 0.0405 | 0.9757 |
| 890678 | 26.88 | 0.9683 | 0.8864 | 0.9696 | 0.9327 | 0.7712 | 0.6648 | 0.7308 | 0.0490 | 0.9729 |
| Mean | 49.11 | 0.9739 | 0.8897 | 0.9629 | 0.9361 | 0.7724 | 0.6672 | 0.7227 | 0.0520 | 0.9828 |

**Table D. 4 -** Test results for 30 runs of the Cauchy-Schwarz CE with different MATLAB seeds and with the common parameters: number of samples 50 000, lb = 0.01 and ub = $v_{t-1}$ for a peak reduction factor of 0.9

| Cauchy-Schwarz EPSO Cross-Entropy distortion $v_i$ | | | | | | | | | | |
|---|---|---|---|---|---|---|---|---|---|---|
| Seed | Time (s) | Group 1 | Group 2 | Group 4 | Group 5 | Group 6 | Group 7 | Group 8 | Group 9 | Group 3 |
| 156412 | 30.12 | 0.9781 | 0.8992 | 0.9771 | 0.9584 | 0.8296 | 0.7827 | 0.4091 | 0.3283 | 0.9801 |
| 348568 | 39.54 | 0.9786 | 0.8941 | 0.9565 | 0.9570 | 0.8304 | 0.7839 | 0.4046 | 0.3330 | 0.9808 |
| 456737 | 26.02 | 0.9794 | 0.8995 | 0.9537 | 0.9560 | 0.8273 | 0.7892 | 0.4102 | 0.3286 | 0.9791 |
| 690896 | 37.60 | 0.9783 | 0.8981 | 0.9761 | 0.9563 | 0.8296 | 0.7826 | 0.3870 | 0.3458 | 0.9898 |
| 324684 | 36.08 | 0.9780 | 0.8957 | 0.9532 | 0.9582 | 0.8312 | 0.7870 | 0.3995 | 0.3378 | 0.9801 |
| 735676 | 37.47 | 0.9799 | 0.9000 | 0.9534 | 0.9600 | 0.8290 | 0.7876 | 0.3945 | 0.3387 | 0.9814 |
| 634235 | 33.55 | 0.9800 | 0.8995 | 0.9565 | 0.9600 | 0.8241 | 0.7896 | 0.3937 | 0.3369 | 0.9798 |
| 978559 | 30.27 | 0.9800 | 0.8998 | 0.9610 | 0.9570 | 0.8230 | 0.7906 | 0.3919 | 0.3419 | 0.9815 |
| 235456 | 38.43 | 0.9785 | 0.8939 | 0.9550 | 0.9575 | 0.8254 | 0.7957 | 0.3949 | 0.3408 | 0.9806 |
| 764868 | 30.44 | 0.9782 | 0.8956 | 0.9578 | 0.9538 | 0.8340 | 0.7807 | 0.3873 | 0.3460 | 0.9805 |
| 542475 | 30.26 | 0.9794 | 0.8976 | 0.9583 | 0.9550 | 0.8239 | 0.7944 | 0.3937 | 0.3417 | 0.9795 |
| 525463 | 31.70 | 0.9779 | 0.8955 | 0.9542 | 0.9532 | 0.8287 | 0.7906 | 0.3933 | 0.3418 | 0.9794 |
| 446367 | 39.29 | 0.9782 | 0.8964 | 0.9597 | 0.9568 | 0.8243 | 0.7912 | 0.3900 | 0.3438 | 0.9834 |
| 895673 | 34.35 | 0.9779 | 0.8956 | 0.9560 | 0.9536 | 0.8272 | 0.7921 | 0.4056 | 0.3327 | 0.9784 |
| 655358 | 28.43 | 0.9770 | 0.8965 | 0.9529 | 0.9572 | 0.8281 | 0.7892 | 0.4028 | 0.3364 | 0.9811 |
| 245365 | 36.53 | 0.9792 | 0.8980 | 0.9550 | 0.9600 | 0.8268 | 0.7876 | 0.3940 | 0.3390 | 0.9827 |
| 213125 | 39.12 | 0.9795 | 0.8981 | 0.9542 | 0.9585 | 0.8255 | 0.7894 | 0.4042 | 0.3330 | 0.9806 |
| 326685 | 32.12 | 0.9789 | 0.8971 | 0.9574 | 0.9585 | 0.8289 | 0.7860 | 0.3864 | 0.3431 | 0.9812 |
| 244765 | 34.57 | 0.9800 | 0.8974 | 0.9548 | 0.9600 | 0.8301 | 0.7874 | 0.3920 | 0.3407 | 0.9800 |
| 425465 | 33.57 | 0.9797 | 0.8973 | 0.9570 | 0.9559 | 0.8224 | 0.7967 | 0.3971 | 0.3391 | 0.9805 |
| 344536 | 28.60 | 0.9800 | 0.8985 | 0.9790 | 0.9600 | 0.8306 | 0.7757 | 0.3645 | 0.3587 | 0.9875 |
| 965734 | 33.79 | 0.9778 | 0.8974 | 0.9616 | 0.9554 | 0.8241 | 0.7925 | 0.3972 | 0.3366 | 0.9800 |
| 907745 | 36.67 | 0.9786 | 0.8956 | 0.9506 | 0.9572 | 0.8269 | 0.7914 | 0.4188 | 0.3239 | 0.9793 |
| 435275 | 37.27 | 0.9775 | 0.8907 | 0.9511 | 0.9535 | 0.8306 | 0.7884 | 0.4184 | 0.3269 | 0.9793 |
| 345546 | 39.72 | 0.9786 | 0.8959 | 0.9515 | 0.9563 | 0.8294 | 0.7889 | 0.4068 | 0.3339 | 0.9798 |
| 423454 | 41.07 | 0.9787 | 0.8968 | 0.9513 | 0.9566 | 0.8291 | 0.7884 | 0.3938 | 0.3398 | 0.9819 |
| 786423 | 30.92 | 0.9778 | 0.8951 | 0.9522 | 0.9575 | 0.8287 | 0.7874 | 0.3955 | 0.3392 | 0.9813 |
| 675678 | 28.87 | 0.9781 | 0.8986 | 0.9523 | 0.9587 | 0.8268 | 0.7928 | 0.4169 | 0.3265 | 0.9786 |
| 453456 | 38.10 | 0.9787 | 0.8977 | 0.9780 | 0.9576 | 0.8287 | 0.7803 | 0.3998 | 0.3399 | 0.9898 |
| 890678 | 34.02 | 0.9797 | 0.8971 | 0.9575 | 0.9591 | 0.8290 | 0.7848 | 0.3914 | 0.3398 | 0.9803 |
| Mean | 34.28 | 0.9787 | 0.8969 | 0.9582 | 0.9572 | 0.8278 | 0.7882 | 0.3978 | 0.3378 | 0.9813 |

**Table D. 5 -** Test results for 30 runs of the Cauchy-Schwarz CE with different MATLAB seeds and with the common parameters: number of samples 50 000, lb = 0.01 and ub = $v_{t-1}$ for a peak reduction factor of 1.0

| Cauchy-Schwarz EPSO Cross-Entropy distortion $v_i$ | | | | | | | | | | |
|---|---|---|---|---|---|---|---|---|---|---|
| Seed | Time (s) | Group 1 | Group 2 | Group 4 | Group 5 | Group 6 | Group 7 | Group 8 | Group 9 | Group 3 |
| 156412 | 29.49 | 0.9601 | 0.8529 | 0.9526 | 0.9224 | 0.8380 | 0.7481 | 0.7030 | 0.4432 | 0.9749 |
| 348568 | 30.25 | 0.9602 | 0.8517 | 0.9543 | 0.9223 | 0.8329 | 0.7510 | 0.6967 | 0.4449 | 0.9746 |
| 456737 | 38.28 | 0.9606 | 0.8507 | 0.9541 | 0.9186 | 0.8355 | 0.7552 | 0.6947 | 0.4383 | 0.9768 |
| 690896 | 32.12 | 0.9597 | 0.8500 | 0.9563 | 0.9238 | 0.8403 | 0.7528 | 0.6948 | 0.4408 | 0.9771 |
| 324684 | 28.72 | 0.9614 | 0.8516 | 0.9569 | 0.9250 | 0.8424 | 0.7491 | 0.6971 | 0.4396 | 0.9762 |
| 735676 | 29.86 | 0.9579 | 0.8458 | 0.9531 | 0.9210 | 0.8290 | 0.7537 | 0.7036 | 0.4415 | 0.9768 |
| 634235 | 30.36 | 0.9566 | 0.8474 | 0.9534 | 0.9182 | 0.8251 | 0.7596 | 0.6893 | 0.4411 | 0.9714 |
| 978559 | 25.50 | 0.9607 | 0.8508 | 0.9556 | 0.9234 | 0.8354 | 0.7516 | 0.6999 | 0.4413 | 0.9748 |
| 235456 | 43.91 | 0.9570 | 0.8480 | 0.9487 | 0.9172 | 0.8254 | 0.7598 | 0.7073 | 0.4391 | 0.9745 |
| 764868 | 27.42 | 0.9601 | 0.8518 | 0.9534 | 0.9247 | 0.8419 | 0.7523 | 0.6972 | 0.4392 | 0.9761 |
| 542475 | 34.38 | 0.9570 | 0.8492 | 0.9533 | 0.9191 | 0.8331 | 0.7547 | 0.6973 | 0.4422 | 0.9733 |
| 525463 | 25.76 | 0.9600 | 0.8495 | 0.9518 | 0.9234 | 0.8293 | 0.7540 | 0.7101 | 0.4431 | 0.9750 |
| 446367 | 39.06 | 0.9588 | 0.8444 | 0.9524 | 0.9185 | 0.8243 | 0.7622 | 0.7017 | 0.4400 | 0.9701 |
| 895673 | 27.85 | 0.9584 | 0.8528 | 0.9520 | 0.9218 | 0.8345 | 0.7503 | 0.7081 | 0.4391 | 0.9758 |
| 655358 | 29.61 | 0.9602 | 0.8505 | 0.9514 | 0.9223 | 0.8327 | 0.7549 | 0.6957 | 0.4409 | 0.9734 |
| 245365 | 30.60 | 0.9597 | 0.8476 | 0.9531 | 0.9236 | 0.8346 | 0.7550 | 0.6975 | 0.4399 | 0.9742 |
| 213125 | 35.43 | 0.9584 | 0.8482 | 0.9546 | 0.9243 | 0.8299 | 0.7584 | 0.6885 | 0.4435 | 0.9732 |
| 326685 | 29.23 | 0.9586 | 0.8479 | 0.9546 | 0.9200 | 0.8304 | 0.7585 | 0.6839 | 0.4409 | 0.9764 |
| 244765 | 30.00 | 0.9602 | 0.8513 | 0.9551 | 0.9211 | 0.8364 | 0.7501 | 0.6992 | 0.4429 | 0.9755 |
| 425465 | 28.78 | 0.9582 | 0.8443 | 0.9523 | 0.9169 | 0.8224 | 0.7606 | 0.6965 | 0.4442 | 0.9735 |
| 344536 | 27.09 | 0.9597 | 0.8533 | 0.9556 | 0.9233 | 0.8371 | 0.7511 | 0.6949 | 0.4387 | 0.9753 |
| 965734 | 30.17 | 0.9603 | 0.8514 | 0.9550 | 0.9234 | 0.8395 | 0.7526 | 0.6902 | 0.4437 | 0.9742 |
| 907745 | 305.33 | 0.9721 | 0.8466 | 0.9764 | 0.9536 | 0.8382 | 0.7381 | 0.7253 | 0.4374 | 0.9842 |
| 435275 | 29.74 | 0.9605 | 0.8522 | 0.9562 | 0.9229 | 0.8372 | 0.7486 | 0.6934 | 0.4435 | 0.9761 |
| 345546 | 38.48 | 0.9570 | 0.8515 | 0.9525 | 0.9212 | 0.8327 | 0.7495 | 0.7050 | 0.4421 | 0.9771 |
| 423454 | 35.76 | 0.9581 | 0.8467 | 0.9533 | 0.9218 | 0.8291 | 0.7552 | 0.7074 | 0.4400 | 0.9733 |
| 786423 | 29.13 | 0.9620 | 0.8528 | 0.9564 | 0.9241 | 0.8386 | 0.7499 | 0.6992 | 0.4392 | 0.9756 |
| 675678 | 26.08 | 0.9588 | 0.8477 | 0.9516 | 0.9202 | 0.8325 | 0.7534 | 0.6995 | 0.4428 | 0.9722 |
| 453456 | 34.83 | 0.9600 | 0.8501 | 0.9551 | 0.9213 | 0.8346 | 0.7541 | 0.6931 | 0.4431 | 0.9736 |
| 890678 | 28.91 | 0.9605 | 0.8507 | 0.9545 | 0.9198 | 0.8344 | 0.7508 | 0.6980 | 0.4427 | 0.9754 |
| Mean | 40.40 | 0.9598 | 0.8496 | 0.9545 | 0.9226 | 0.8336 | 0.7532 | 0.6989 | 0.4413 | 0.9750 |

**Table D. 6 – Test Results comparing the years simulated towards convergence with the Kullback-Leibler (KL) distortion and the Cauchy-Schwarz (CS) distortion for the different peak reduction factors (PRF)**

| Seed | PRF = 0.6 | | PRF = 0.7 | | PRF = 0.8 | | PRF = 0.9 | | PRF = 1.0 | |
|---|---|---|---|---|---|---|---|---|---|---|
| | KL | CS | KL | CS | KL | CS | KL | CS | KL | CS |
| | Years simulated | | Years simulated | | Years simulated | | Years simulated | | Years simulated | |
| 34563457 | 76 | 61 | 53 | 35 | 54 | 133 | 33 | 52 | 29 | 60 |
| 45667 | 65 | 65 | 57 | 41 | 37 | 137 | 43 | 41 | 37 | 43 |
| 64356345 | 59 | 78 | 37 | 31 | 68 | 110 | 32 | 47 | 59 | 44 |
| 562434 | 67 | 87 | 41 | 42 | 74 | 147 | 32 | 33 | 49 | 49 |
| 45645634 | 67 | 85 | 42 | 45 | 44 | 147 | 43 | 47 | 36 | 46 |
| 673456586 | 69 | 95 | 34 | 43 | 48 | 132 | 41 | 57 | 42 | 72 |
| 6574564 | 56 | 116 | 48 | 33 | 62 | 158 | 37 | 95 | 41 | 46 |
| 6767867 | 77 | 80 | 36 | 52 | 58 | 113 | 39 | 43 | 31 | 51 |
| 467467 | 62 | 129 | 47 | 43 | 51 | 136 | 24 | 44 | 37 | 69 |
| 645645664 | 64 | 72 | 34 | 38 | 35 | 162 | 49 | 70 | 29 | 44 |
| 3635643 | 79 | 103 | 47 | 23 | 56 | 138 | 47 | 45 | 30 | 57 |
| 363543453 | 66 | 53 | 29 | 33 | 49 | 158 | 26 | 70 | 36 | 52 |
| 3636 | 79 | 105 | 46 | 30 | 41 | 173 | 2 | 68 | 35 | 44 |
| 435687 | 70 | 62 | 40 | 41 | 51 | 183 | 45 | 51 | 48 | 47 |
| 9078345 | 43 | 89 | 48 | 45 | 53 | 157 | 30 | 57 | 53 | 52 |
| 39047589 | 52 | 121 | 48 | 40 | 34 | 194 | 38 | 49 | 25 | 2 |
| 507858936 | 69 | 67 | 48 | 56 | 51 | 145 | 33 | 52 | 48 | 44 |
| 8973478 | 58 | 64 | 45 | 28 | 42 | 156 | 41 | 71 | 42 | 59 |
| 97345873 | 65 | 87 | 44 | 28 | 50 | 145 | 36 | 36 | 25 | 50 |
| 893246583 | 67 | 99 | 45 | 34 | 49 | 188 | 29 | 51 | 20 | 60 |
| 86345873 | 67 | 77 | 58 | 35 | 43 | 155 | 35 | 41 | 47 | 46 |
| 21763 | 52 | 56 | 44 | 38 | 45 | 158 | 40 | 2 | 35 | 58 |
| 3456789 | 53 | 90 | 66 | 40 | 49 | 114 | 24 | 58 | 48 | 56 |
| 5636 | 51 | 87 | 32 | 34 | 44 | 204 | 39 | 34 | 37 | 54 |
| 90854902 | 65 | 100 | 49 | 17 | 55 | 146 | 26 | 35 | 30 | 69 |
| 87539 | 49 | 92 | 64 | 26 | 41 | 153 | 29 | 54 | 30 | 68 |
| 35773456 | 71 | 74 | 46 | 38 | 48 | 186 | 28 | 38 | 39 | 61 |
| 538754 | 57 | 85 | 43 | 54 | 32 | 167 | 33 | 51 | 24 | 65 |
| 38975983 | 76 | 2 | 38 | 45 | 43 | 186 | 34 | 53 | 33 | 52 |
| 908734 | 84 | 69 | 47 | 29 | 59 | 180 | 2 | 44 | 42 | 56 |
| 34563457 | 76 | 61 | 53 | 35 | 54 | 133 | 33 | 52 | 29 | 60 |
| Mean | 64.50 | 81.67 | 45.20 | 37.23 | 48.87 | 155.37 | 33.00 | 49.63 | 37.23 | 52.53 |